MICROBIAL METABOLISM OF ABIETANE DITERPENOIDS BY *PSEUDOMONAS ABIETANIPHILA* BKME-9 AND *BURKHOLDERIA XENOVORANS* LB400

by

Daryl James Smith

B.Sc., Dalhousie University, 1989

A THESIS SUBMITTED IN PARTIAL FULFILMENT OF THE REQUIREMENTS FOR THE DEGREE OF

DOCTOR OF PHILOSOPHY

in

THE FACULTY OF GRADUATE STUDIES

(Microbiology and Immunology)

UNIVERSITY OF BRITISH COLUMBIA

August 2006

ABSTRACT

This dissertation has elucidated initial steps in the degradation of abietane diterpenoids by *Pseudomonas abietaniphila* BKME-9 and *Burkholderia xenovorans* LB400. A 10.4-kbp extension of the *dit* cluster in BKME-9 containing genes involved in abietane diterpenoid degradation has been sequenced. The *ditQ* gene was found to encode a cytochrome P450 monooxygenase. Knocking out *ditQ* had little effect on growth of BKME-9 on abietic acid (AbA) but impaired growth on dehydroabietic acid (DhA) and palustric acid (PaA). A *xylE* transcriptional fusion showed that a range of diterpenoids induced transcription of *ditQ*. Substrate binding assays of DitQ revealed that DhA binds to the enzyme ($K_d = 0.43 \pm 0.03$ μM). These results indicate that DitQ is involved in the metabolism of DhA and PaA and are consistent with its putative role in converting DhA to 7-hydroxy-DhA.

The genome of LB400 was found to contain a large cluster of genes with high similarity to the BKME-9-*dit* cluster. Microarray transcriptional analysis revealed that of the 72 genes encoded by an 80.5-kb cluster, 43 are up-regulated at least 2-fold in expression during growth on DhA versus on succinate. This cluster has been named the LB400 *dit* cluster. Through 2D gel proteomic analysis, we have determined that a key difference in the catabolism of the abietane diterpenoids, DhA and AbA lies in the differential expression of a cytochrome P450, DitU (CYP226A2) encoded by the *dit* cluster. DitQ was expressed during growth on both DhA and AbA, whereas DitU expression was only detectable during growth on AbA. Phenotypic studies of knockout mutants in LB400 containing insertion mutations of *ditQ* or *ditU* showed that *ditQ* was required for growth on DhA, whereas *ditU* was required for growth on AbA. In cell suspension assays, patterns of metabolite accumulation confirmed the role of DitU in AbA transformation and DitQ in DhA transformation. Substrate binding assays revealed that DitQ binds both DhA ($K_d = 0.98 \pm 0.01$ μM) and PaA ($K_d = 1.6 \pm 0.1$ μM). An in vitro P450 assay confirmed that DitQ transforms DhA to 7-hydroxy-DhA. These results demonstrate distinct roles

of DitQ and DitU in the transformation of DhA and AbA to the central intermediate, 7-oxo-DhA, in a convergent degradation pathway.

TABLE OF CONTENTS

LIST OF TABLES

LIST OF FIGURES

LIST OF ABBREVIATIONS

AbA	abietic acid
Asp	aspartate
ATPase	adenosine triphosphate synthase
BCA	bicinchoninic acid
Bcc	*Burkholderia cepacia* complex
BLAST	Basic Local Alignment Search Tool
BLASTP	protein-protein BLAST
C23O	catechol 2,3-dioxygenase
CDS	coding sequences
CFU	colony forming unit
CO	carbon monoxide
CoA	Coenzyme A
COGs	clusters of orthologous groups
cpm	counts per minute
CTP	cytidine triphosphate
dATP	deoxyadenosine triphosphate
dCTP	deoxycytidine triphosphate
dGTP	deoxyguanosine triphosphate
DhA	dehydroabietic acid
DMAPP	dimethylallyl diphosphate
DMDHA	dimethyl heptanedioic acid
DMSO	dimethylsulfoxide
DNA	deoxy ribose nucleic acid
DXP	deoxyxylulose pathway
dNTP	deoxyribonucleotide triphosphate
DTT	dithiothreitol
dUTP	deoxyuridine triphosphate
EB	elution buffer
EDTA	ethylenediaminetetraacetic acid
EI	electron impact
EMP	Embden-Meyerhof-Parnas
FAD	flavin adenine dinucleotide
FID	flame ionization detector
FMN	flavin adenine mononucleotide
FPP	farnesyl diphosphate
GC	gas chromotography
GCMS	gas chromatography-mass spectroscopy
GFPP	geranylfarnesyl disphosphate
GGPP	geranylgeranyl diphosphate
Gm	gentamicin
GPP	geranyl diphosphate
h	hour
HIV	human immunodeficiency virus
HMM	hidden Markov model
IPG	immobilized pH gradient
IPP	isopentyl diphosphate
IPTG	isopropyl-beta-D-thiogalactopyranoside

LB	Luria-Bertani
NADH	reduced nicotinamide adenine dinucleotide
NADPH	reduced nicotinamide adenine dinucleotide phosphate
NCBI	National Center for Biotechnology Information
NIST	National Institute of Standards and Technologies
NPLC1L1	Niemann-Pick C1-like 1
MFS	Major Facilitator Superfamily
min	minute
MS	mass spectroscopy
OD	optical density
OPP	pyrophosphate
P450	cytochrome P450
PaA	palustric acid
PAGE	polyacrylamide gel electrophoresis
PCR	polymerase chain reaction
pI	Isoelectric point
PMSF	phenylmethylsulphonylfluoride
psi	pounds per square inch
TCA	tricarboxylic acid
TE	tris EDTA
TMS	transmembrane subunits
UV	ultra violet
UV-Vis	ultra violet-visible
X-gal	5-bromo-4-chloro-3-indolyl-beta-D-galactopyranoside

ACKNOWLEDGEMENTS

First, I would like to thank my supervisor, Dr. William Mohn, for giving me the opportunity and for his understanding, patience, guidance and support. I would also like to thank my supervisory committee, Drs. Tom Beatty, Lindsay Eltis and Michael Murphy for their guidance. Lindsay was instrumental in work on the P450s by providing helpful suggestions on both experimentation and data interpretation. He also provided purified DitA3, BphF and BphG for in vitro P450 assays. I would like to thank Leticia Gomez for assistance with the in vitro P450 assays. I would like to thank Gord Stewart for everything from un-jamming the printer to help with operation of the GCMS. I would like to thank all members, past and present, of the Mohn Lab group for support and camaraderie. I am also grateful to all members of the "RHA1 group" for support and guidance in annotation and interpretation of genomic data. In particular, I would thank Dr. Marianna Patrauchan and Christine Florizone for valuable assistance on all aspects of the 2D gel work. I would like to thank Nancy Smith and Dr. Dominic Frigon for proofreading parts of this dissertation.

I also acknowledge Dr. J. Tiedje for the use of his laboratory at Michigan State University to conduct microarray experiments and Dr. Joonhong Park for helpful discussion and assistance with the microarray work. I also thank Dr. R.C. Wyndham for *tdt* cluster sequence data prior to publication, cloned *tdtD*, and helpful discussions. This work was supported by the Natural Science and Engineering Research Council of Canada.

To Kristen, my appreciation for accepting me, and all that goes along with that, including grad school. To Simon, Regan, and Talia, my appreciation for putting a smile on my face on those days when nothing was going right.

CONTRIBUTIONS OF OTHERS

Chapter 2 Vince Martin conducted Southern hybridization reactions. Lindsay Eltis suggested P450 substrate binding assays at a Committee meeting. Lindsay Eltis also helped interpret difference spectra.

Chapter 3. Summer student Ryan Farnsworth contributed to growth assay of LB400. Xeotron microarray hybridization and scanning were conducted by Joonhong Park at Michigan State University.

Chapter 4. Summer student, Angle Yu, provided help with preparation of knockouts. A portion of 2D gel analysis was conducted by Chirstine Florizone, including running and scanning gels. Marianna Patrauchan provided valuable assistance with Progenesis Workstation software. Excision of protein from gels, in-gel digests of selected protein spots and MALDI-TOF were conducted by Christine Florizone. Lindsay Eltis suggested the P450 in vitro assay and kindly provided the both BphG and DitA3.

1. Introduction

1.1 Preface

Resin is produced by most species of coniferous trees including grand fir (*Abies grandis*) (28) and Norway spruce (*Picea abies*) (56). Resin consists of a volatile turpentine fraction, containing mostly monoterpenes and sesquiterpenes, and a non-volatile rosin fraction. The rosin fraction, which consists mostly of diterpenoids, has been reported to constitute up to 0.8% of the total dry weight of wood (21). Considering the total biomass of conifers on the planet and their continual growth and decay, these compounds contribute significantly to the global carbon cycle. The most abundant diterpenoids in the rosin fraction are acidic abietanes and pimeranes (56). Acidic abietanes are tricyclic C-20 carboxylic acid-containing compounds with an isopropyl group at C13 (Fig. 1.1), whereas the pimeranes have a vinyl and methyl substituents at this position. They are both produced in conifers through the cyclization of geranylgeranyl diphosphate by diterpene synthase and subsequent oxidations involving cytochromes P450 (27, 71).

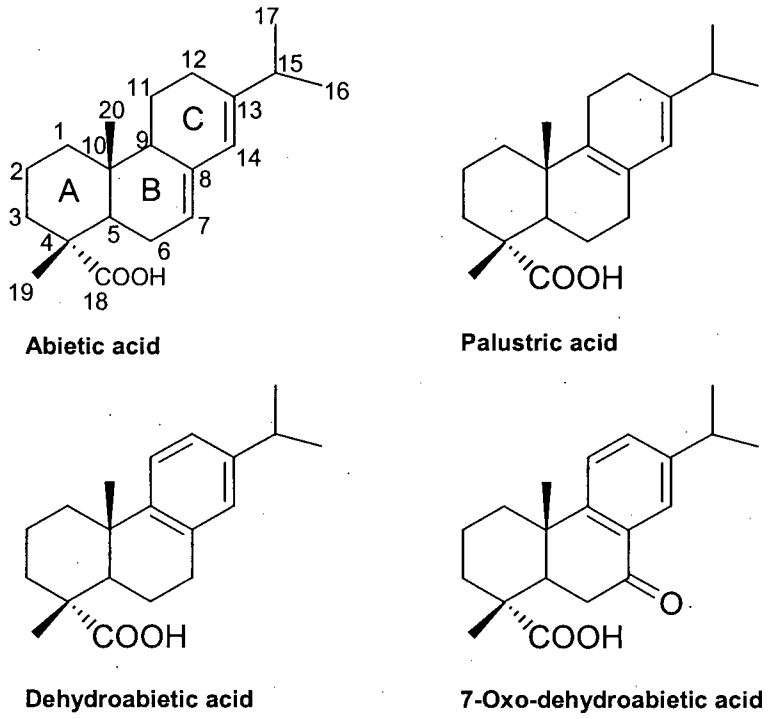

Figure 1.1 Chemical structures of abietane diterpenoids.

This dissertation will focus on the microbial metabolism of abietic acid (AbA), dehydroabietic acid (DhA), palustric acid (PaA), and 7-oxo-dehydroabietic acid (7-oxo-DhA) (Fig. 1.1).

One of the first documented applications of these tree derived natural products was in shipbuilding (12). Rosin from conifers in the form of pitch or tar was used as a sealant for wooden ships. In the biblical account of Noah and the ark, Noah is commanded by God in Genesis 6:14 "...So make yourself an ark of cypress wood and coat it with pitch inside and out." Rosin was also used as a sealant for wine vessels in ancient Rome (55) leaving the contents with a unique terpene flavour. This taste sensation can still be found today in the Retsina wines of Greece.

To gain a better understanding of the metabolism of these compounds this introduction will first look at their biosynthesis and significance. This will be followed by a brief overview of cytochromes P450 (P450), key enzymes involved in both the synthesis and degradation of several terpenes, and conclude by reviewing what was known about the microbial degradation of diterpenoids prior to the work presented in the following chapters.

1.2 Terpenoid Synthesis

1.2.1 IPP/DMAPP synthesis

Terpenoids constitute the largest single family of natural products with estimates of the number of characterized terpenoids ranging from 25,000 to 50,000. Isopentyl pyrophosphate (IPP) and its allylic isomer, dimethyl allyl pyrophosphate (DMAPP) are the precursors for a vast array of biologically important compounds (Fig. 1.2). These two 5-C isomers are the structural

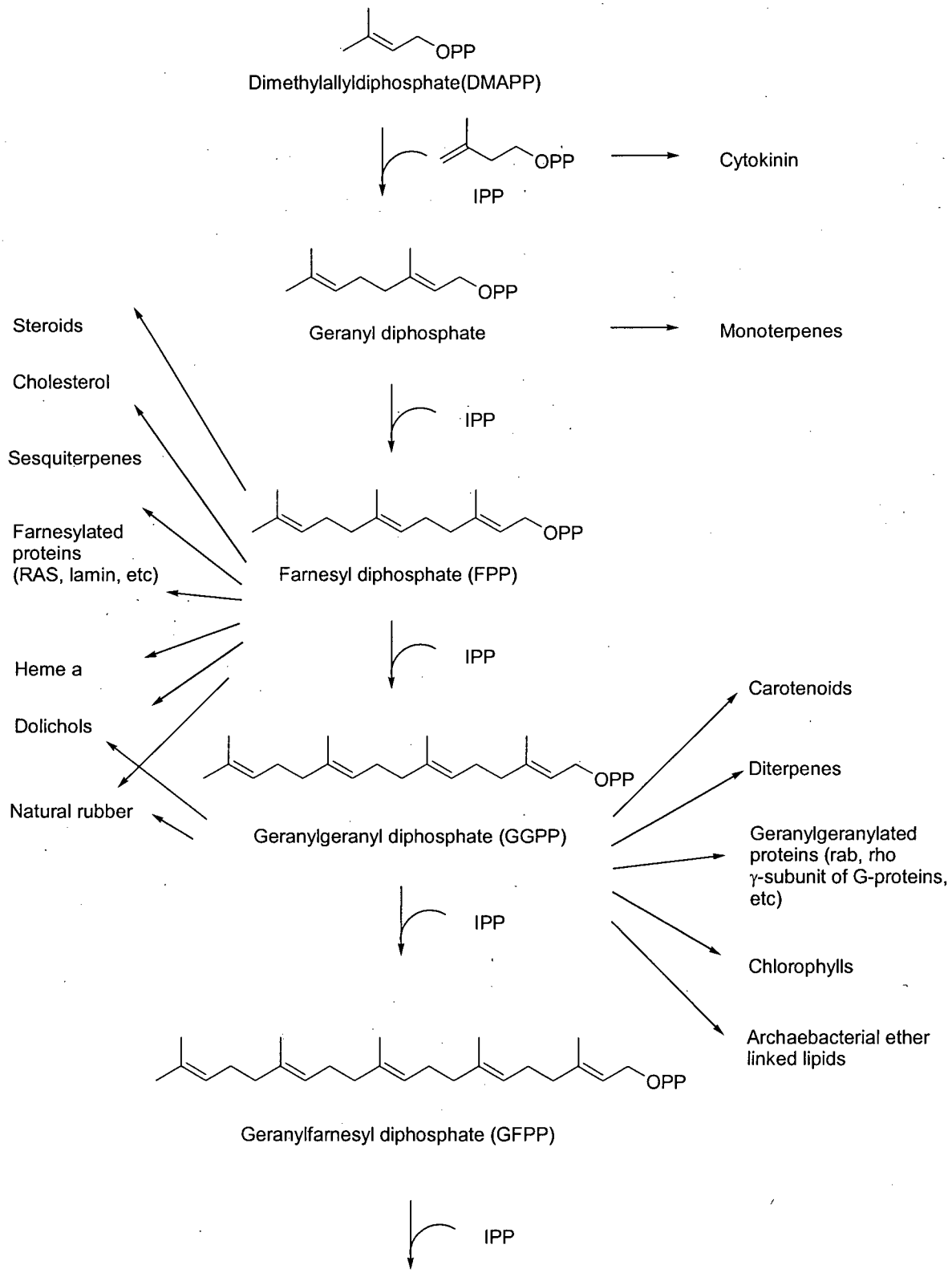

Figure 1. 2. Consecutive condensation of isopentyl pyrophosphate in the prenyl transferase reaction. Adapted from (68)

subunits from which all terpenes are synthesized. Two pathways have been identified in the synthesis of IPP and DMAPP, the mevalonate pathway and the mevalonate-independent or deoxyxylulose (DXP) pathway (Fig. 1.3). (17, 19, 73). Until the early nineties the mevalonate pathway was considered the only route of IPP production, however recent work has demonstrated a major reliance on the DXP pathway in both plants and many bacteria.

1.2.2 Mevalonate pathway

All Archaea and Eukarya, and some Bacteria, utilize the mevalonate pathway. Mevalonate is formed from 3 acetyl Coenzyme A (acetyl-CoA) subunits via acetoacetyl-CoA and 3-hydroxy-3-methylglutaryl-CoA (Fig. 1.3 A). Mevalonate is then reduced, phosphorylated and decarboxylated to yield IPP which undergoes isomerization to DMAPP through the activity of IPP isomerase.

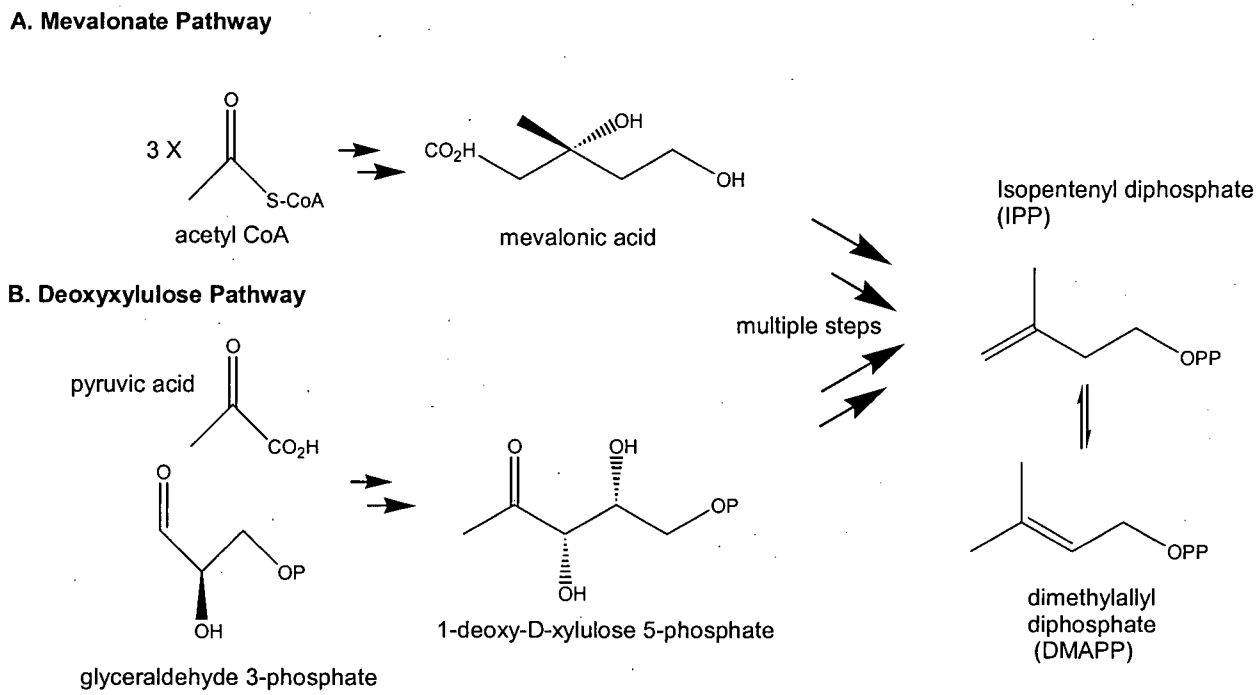

Figure 1.3 The mevalonate and DXP pathways of IPP production.

1.2.3 Mevalonate-independent pathway

This route of IPP and DMAPP production is essential in plant plastids and many Bacteria, but not in animals or Archaea (Fig. 1.3 B). The absence of this pathway in animals has made it an attractive area of research in antimicrobial therapies (19). Observations of unexpected isotope patterns in radiolabeled terpenoids in eubacteria growing on [^{13}C]glucose, which were not compatible with the classic mevalonate pathway predictions, led to further investigation of an alternate pathway (as reviewed in (19)). In one report, the fermentative ethanologenic bacterium *Zymomonas mobilis* was grown on radiolabeled glucose. The 2-megabase genome of *Z. mobilis* has recently been sequenced (78). Gene annotation confirmed the absence of essential genes for the Embden-Meyerhof-Parnas (EMP) and tricarboxylic acid (TCA) cycle pathways. *Z. mobilis* exclusively uses the Entner-Doudoroff pathway for the metabolism of glucose. Growth on [^{13}C]glucose showed the incorporation of 3 contiguous carbons from glucose into IPP which cannot be accounted for in the mevalonate pathway utilizing 2-C Acetyl CoA (74). In the DXP pathway IPP is synthesized via the condensation of pyruvate and glyceraldehyde 3-phosphate to form deoxy-D-xylose-5-phosphate through decarboxylation and rearrangement. This condensation of two 3-C subunits accounts for the isotope pattern observed in *Z. mobilis* terpenoid production.

1.2.4 The isoprene rule

After production of IPP, biosynthesis of the terpenoids follows the "biogenic isoprene rule" which was originally proposed by Nobel laureate Leopold Ruzicka in 1953 using the limited structural and enzymatic data available at the time (77). Ruzicka proposed that the structural precursors of the various classes of terpenoids were composed from linear chains of specific lengths which were synthesized from "head to tail" joining of 5 carbon isoprene units. It is now known that the parents of the various classes include, 10-C geranyl pyrophosphate (GPP),

15-C farnesyl pyrophosphate (FPP), 20-C geranylgeranyl pyrophosphate (GGPP), 25-C geranylfarnesyl pyrophosphate (GFPP), 30-C squalene and 40-C phytoene (Fig. 1.2).

1.2.5 Prenyltransferases

Prenyltransferases catalyze the synthesis of linear prenyl pyrophosphate in a 1,4 head to tail condensation reaction via a positively charged carbon ion (carbocation) intermediate from IPP and DMAPP. This is the first committed step in the synthesis of terpenoids (52). Structural analysis of prenyltransferases show two juxtaposed conserved aspartate-rich regions, which coordinate substrate binding and catalysis via divalent cations in these alpha helical proteins. DMAPP is the electrophilic allylic isomer of IPP, produced by IPP isomerase, which facilitates the 1'-4 condensation of these two 5 carbon units (16). Chain elongation involves the consecutive addition of an IPP to DMAPP or its growing allylic pyrophosphate counterpart (85) (Fig. 1.4). The reaction is initiated by formation of a carbocation at C1 of the allylic pyrophosphate generated by elimination of pyrophosphate via C-O bond cleavage. Condensation occurs through the nucleophilic attack of the terminal double bond of IPP on the carbocation at C1 of the allylic pyrophosphate leading to a new C-C bond. This forms a tertiary carbocation, which is eliminated through deprotonation at C2 of the now condensed IPP, leading to double bond formation between C2 and C3 of the growing chain. The reaction may be repeated with the addition of more IPPs.

Chain length is determined by the transferase catalyzing the elongation. For example, farnesyl pyrophosphate synthase only produces 15-C isoprenes and chain elongation is completed after the condensation of geranyl pyrophosphate with IPP, whereas geranylgeranyl pyrophosphate synthase produces a 20-C isoprene from the condensation of farnesyl pyrophosphate with an IPP. Chain length is governed by the presence of a "large" amino acid residue, such as phenylalanine, located near the aspartate rich motif. The larger residue blocks

further increases in chain length and leads to termination (68). Substitution of these large amino acids with smaller amino acids, such as alanine, allows for increases in chain length.

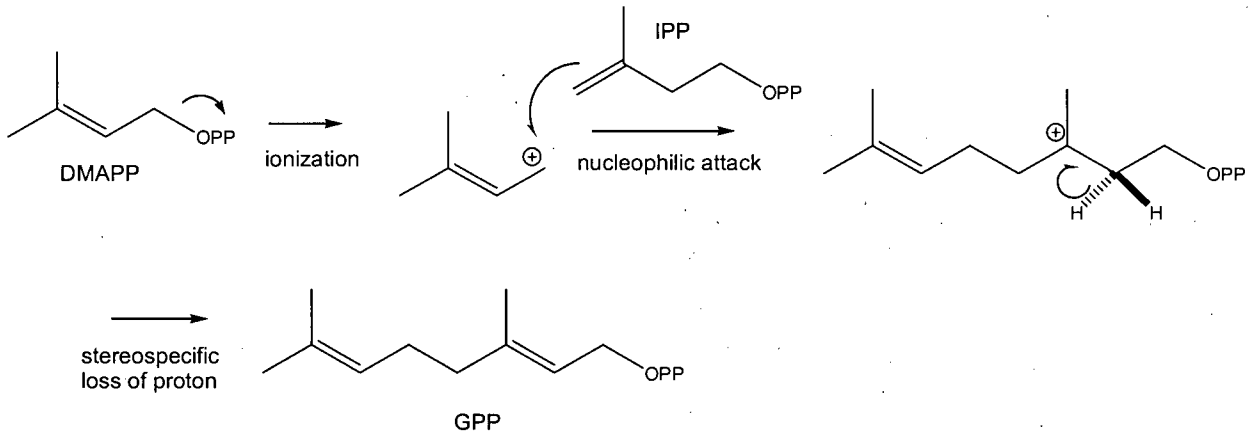

Figure 1.4 General scheme – prenyltransferase reaction. The reaction is initiated by elimination of the pyrophosphate group from DMAPP yielding a carbocation at C1. Nucleophilic attack of IPP on the carbocation yields a new C-C bond. Stereospecific deprotonation at C2 yields a new allylic pyrophosphate that is available for addition of another IPP.

1.2.6 Terpene synthase

After production of linear universal precursor prenyl pyrophosphates (GPP, FPP, GGPP, and GFPP), terpene production reaches a second flux point catalyzed by the terpene synthases. These enzymes determine the subclass of terpene formed. The reaction mechanism of both chain elongation and cyclization involve similar steps, which has led to speculation that both enzymes share a common ancestor (52). Both share conserved catalytic residues in primary sequence analysis as well as overall structural similarity. However, the diversity in the type and mechanistic complexity of the synthases far outweighs the relatively conserved transferases.

In the cyclization of C-10 monoterpenes and C-15 sesquiterpenes, catalysis is similar to the prenyltransferase reaction in that it begins with a carbocation formation through cleavage of the pyrophosphate. This is followed by intramolecular attack of the prenyl chain at C1 to yield a cyclic carbocation intermediate. After cyclization, rearrangement and modification of the ring

structure may occur, including internal additions involving the remaining double bonds to generate additional rings, hydride shifts, methyl migrations and Wagner-Meerwein rearrangements before water capture or deprotonation (as reviewed in (13)). In some cases a single synthase may produce more than one product, as seen below with abietadiene synthase.

1.2.7 Diterpene cyclization

The major routes of diterpene cyclization are, macrocyclic leading to the taxane (see Fig. 1.7 pg. 13) and casbene skeletal structures, or cyclization via a copalyl diphosphate intermediate (see Fig. 1.5) leading to tricyclic kaurene (see Fig. 1.9 pg. 20) and abietadiene structures (Fig. 1.5). The latter cyclization reaction has two key intermediates, the A/B ring closure to form the copalyl diphosphate intermediate and C ring closure to yield a pimaradiene intermediate. A/B ring closure is initiated by protonation of the terminal C20 double bond, followed by internal additions and proton eliminations to (-)-copalyl pyrophosphate in the case of kaurene and (+)-copalyl pyrophosphate with abietadiene. A common mechanism of A/B ring closure in tricyclic diterpenoid formation leads to a common A/B ring structure. C ring closure is similar to the cyclization reaction of the monoterpene and sesquiterpenes in that it is initiated by carbocation formation through pyrophosphate cleavage. Intramolecular proton shift, a 1,2 methyl migration and deprotonation complete the reaction and lead to the final product. It has been determined that this second step in catalysis may result in multiple product formations, as seen in abietadiene cyclization. In kaurene synthesis, two enzymes catalyze the two steps, whereas in abietadiene synthesis a single enzyme catalyzes both steps (70). There is evidence that the single abietadiene synthase has two active sites, one for formation of the copalyl intermediates and the second for C ring closure and other structural modifications (70).

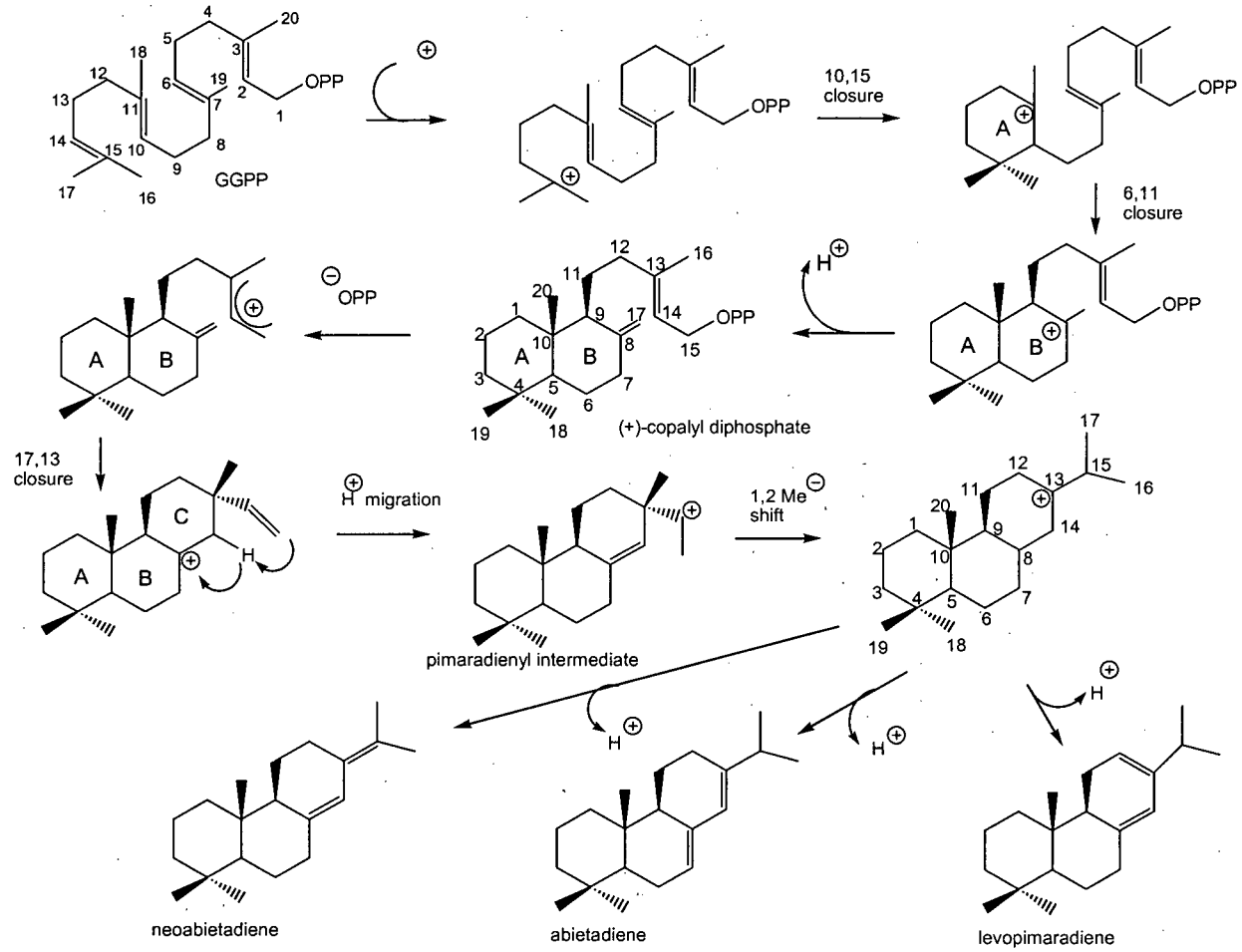

Figure 1.5 Abietane diterpenoid cyclization reactions. Protonation of GGPP's terminal double bond yields a carbocation at C15. Internal addition of C15 carbocation to C10 yields the A ring and a C11 carbocation. Internal addition of C11 carbocation to C6 yields the B ring and a C8 carbocation. Deprotonation at the C8 carbocation yields (+)-copalyl diphosphate. Elimination of pyrophosphate via C-O bond cleavage yields a charged delocalized carbocation at C13-C15. Internal addition of C13 carbocation to C17 yields the C ring and a carbocation at C8. An intramolecular proton shift from C15 to C17 yields the pimaradienyl intermediate. A 1,2 methyl shift from C13 to C14 yields a carbocation at C13. Finally, deprotonation yields one of several tricyclic products. Adapted from (13)

The enzyme catalyzing the cyclization of geranylgeranyl pyrophosphate to abietadiene, the precursor of abietic acid in *A. grandis*, has been purified and the gene encoding it has been cloned and expressed in *Escherichia coli* (47, 84). The proposed pathway for abietadiene formation proceeds via (+)-copalyl pyrophosphate and pimaradiene intermediates (70) (Fig. 1.5). An abietadiene synthase in vitro activity assay yielded 3 major products (abietadiene, levopimaradiene, and neoabietadiene) and 3 minor products (pimaradiene, sandaracopimaradiene

and palustradiene). These 6 products constitute the skeletal precursors of all resin acids produced in *A. grandis* (70).

1.2.8 Oxidative formation of acidic abietane diterpenoids

Sequential oxidation of the C18 methyl group by two cytochromes P450 and an aldehyde dehydrogenase are proposed to lead to the carboxylic functional group on C18 of diterpenes in *A. grandis* (27) (Fig. 1.6). Recently, a methyl jasmonate-induced cytochrome P450 (CYP720B1)

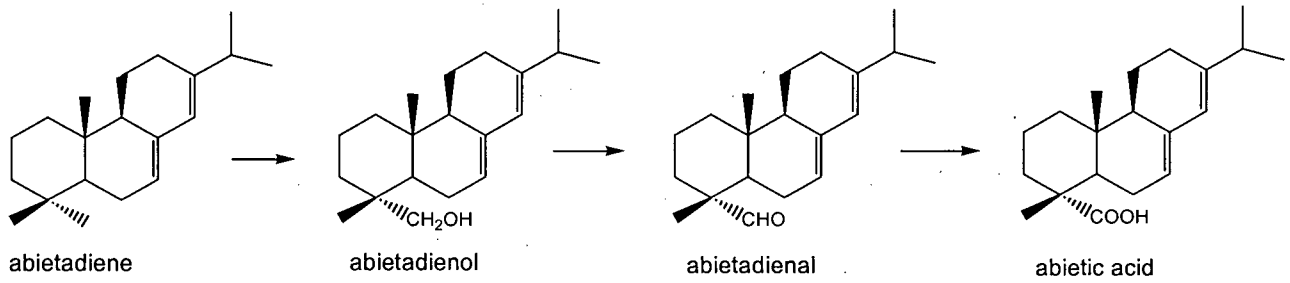

Figure 1.6 . Consecutive oxidation of abietadiene to abietic acid. Oxidation of abietadiene at C18 yields abietadienol. Oxidation of abietadienol at C18 yields abietadienal. Oxidation of abietadienal at C18 yields abietic acid.

from Loblolly pine (*Pinus taeda*) was cloned, sequenced and characterized (71). In vitro, CYP720B1 was found to catalyze consecutive C18 oxidations of diterpene alcohols and aldehydes. When expressed in yeast, this single P450 could completely oxidize C18 abietadiene to abietic acid but with lower activity than seen for transformations of the alcohol or aldehyde (71). The authors suggested that an additional P450 might be required for the first oxidative step.

In summary, production of a wide array of acidic diterpenoids from IPP and DMAPP subunits in several conifers requires a total of only five enzymes. GGPP prenyltransferase synthesizes a 20-C linear diterpenoid, and abietadiene synthase catalyzes cyclization and skeletal rearrangements to produce of a variety of diterpene structures. Finally, 1 or 2 cytochromes P450 and in some conifers, an aldehyde dehydrogenase catalyze oxidations to yield the carboxylic functional group.

1.3 Terpenoid significance

1.3.1 Plant defense and growth

A number of plant and fungal terpene products are used for plant defense or stimulation of plant growth. It has been proposed that the large number of terpenes may be the result of evolutionary development of plant defense against insect attack, or signaling to enhance growth (38). Gibberellins are a family of tetracyclic diterpenoid carboxylic acids produced in plants and fungi by transformations of *ent*-kaurene that act to stimulate plant growth (81) (see Fig. 1.9). The genes required for synthesis of various gibberellins from *ent*-kaurene have been sequenced and characterized. The microbial metabolism of *ent*-kaurene is discussed below.

Both monoterpenes and diterpenes play a role in plant defence against attacks from herbivores and pathogens (50). Fungal inoculation or wounding resulted in the production of terpenoids in Maritime pine (*Pinus pinaster*) (10). Mechanical wounding or insect attack of *A. grandis* stems leads to an induction of enzymes required for synthesis of resin components (28). In addition to the induced terpene synthesis some plant species performed terpenes, which are stored in specialized structures such as resin ducts in *Pinus contorta* (Lodgepole pine) or resin blisters in *A. grandis*.

Terpene production is induced by methyl jasmonate in Norway spruce stems (56). Both monoterpene and diterpene synthases are induced following wounding with a peak in production at 10 days post wounding. The simultaneous production of both monoterpenes and diterpenes is consistent with their combined role in plant defence. The volatile monoterpenes solubilize and facilitate mobilization of the lipophilic diterpenes for transfer to the point of attack. Here, following volatilization of the monoterpenes, the diterpenes can then crystallize to form a protective barrier that seals the plant off from further damage. Meanwhile the volatile monoterpenes are potentially toxic to invading plant pathogens.

1.3.2 Acidic diterpenoids as pollutants in pulp and paper production

Usually when one thinks of natural products from trees, the first thought that comes to mind is not pollution. However, during pulp and paper making, resin acids including abietane diterpenes are extracted from wood and discharged in wastewater at concentrations far above those occurring naturally (2, 54). Research on the microbial removal of these compounds from wastewater treatment systems has been the driving force behind investigations of the degradation of resin acids. Removal of resin acids from the wastewater is necessary before it is discharged into receiving water because of the acute toxicity of resin acids to fish (2). Additionally, resin acids are a major component of pitch. Pitch is formed during pulp and paper making by lipophilic wood extracts which coalesce to form droplets. Pitch deposits lower pulp quality and interfere with the operation of papermaking equipment. Accumulation of pitch in the papermaking water limits re-use of that water, which otherwise would reduce the environmental impact of papermaking (32). The resin acids from pulp and paper production are usually removed in biotreatment systems. Several resin acid degrading microorganisms isolated from pulp and paper mill biological treatment systems have been characterized (6, 54, 60, 62-65).

1.3.3 Medicinal significance

Greater than half of chemotherapeutic drugs for cancer treatment and infectious disease are of natural origin (67). Terpenoids are the largest class of natural products and comprise a significant portion of treatments in use today.

1.3.3.1 Monoterpenoids – limonene and perillyl alcohol

Limonene is one of the most abundant monoterpenes found in nature (Fig. 1.7). It is the major component of peel oil from oranges, citrus, and lemons, and is the oil of caraway. Monoterpenoids are C-10 isoprene compounds that differ from other classes of terpenoids in

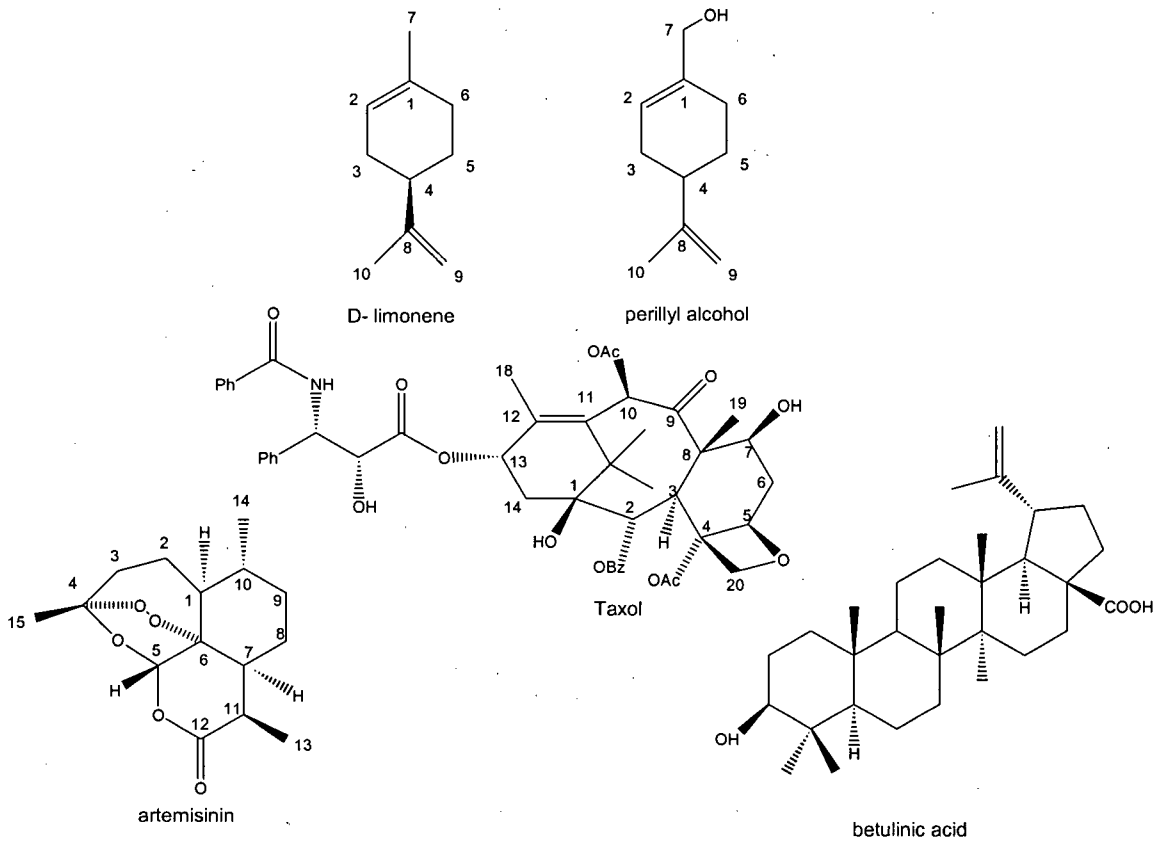

Figure 1.7 Medically significant terpenoids. D-limonene and perillyl alcohol are monoterpenoids currently being studied for their potential use as chemotherapeutic agents. Artemisinin is a sesquiterpenoid with antimalarial activity. Taxol is a taxane diterpenoid with potent chemotherapeutic activity (Ph, phenyl; Ac, acetate; Bz, benzoate). Betulinic acid is a triterpenoid currently under investigation for use in prevention and treatment of HIV infection and cancer.

their volatility and aromaticity. Much of the work on monoterpenoids in the past has been focused on the development of flavours and fragrances related to the food and cosmetic industry. Recently, additional interest has centred on these compounds as chemotherapy agents against tumors (88). Limonene and its hydroxylated derivative perillyl alcohol, respectively, are undergoing Phase 1 and Phase II clinical testing of their chemotherapeutic activity (88). The proposed mechanisms of action against tumors are (a) the interference of protein prenylation of key regulatory proteins including RAS (29) or (b) induction of apoptosis (3).

1.3.3.2 Sesquiterpenoids - artemisinin

Multiple drug resistance of *Plasmodium falciparum* has led to the necessity for development of alternative forms of treatment against malaria (87, 88). Artemisinin is a potent antimalarial extract of sweet wormwood (*Artemisia annua*), which has been used in traditional Chinese medicine for centuries under the name Qinghaosu (Fig. 1.7). It is a sesquiterpene lactone with an endoperoxide trioxane ring structure, which is required for medicinal activity. It is postulated to act through the proliferation of free radicals (61), or more likely through inhibition of the parasite's calcium ATPase (18).

1.3.3.3 Diterpenoids – Taxol and others

AbA and its derivatives have recently been evaluated for their ability to function as inhibitors of fungi (20), tumors, mutagenesis, viruses, nitric oxide production (30, 44), inflammation, (22) and lipoxygenase activity (82). A recent increase in the interest in natural products isolated from marine organisms has led to the discovery of a wide range of novel diterpenoids. These novel products could potentially lead to the development of new medicinal applications (4, 33).

One of the most widely recognized diterpenoids in pharmaceutical applications today is Taxol (Fig. 1.7). This taxane diterpenoid extracted from the bark of Pacific Yew (*Taxus brevifolia*) has proven to be a potent chemotherapeutic agent. Taxol acts by stabilizing microtubules, which in turn hinders the rearrangement of microtubule networks required for mitosis and cell proliferation (88). Extraction of Taxol from its natural source is not practical in quantities required for widespread clinical use. At present, research is underway to better understand the synthesis of Taxol in Yew to enhance cell culture and semisynthetic means of production (41, 42).

1.3.3.4 Triterpenoids - betulinic acid

Betulinic acid is a pentacyclic lupane-type triterpenoid found in several plant species, including the birch tree (*Betula* spp. Betulaceae) (11). Recently, much of the focus on betulinic acid and its derivatives has centered on prevention and treatment of HIV infection and cancer. In HIV infection treatment a betulinic acid derivative was found to disrupt the cellular entry of HIV-1, while in cancer treatment it was found to induce apoptosis (11).

1.3.3.5 Obstacles in the production of terpene pharmaceuticals

Significant obstacles exist in our ability to extract large quantities of potentially beneficial terpenoids from their natural sources. Complications include multiple biosynthetic pathways in plants resulting in a mixture of products, and low product concentrations and product yields (88). For example, extraction of 1 kg of Taxol required 6.7 t of *Taxus* bark, which is roughly equivalent to 2000-3000 trees (as reviewed in (40)). Cell culture, aquaculture, semi, and total synthesis are being investigated as means to circumvent some of the issues related to production of terpenoids. Metabolic engineering is also a viable option.

1.3.3.6 Metabolic engineering

Recently, Martin et al. (59) reported the synthesis of amorphadiene in *E. coli*. Amorphadiene is a cyclic sesquiterpene that is a precursor in the synthesis of artemisinin. As mentioned above, artemisinins are potent antimalarial drugs produced naturally in sweet wormwood. Extraction of this natural product is costly and therefore prohibitive to treatment of large human populations. Therefore a cost-effective means of production is currently under investigation. A significant advancement toward this goal was achieved by the expression of the mevalonate pathway for IPP production in *E. coli* (59). By using the mevalonate pathway for IPP production as opposed to *E. coli*'s DXP pathway, it was possible to circumvent regulatory controls of IPP production in *E. coli* and produce large quantities of the terpenoid precursor.

Another example of metabolic engineering for terpene production is perillyl alcohol. Van Beilen et al. (83) screened 1800 bacterial strains for the ability to transform limonene to perillyl alcohol. *Mycobacterium* sp. HXB–1500 expressing cytochrome P450 (CYP 153 family) had the most promising transformation activity. The P450 system from HXB-1500, including a ferredoxin and ferredoxin reductase, was expressed in *Pseudomonas putida* (83). This strain was able to convert 3 μmol of limonene to perillyl alcohol per minute per gram of cells (dry weight).

1.4 Cytochromes P450 in terpenoid metabolism

1.4.1 P450 heme-thiolate proteins

Cytochromes P450 are heme-thiolate proteins present in all domains of life, which catalyze a wide variety of oxygenation reactions. During terpene synthesis, many of the post cyclization reactions required for production of active terpenoid compounds are catalyzed by P450s, as seen above in the synthesis of diterpene resin acids (71). P450s produce regiospecifically and stereospecifically modified terpene products (36). Understanding the role of these enzymes is of interest in the metabolic engineering of pharmaceuticals and the metabolism of xenobiotics. As cytochromes P450 form a significant portion of the findings of this dissertation, the following section will briefly consider this extremely interesting enzyme group.

1.4.2 Classification of P450s

P450-dependent oxygenation systems can be classified into four groups depending on the number of proteins involved in electron transfer from reduced nicotinamide adenine dinucleotide (NADH) or reduced nicotinamide adenine dinucleotide phosphate (NADPH) (26). Type I systems have 3 proteins including a reductase - containing either flavin adenine dinucleotide (FAD) or flavin adenine mononucleotide (FMN), a ferredoxin, and the catalytic P450 subunit. This is the most common scheme found in prokaryotes and mitochondria. Type II systems

involve 2 proteins; an NAD(P)H reductase and a catalytic subunit. The reductase component contains both an FAD and FMN. Electrons are transferred from FAD to FMN and then to the catalytic P450 component. Type II enzymes are found in the endoplasmic reticulum of higher animals and most other eukaryotic cells. Type III systems are composed of a single protein, which contains both a reductase and a catalytic domain. This protein contains an FAD, FMN and heme group associated with a P450 and requires NADPH as an electron donor. Type III enzymes were first reported in *Bacillus megaterium* (P450 BM-3) (66) and then later found in *Fusarium oxysporum* ($P450_{foxy}$) (45).

Recently Roberts et al. (72) identified a new class of cytochrome P450 from the genus *Rhodococcus*. In these type IV systems, electron transport is mediated through a dioxygenase-reductase-like activity. Electrons are transferred from NADH to the P450 active site via an FMN centre and a 2Fe2S ferredoxin-like component. As in Type III P450s, the electron transport proteins are linked to the Type IV P450 in one polypeptide. Heterologous expression of Type IV P450, P450Rhf, in *E. coli* produced the expected 85-kilodalton protein. Although the natural function of this P450 is unknown, it was able to mediate the O-dealkylation of 7-ethoxycoumarin. Additional Type IV cytochromes P450 have been identified in the recently sequenced genome of *Rhodococcus* sp. RHA1 (86), however the proteins and not fused suggesting a type V classification. A Basic Local Alignment Search Tool (BLAST) search of the National Center for Biotechnology Information (NCBI) non-redundant database using the P450RhF sequence identified several putative Type IV P450s from the genus *Burkholderia*.

1.4.3 General mechanism

Much of our knowledge of the structure and mechanism of P450s has been determined by work on $P450_{cam}$ (CYP101). This enzyme, isolated from *P. putida*, stereospecifically hydroxylates the monoterpene camphor to 5-exo-hydroxy camphor. The general mechanism of

oxygen activation is described as follows (15, 31, 51) (Fig. 1.8). In the resting state, the heme

335 ferric iron is hexacoordinated by the conserved cysteine residue of the heme-binding pocket, the

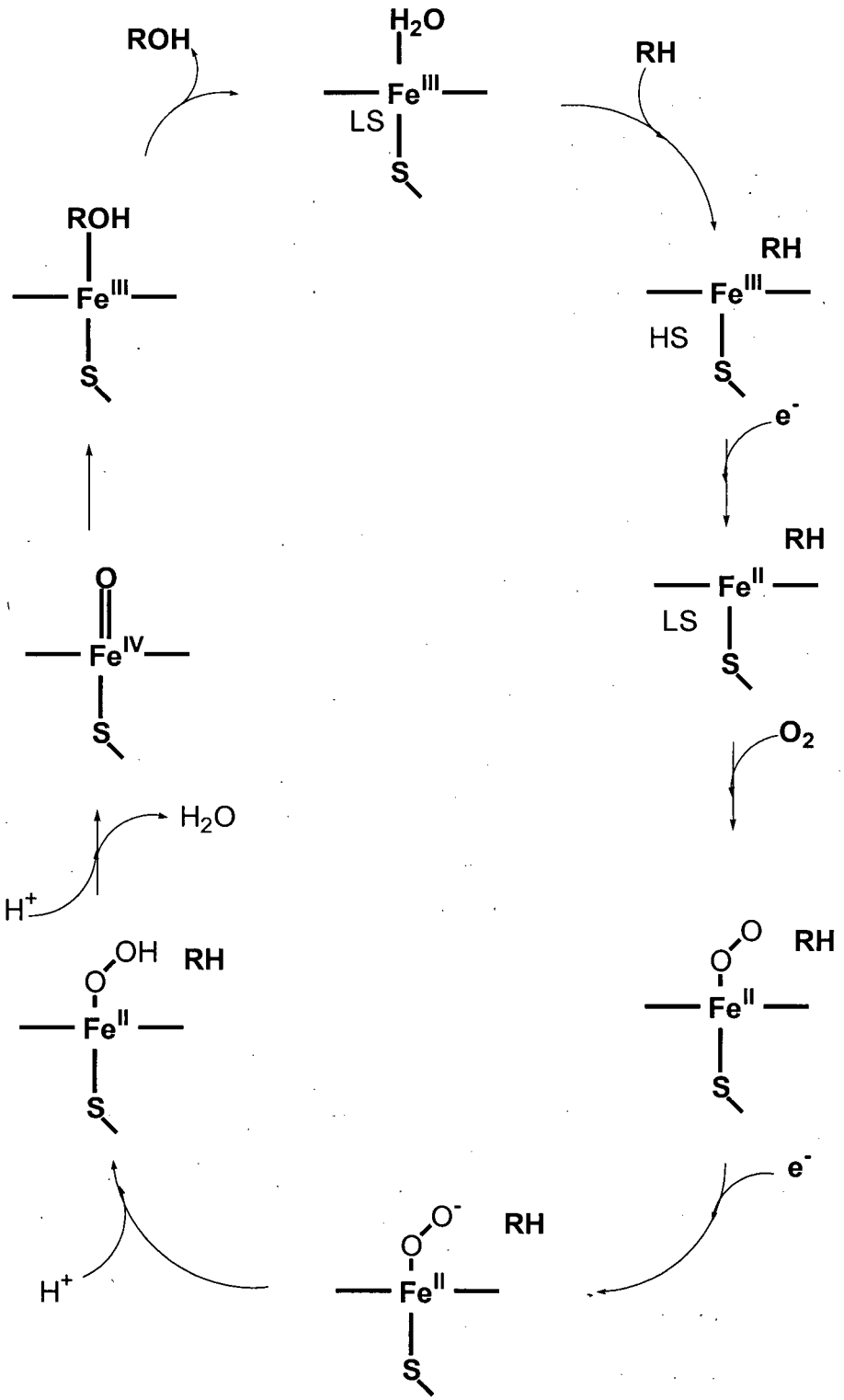

Figure 1.8 General mechanism of P450 catalytic cycle. RH – substrate, ROH – hydroxylated product, LS-low spin iron, HS- high spin iron. Adapted from (51) and (15).

4 nitrogens of the heme pyrrole rings, and a distal water molecule. Binding of the substrate, in most cases, leads to the displacement of the iron-bound water which in turn changes the spin state of the heme iron. This change of spin increases the reduction potential of the heme iron, facilitating the first electron transfer from NAD(P)H leading to ferrous iron. The production of ferrous iron facilitates dioxygen binding generating an Fe^{II}-O_2 complex followed by a second electron transfer generating Fe^{II}-O_2^-. Protonation of the distal oxygen with heterolytic cleavage of O-O bond leads to water formation and Fe^{IV}=O. This high valent complex drives most of the P450 reactions (31). In a typical hydroxylation reaction, the high valent complex abstracts a hydrogen atom from an unactivated C atom of the substrate followed by rebound and transfer of oxygen to bound substrate and dissociation of product regenerating the ferric heme iron.

1.4.4 P450s in diterpenoid metabolism

As mentioned above, P450s are required for post-synthase modification of terpenes to functional compounds. This is well documented in the production of gibberellins from the diterpenoid *ent*-kaurene (81) (Fig. 1.9). A cluster of genes in *Gibberlla fujikuroi* encodes 4 cytochromes P450 designated P450-1 through P450-4. P450-4 is required for carboxylic acid formation. Three consecutive oxidations by P450-4 of the diterpenoid *ent*-kaurene at C19 proceed from an alcohol, to an aldehyde, and finally to *ent*-kaurenoic acid (Fig. 1.7). This is similar to the transformation of abietadiene to abietic acid in Loblolly pine discussed above.

P450-1 is required for several oxidation steps in the production of gibberellins in *G. fujikuroi,* including a 7-alpha-OH (Fig. 1.9). Rojas et al. (75) characterized the C7 α hydroxylation reaction of *ent*-kaurenoic acid by P450-1 through gene knockout and expression of *P450-1* in a fungal strain lacking several gibberellin genes. *P450-1* mutant strains failed to transform *ent*-kaurenoic acid to *ent*-7α-hydroxykaurenoic acid. The *ent*-7-α-hydroxykaurenoic

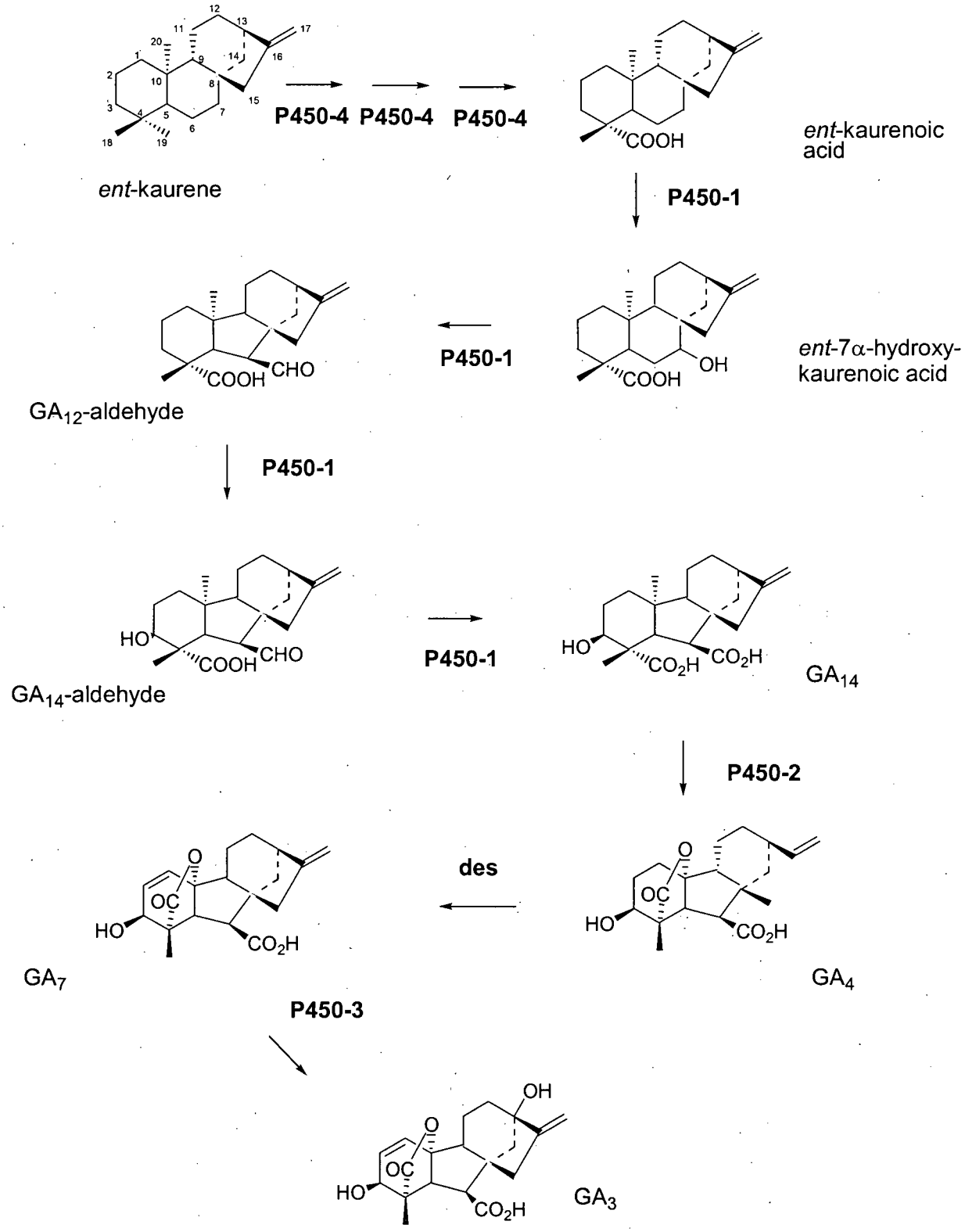

Figure 1.9 Main route of gibberellin biosynthesis of gibberellins in *Gibberlla fujikuroi*. Des – desaturase, GA- gibberellin, Adapted from (81)

acid product is a precursor of B ring contraction, an essential step in gibberellin synthesis. The enzyme was also found to catalyze 3C β hydroxylation. In fact, this single P450 was found to be involved in oxidations at four different carbon atoms on the tetracyclic compounds. (C3, C6, C7, C18). This allows for the production of several types of gibberellins, which in turn increases the range of plants these compounds can affect during fungal infection. Given that the enzyme contains a single heme and substrate binding requires a specific orientation of substrate proximal to the heme iron, subsequent hydroxylations must require flexibility in substrate binding to accommodate variable substrates. In their discussion, the authors give some possibilities including shifts in substrate binding brought about by subsequent hydroxylation reactions (75).

1.5 Biotransformation of terpenoids

Cytochromes P450 play a key role in the metabolism of xenobiotics in mammals. Much of the research on microbial metabolism of terpenes focuses on creating mammalian models of metabolism (76). This research aims to predict metabolites that are produced in mammalian systems and then produce large enough quantities of these metabolites for further study. Fungal biotransformation experiments are most often used because of the similarities between cytochrome P450 systems in fungi and mammals. Typically these fungal transformations are limited and the organisms do not mineralize the substrates. Such partial transformation suggests that the reactions may be fortuitous or cometabolic. In these types of investigations little attention is given to the genetics or enzymology behind the transformations occurring in the microbes. These reports therefore are not very informative regarding the mineralization of growth substrates by bacterial systems. However, by considering the results of this type of work it is possible to gain insight into reactions that may initiate metabolism and identify susceptible carbon positions on the substrate. Table 1.1 contains a selection of the microbial metabolism of cyclic diterpene compounds illustrating the general range of activities reported. For a review of these transformations see (34).

1.5.1 Isosteviol

Stevioside, a natural non-caloric sweetener extracted from the leaves of *Stevia rebaudiana,* is reported to be 250-300x sweeter than sucrose (35). It is presently used in many parts of Asia and South America as a substitute sweetener. Isosteviol (Table 1.1) is a beyerane diterpene produced from the acid hydrolysis of the 3 glucose side chains of stevioside. Isosteviol and its derivatives have several reported bioactive properties including antibacterial activity (53), inhibitory effects on Epstein Barr Virus activation (1) and DNA polymerase and DNA topoisomerase inhibitors. In an effort to increase the bioactivity of isosteviol compounds, de Oliveira et al. (14) examined transformation of isosteviol by *Aspergillus niger, Penicillium chrysogenum* and *Rhizopus arrhizus.* Transformation of this beyerane diterpenoid resulted in the production of 3 identified products, two monohydroxylated products (at C7 and C17) and one dihydroxylated product (C1 and C7).

1.5.2 Kaurene/pimerane diterpenoids

9-*epi-ent* Pimaradiene diterpenes resemble AbA's B ring structure, with a C7,8 double bond (24) (Table 1.1). Biotransformation of 2α, 19-dihydroxy-9-*epi-ent*-pimara-7,15-diene by *G. fujikuroi* resulted in the accumulation of more than 7 compounds. Three compounds contained a 7,8 epoxide, 2 were C7-keto and 2 were C7-hydroxylated. The main reaction with this substrate was the alpha epoxidation of the 7,8 double bond. It was suggested that the epoxide was subsequently converted to the 7-keto compound. Similar results were found for biotransformation of 18-hydroxy-9-*epi-ent*-pimara -7,15-diene, and 18-hydroxy-9,13-epi-*ent*-pimara-7-15-diene by *G. fujikuroi* (23, 25). Fraga et al. suggested that the 7,8 epoxide rearranged to the 7-ketone or the allylic alcohol 7-hydroxy by opening of the oxirane ring.

410

Table 1.1 Biotransformation of selected diterpenoids

Name & Structure	Microbe(s)	Transformation(s)	Reference
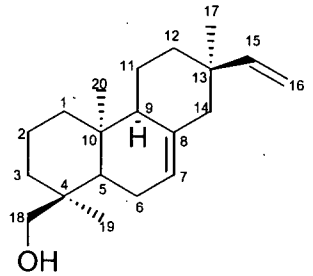 18-hydroxy-9,13-*epi*-*ent*-pimara-7,15-diene	*Gibberella fujikuroi*	-Epoxidation of 7,8 double bond (main product) -Rearrangement of 7,8 epoxy to 7-hydroxy or 7-keto derivative -Other hydroxylations	(23)
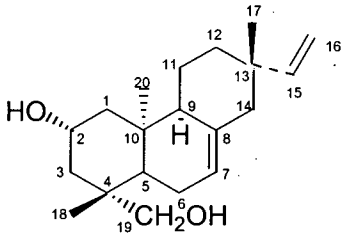 2a,19-dihydroxy-9-*epi*-*ent*-pimara-7,15-diene	*Gibberella fujikuroi*	- -Epoxidation of 7,8 double bond (main product) -Rearrangement of 7,8 epoxy to 7-hydroxy or 7-keto derivative -Other hydroxylations	(24)
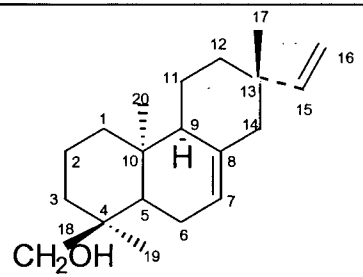 18-hydroxy-9-*epi*-*ent*-pimara-7,15-diene	*Gibberella fujikuroi*	-Epoxidation of 7,8 double bond (main product) -Rearrangement of 7,8 epoxy to 7-hydroxy or 7-keto derivative -Other hydroxylations	(25)

Name & Structure	Microbe(s)	Transformation(s)	Reference
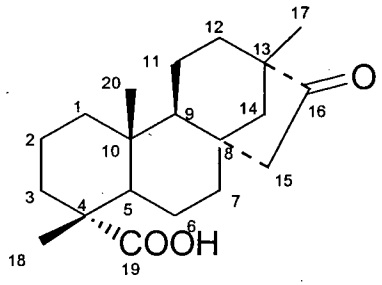 isosteviol	*Aspergillus niger* *Penicillium chrysogenum* *Rhizopus arrhizus*	C12, C17, C1, C7 hydroxylation	(14)
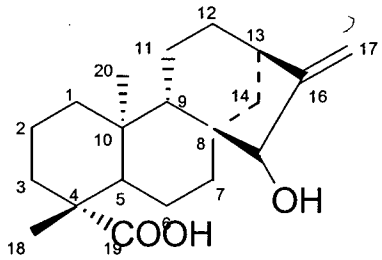 15a-hydroxy-*ent*-kaurenoic acid	*Gibberella fujikuroi*	C7 hydroxylation	(5)
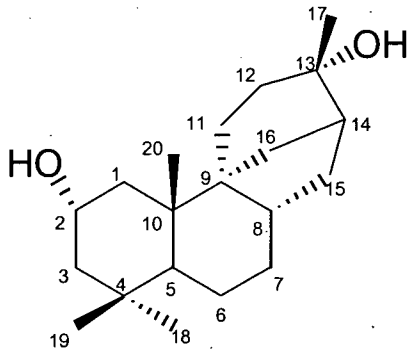 stemodin	*Rhizopus arrhizus*	C7, C14, C16, C17, C18, C19 hydroxylation	(39)

Name and Structure	Microbe(s)	Transformations	Reference
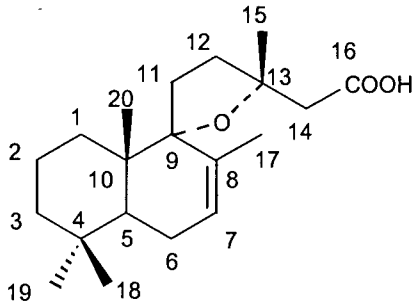 grindelic acid	*Aspergillus niger* *Penicillium brevi-compactum*	Major product was 3β-hydroxy derivative Minor products include 3-ketone, 18-alcohol, and 7α,8α-epoxide	(37),(69)
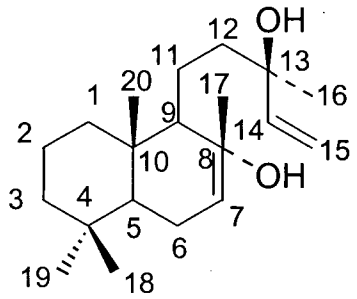 sclareol	*Septomyxa affinis* *Cunningham-ella* sp.	3β-alcohol, 3-ketone, 2α-alcohol, 18-alcohol	(34, 46)

1.5.3 Abietane diterpenoids

Several strains capable of growth on abietane or pimerane diterpenoids have been described as mentioned above. Few studies, however, have focused on the mechanism of mineralization of these compounds. What is known regarding the catabolism of abietane diterpenoids was recently reviewed (54, 60). Early reports of the microbial degradation of abietane diterpenoids (as reviewed in (43)) focused on the identification of metabolites, which accumulated during growth in typical salt media, in cation deficient media, or in the presence of the metabolic inhibitor, bipyridyl. *Flavobacterium resinovorum*, isolated from the soil of a *Pinus maritima* forest, was found to grow on the non-volatile components of pine oleoresin as a sole source of carbon and electrons. During growth on DhA, Biellmann and Wennig (9) identified a single metabolite extracted from the growth medium, the 3-oxo, decarboxylated derivative of DhA (Fig. 1.10, III). This compound was not expected as degradation was thought to begin at the aromatic ring. Growth of *F. resinovorum* on DhA using metabolic inhibitors (alpha, alpha'-dipyridyl) or in cation deficient media resulted in slower growth allowing for identification of additional metabolites including, VI the diphenol, diketone, decarboxylated derivative of DhA (7). From the identification of additional metabolites they proposed a degradation pathway for DhA by *F. resinovorum* (Fig. 1.10 B).

The same group used similar methods to investigate the degradation of DhA by *Pseudomonas* sp. and *Alcaligenes* sp. (8). Both strains were isolated by aerobic enrichment on DhA. Unlike metabolites found with *F. resinovorum*, only 7-oxo-DhA was isolated and not the 3-oxo derivatives. As before, based on isolated metabolites they proposed a degradation pathway, which differs from the *F. resinovorum* in that no C3 oxidation or decarboxylation occurs in the initial steps (Fig. 1.10 C).

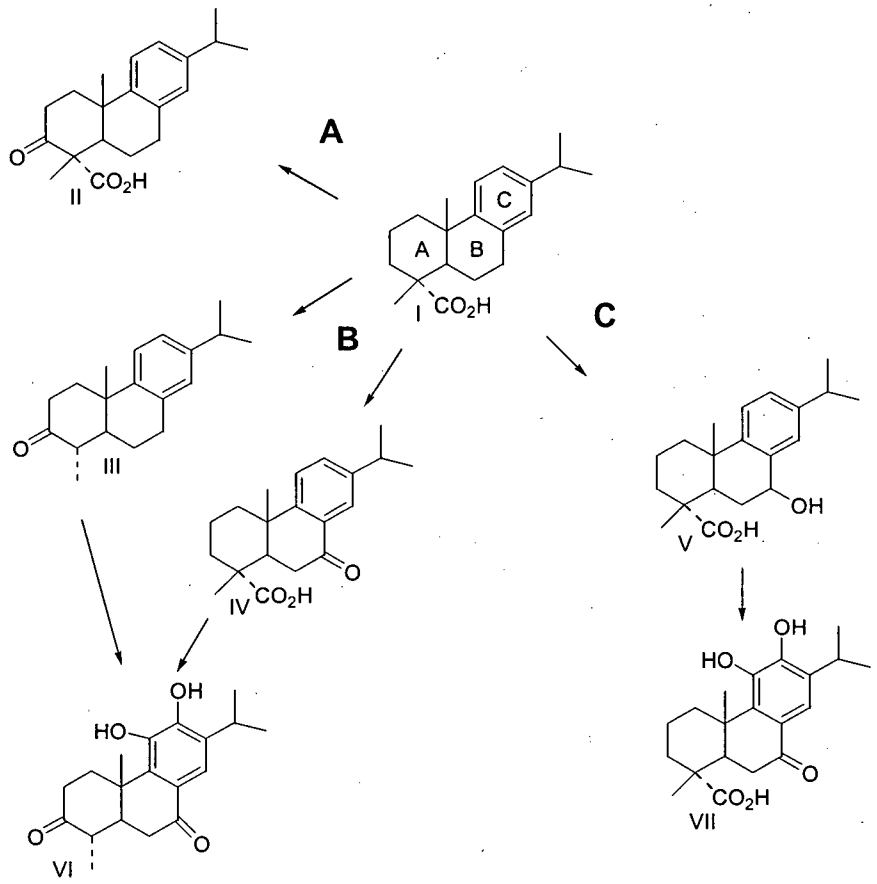

Figure 1.10 Initial steps in the proposed degradation pathway of DhA by A. *Arthrobacter* sp., B. *F. resinovorum* and C. *Alcaligenes* sp. and *Pseudomonas* sp. I, dehydroabietic acid; II, 3-oxo-dehydroabietic acid III, 2-oxo-dehydroabietin; IV, 7-oxo-dehydroabietic acid; V, 7-hydroxy-dehydroabietic acid; VI, 5,6-dihydroxy-2,9-dioxo-dehydroabietin; VII, 11,12-dihydroxy-7-oxo-dehydroabietic acid.

Additionally, Levinson and Carter (49) reported an *Arthrobacter* sp. isolated from Lodgepole pine which when incubated with methyl dehydroabietate produced 3-oxo-DhA without identification of any 7-oxo-DhA. They also tentatively reported an A ring degradation product of DhA with an intact B and C ring. This collection of early work indicated 3 possible degradation pathways for DhA degradation, one via 3-oxo-DhA, a second via 7-oxo-DhA and a third combining both 3 and 7-oxo-DhA derivatives.

As mentioned above, biodegradation of abietane diterpenoids in pulp and paper mill effluent has been a driving force behind research into the microbial metabolism of terpenes. Recently, molecular investigations have focused on a bacterium isolated from bleach kraft pulp

mill effluent, *Pseudomonas abietaniphila* BKME-9, that mineralizes and grows on the abietane diterpenoids, AbA, DhA, PaA, and 7-oxo-DhA as its sole organic substrates (6). The *dit* gene cluster of BKME-9 encodes enzymes required for the catabolism of these compounds (57, 58). Several genes of the *dit* cluster were sequenced and characterized, and a convergent pathway for abietane diterpenoid metabolism was proposed (Fig. 1.11). Evidence for a convergent pathway for AbA, DhA and PaA catabolism came from studies of a *ditA1* knockout mutant (57). DitA ring hydroxylating dioxygenase catalyzes the formation of a catecholic intermediate in the proposed pathway (58). 7-Oxo-DhA accumulated in cell suspensions of the *ditA1* mutant strain incubated with AbA or DhA, while DhA and 7-oxo-DhA accumulated in cell suspensions incubated with PaA. The aromatisation of the C ring of both AbA and PaA suggested a convergent pathway with DhA serving as an intermediate.

The initial steps in the biodegradation pathway have not been elucidated, but some evidence suggests that a P450 monooxygenase is involved. A putative P450, encoded by *tdtD* that may function in abietane diterpenoid degradation, was recently identified in *Pseudomonas diterpeniphila* A19-6a, another resin acid-degrading bacterium closely related to BKME-9 (64, 65). Morgan and Wyndham (64) reported that a *tdtD* knockout mutant of A19-6a was retarded in its removal of DhA or AbA from its growth medium when compared to that of the wild type. The mutant retained the ability to grow on DhA and AbA as sole organic substrates; however, any effects of the mutation on growth rates were not reported. These results suggest involvement of the *tdtD* gene in diterpenoid metabolism but give no conclusive evidence for a functional P450 gene product or the role of such an enzyme in resin acid metabolism. Morgan and Wyndham also provided evidence for a homologue of the *tdtD* gene in BKME-9 but were unable to conclude whether this gene was linked to the previously described *dit* cluster.

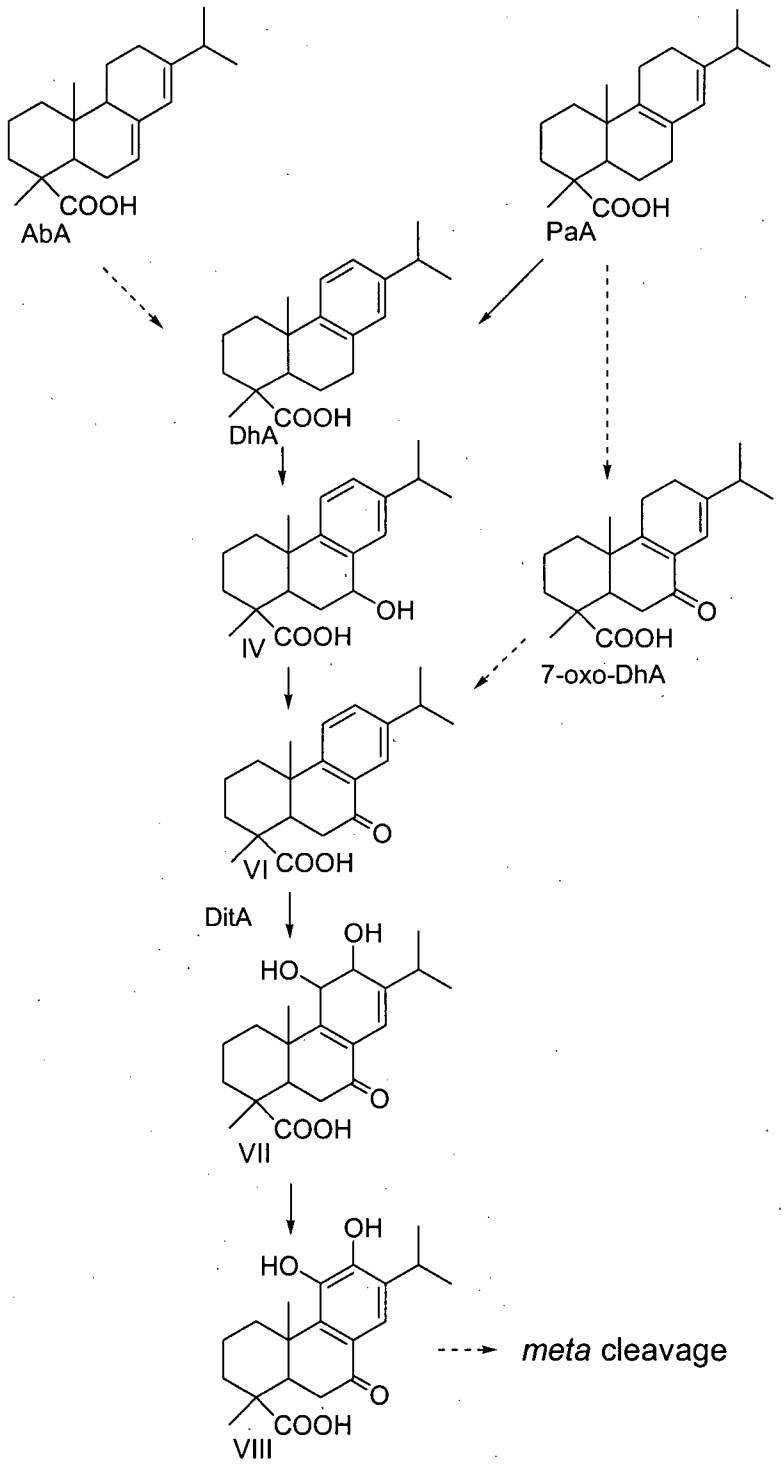

475

Figure 1.11 Proposed convergent pathway for abietane diterpenoid degradation pathway by *Pseudomonas abietaniphila* BKME-9. Adapted from (57) Chemical Designations AbA, abietic acid; PaA, palustric acid; DhA, dehydroabietic acid, IV, 7-hydroxy-dehydroabietic acid; V, 7-oxo palustric acid; 7-oxo-DhA, 7-oxo-dehydroabietic acid; VII, 7-oxo-11, 12-dihydroxy-
480 8,13-abietadien acid; VII, 7-oxo-11,12-dihydroxydehydroabietic acid.

Little is known about the anaerobic degradation of abietane diterpenoids (60). A pathway for the anaerobic metabolism of DhA has been proposed using results obtained from experiments with deuterium labelled DhA. Deuterium labelled DhA was incubated in sediment collected downstream of a pulp and paper mill and compared to DhA transformation in autoclaved sediment under the same conditions (79, 80). The main intermediates in the pathway are decarboxylated and aromatized products with intact tricyclic abietane structures. After 264 days of incubation, d-tetrahydroretene (10-d-1-methyl-7- methylethyl-1,2,3,4-tetrahydrophenanthrene) was found to be the major product. A small amount of retene (7-isopropyl-1-methylphenantrene) was also observed. Retene has also been identified in sediment particles in lakes receiving pulp and paper mill effluent (48).

1.6 Summary

Terpenoids are ubiquitous and play a variety of critical roles in biology. Not only do they constitute an important part of the carbon cycle, they also raise concerns in pollution control, and have potential benefits as pharmaceutical agents. This introduction has presented several elements of the abietane diterpenoid carbon cycle. Synthesis of a wide variety of compounds from a simple 5-carbon "building block", utilizing relatively few enzymes, leads to common structural intermediates while additional enzymes are used for modification to produce functional compounds.

While much attention has been given to the synthesis of these compounds, little is known about their catabolism. A survey of biotransformation of terpenes above and in Table 1.1 shows the prevalence of the oxidation of these hydrophobic compounds to more polar products. Most aerobic biotransformations of terpenes are initiated by hydroxylations or epoxidations. Carbons 7 and 3 of diterpenes synthesized via copalyl diphosphate (Fig. 1.5) are most often hydroxylated. Diterpenes containing a C7-C8 single bond are susceptible to alpha or beta hydroxylation at C7,

which may be followed by further oxidation to a ketone. In the case of a C7-C8 double bond there is support for C7-C8 epoxidation also leading to a C7 hydroxyl or ketone. The transformations presented in Table 1.1 and studies involving strains capable of growth on diterpenoids, emphasize the importance of C7 and C3 oxidations in their metabolism. To date, however, no genes or enzymes catalyzing these transformations leading to substrate degradation have been reported. We hypothesize that a cytochrome P450 is required for this transformation and represents the first required step in aerobic abietane diterpenoid catabolism following substrate uptake.

1.7 Conclusions

A review of both the synthesis and the limited data that is available concerning the degradation of tricyclic diterpenoids has shed some light on the unknowns regarding their metabolism. It is interesting to note that the three proposed pathways for abietane diterpenoid degradation are initiated by oxidation of the A ring at C3 or the B ring at C7 (Fig 1.10). This same type of initial reaction is often observed in biotransformations of other terpenoid compounds (Table 1.1). This raises the possibility that there are common catabolic pathways for degradation. Alternatively, this suggests that these carbons are simply most susceptible to hydroxylation. Looking again at the synthesis of these compounds it is worth noting that the formation of the A and B ring in all known tricyclic diterpenoids is similar, while the variability between the classes of tricyclic diterpenoids is found mainly in the formation of the C ring (Fig. 1.5, Table 1.1). If the C ring is cleaved and removed, then resulting intermediates would have similar structures resembling a decalin derivative. Little is known about the microbial catabolism of this fused two-ring structure, however, this compound could be a common intermediate in tricyclic diterpenoid degradation. At this point there is little evidence to support this hypothesis.

These possibilities raise further issues regarding the enzymes involved in catabolism. Degradation may rely on relatively few enzymes, perhaps with broad specificities or, possibly

there is a proliferation of divergent degradative enzymes specific for the broad range of terpenoids. Similar to a divergent synthetic pathway utilizing relatively few enzymes to produce a variety of compounds (Fig. 1.5), the same may be true for their catabolism, that is relatively few enzymes are used to transform the broad range of diterpenoids into a common intermediate in a convergent degradation pathway (Fig. 1.1). This thesis will focus on the microbial metabolism of abietane diterpenoids and attempt to shed more light on some of the above issues.

1.8 Thesis Objectives

The overall objective of this doctoral research is to characterize the initial steps in the aerobic degradation pathway of abietane diterpenoid catabolism by *Pseudomonas abietaniphila* BKME-9 and *Burkholderia xenovorans* LB400. This overall objective was pursued through 3 specific aims that focused on genes of the BKME-9 and LB400 *dit* clusters, including 3 cytochrome P450 genes: (1) to identify, clone and sequence a P450 contiguous with the *dit* gene cluster of BKME-9 and determine its involvement in the initial steps of abietane diterpenoid degradation; (2) to characterize the growth of LB400 on abietane diterpenoids, particularly looking at the induction of genes of the LB400 *dit* cluster using microarray transcriptomic analysis and using a knockout of *ditA1* encoding a ring hydroxylating dioxygenase, an enzyme critical in the degradation pathway; and, (3) to investigate the roles of two cytochromes P450 in the degradation of abietane diterpenoids by LB400. The three cytochromes P450 that were studied were DitQ-BKME-9, DitQ-LB400 (CYP226A1), and DitU-LB400 (CYP226A2). Expression of the enzymes during growth on abietane diterpenoids was assessed using a fused reporter construct in the case of DitQ-BKME-9 and both microarray transcriptomic analysis and 2D gel proteomic analysis in the cases of CYP226A1 and CYP226A2. The functions of these P450s in the catabolism of abietane diterpenoids were determined by gene knockout phenotypes, substrate-binding assays, and in the case of CYP226A1, an in vitro activity assay. The results are discussed and the physiological relevance of the observed activities is addressed.

1.9 References

1. **Akihisa, T., Y. Hamasaki, H. Tokuda, M. Ukiya, Y. Kimura, and H. Nishino.** 2004. Microbial transformation of isosteviol and inhibitory effects on Epstein-Barr virus activation of the transformation products. J Nat Prod **67:**407-10.

2. **Ali, M., and T. R. Sreekrishnan.** 2001. Aquatic toxicity from pulp and paper mill effluents: a review. Advances in Environmental Research **5:**175-196.

3. **Ariazi, E. A., Y. Satomi, M. J. Ellis, J. D. Haag, W. Shi, C. A. Sattler, and M. N. Gould.** 1999. Activation of the transforming growth factor β signaling pathway and induction of cytostasis and apoptosis in mammary carcinomas treated with the anticancer agent perillyl alcohol. Cancer Res **59:**1917-1928.

4. **Baker, D. D., and K. A. Alvi.** 2004. Small-molecule natural products: new structures, new activities. Curr Opin Biotechnol **15:**576-83.

5. **Barrero, A. F., J. E. Oltra, E. Cerda-Olmedo, J. Avalos, and J. Justicia.** 2001. Microbial transformation of *ent*-kaurenoic acid and its 15-hydroxy derivatives by the SG138 mutant of *Gibberella fujikuroi*. J. Nat. Prod. **64:**222-225.

6. **Bicho, P. A., V. Martin, and J. N. Saddler.** 1995. Growth, induction, and substrate specificity of dehydroabietic acid-degrading bacteria isolated from a kraft mill effluent enrichment. Appl Environ Microbiol **61:**3245-50.

7. **Biellmann, J. F., G. Branlant, M. Gero-Robert, and M. Poiret.** 1973. Degradation bacterienne de l'acide dehydroabietique par *Flavobacterium resinovorum*. Tetrahedron **29:**1227-1236.

8. **Biellmann, J. F., G. Branlant, M. Gero-Robert, and M. Poiret.** 1973. Degradation bacterienne de l'acide dehydroabietique par un *Pseudomonas* et une *Alcaligenes*. Tetrahedron **29:**1237-1241.

9. **Biellmann, J. F., and R. Wennig.** 1970. Microbial degradation of dehydroabietic acid. Chemical Communication **6:**346.

10. **Cheniclet, C.** 1987. Effects of wounding and fungus inoculation on terpene producing systems of maritime pine. Journal of Experimental Botany **38:**1557-1572.

11. **Cichewicz, R. H., and S. A. Kouzi.** 2004. Chemistry, biological activity, and chemotherapeutic potential of betulinic acid for the prevention and treatment of cancer and HIV infection. Med Res Rev **24:**90-114.

12. **Coppen, J. J. W., G. A. Hone, Food and Agriculture Organization of the United Nations., and Natural Resources Institute (Great Britain).** 1995. Gum naval stores : turpentine and rosin from pine resin. Food and Agriculture Organization of the United Nations, Rome.

13. **Davis, E. M., and R. Croteau.** 2000. Cyclization enzymes in the biosynthesis of monoterpenes, sesquiterpenes, and diterpenes. Topics in Current Chemistry **209**:53-95.

14. **de Oliveira, B. H., M. C. dos Santos, and P. C. Leal.** 1999. Biotransformation of the diperpenoid, isosteviol, by *Aspergillus niger*, *Penicillium chrysogenum* and *Rhizopus arrhizus*. Phytochemistry **51:**737-41.

15. **Denisov, I. G., T. M. Makris, S. G. Sligar, and I. Schlichting.** 2005. Structure and chemistry of cytochrome P450. Chem Rev **105:**2253-77.

16. **Dewick, P. M.** 2002. The biosynthesis of C5-C25 terpenoid compounds. Nat Prod Rep **19:**181-222.

17. **Dubey, V. S., R. Bhalla, and R. Luthra.** 2003. An overview of the non-mevalonate pathway for terpenoid biosynthesis in plants. J Biosci **28:**637-46.

18. **Eckstein-Ludwig, U., R. J. Webb, I. D. A. van Goethem, J. M. East, A. G. Lee, M. Kimura, P. M. O'Neill, P. G. Bray, S. A. Ward, and S. Krishna.** 2003. Artemisinins target the SERCA of Plasmodium falciparum. Nature **424:**957-961.

19. **Eisenreich, W., A. Bacher, D. Arigoni, and F. Rohdich.** 2004. Biosynthesis of isoprenoids via the non-mevalonate pathway. Cell Mol Life Sci **61:**1401-26.

20. **Feio, S. S., S. Franca, A. M. Silva, B. Gigante, J. C. Roseiro, and M. J. Marcelo Curto.** 2002. Antimicrobial activity of methyl cis-7-oxo deisopropyldehydroabietate on *Botrytis cinerea* and *Lophodermium seditiosum*: ultrastructural observations by transmission electron microscopy. J Appl Microbiol **93:**765-71.

21. **Fengel, D., and G. Wegener.** 1984. Wood : chemistry, ultrastructure, reactions. W. de Gruyter, Berlin ; New York.

22. **Fernandez, M. A., M. P. Tornos, M. D. Garcia, B. de las Heras, A. M. Villar, and M. T. Saenz.** 2001. Anti-inflammatory activity of abietic acid, a diterpene isolated from Pimenta racemosa var. grissea. J Pharm Pharmacol **53:**867-72.

23. **Fraga, B. M., P. Gonzalez, M. G. Hernandez, M. C. Chamy, and J. A. Garbarino.** 2003. Microbial transformation of 18-hydroxy-9,13-epi-ent-pimara-7,15-diene by *Gibberella fujikuroi*. J Nat Prod **66:**392-7.

24. **Fraga, B. M., P. Gonzalez, M. G. Hernandez, M. C. Chamy, and J. A. Garbarino.** 1998. The microbiological transformation of a 9-epi-ent-pimaradiene diterpene by *Gibberella fujikuroi*. Phytochemistry **47:**211-215.

25. **Fraga, B. M., M. G. Hernandez, P. Gonzalez, M. C. Chamy, and J. A. Garbarino.** 2000. The biotransformation of 18-hydroxy-9-epi-ent-pimara-7,15-diene by *Gibberella fujikuroi*. Phytochemistry **53:**395-399.

26. **Fulco, A. J.** 1991. P450BM-3 and other inducible bacterial P450 cytochromes: biochemistry and regulation. Annu Rev Pharmacol Toxicol **31:**177-203.

27. **Funk, C., and R. Croteau.** 1994. Diterpenoid resin acid biosynthesis in conifers: characterization of two cytochrome P450-dependent monooxygenases and an aldehyde dehydrogenase involved in abietic acid biosynthesis. Arch Biochem Biophys **308:**258-66.

28. **Funk, C., E. Lewinsohn, B. S. Vogel, C. L. Steele, and R. Croteau.** 1994. Regulation of oleoresinosis in Grand Fir (*Abies grandis*) (coordinate induction of monoterpene and diterpene cyclases and two cytochrome P450-dependent diterpenoid hydroxylases by Stem Wounding). Plant Physiol **106:**999-1005.

29. **Gelb, M. H., F. Tamanoi, K. Yokoyama, F. Ghomashchi, K. Esson, and M. N. Gould.** 1995. The inhibition of protein prenyltransferases by oxygenated metabolites of limonene and perillyl alcohol. Cancer Letters **91:**169-175.

30. **Gigante, B., C. Santos, A. M. Silva, M. J. Curto, M. S. Nascimento, E. Pinto, M. Pedro, F. Cerqueira, M. M. Pinto, M. P. Duarte, A. Laires, J. Rueff, J. Goncalves, M. I. Pegado, and M. L. Valdeira.** 2003. Catechols from abietic acid. synthesis and evaluation as bioactive compounds. Bioorg Med Chem **11:**1631-8.

31. **Guengerich, F. P.** 2001. Common and uncommon cytochrome P450 reactions related to metabolism and chemical toxicity. Chem Res Toxicol **14:**611-50.

32. **Gutierrez, A., J. C. del Rio, M. J. Martinez, and A. T. Martinez.** 2001. The biotechnological control of pitch in paper pulp manufacturing. Trends Biotechnol **19:**340-8.

33. **Hanson, J. R.** 2004. Diterpenoids. Nat Prod Rep **21:**785-93.

34. **Hanson, J. R.** 1992. The microbiological transformation of diterpenoids. Nat Prod Rep **9:**139-51.

35. **Hanson, J. R., and B. H. De Oliveira.** 1993. Stevioside and related sweet diterpenoid glycosides. Nat Prod Rep **10:**301-9.

36. **Hefner, J., S. M. Rubenstein, R. E. Ketchum, D. M. Gibson, R. M. Williams, and R. Croteau.** 1996. Cytochrome P450-catalyzed hydroxylation of taxa-4(5),11(12)-diene to taxa-4(20),11(12)-dien-5alpha-ol: the first oxygenation step in taxol biosynthesis. Chem Biol **3:**479-89.

37. **Hoffmann, J. J., Punnapayak, H. Jolad, S.D., Bate, R.B., Camou, F.A.** 1988. Bioconversion of Grindelic Acid into 3-alphahydroxygrindelic acid. J Nat Prod **51:**125-128.

38. **Huber, D. P. W., S Ralph, and J.R. Bohlmann**. 2004. Genomic hardwiring and phenotypic plasticity of terpenoid-based defenses in confiers. Journal of Chemical Ecology **30:**2399-2418.

39. **Hufford, C. D., F. A. Badria, M. Abou-Karam, W. T. Shier, and R. D. Rogers.** 1991. Preparation, characterization, and antiviral activity of microbial metabolites of stemodin. J Nat Prod **54:**1543-52.

40. **Jennewein, S., and R. Croteau.** 2001. Taxol: biosynthesis, molecular genetics, and biotechnological applications. Appl Microbiol Biotechnol **57:**13-9.

41. **Jennewein, S., R. M. Long, R. M. Williams, and R. Croteau.** 2004. Cytochrome p450 taxadiene 5alpha-hydroxylase, a mechanistically unusual monooxygenase catalyzing the first oxygenation step of taxol biosynthesis. Chem Biol **11:**379-87.

42. **Jennewein, S., C. D. Rithner, R. M. Williams, and R. B. Croteau.** 2001. Taxol biosynthesis: taxane 13 alpha-hydroxylase is a cytochrome P450-dependent monooxygenase. Proc Natl Acad Sci U S A **98:**13595-600.

43. **Kieslich, K.** 1976. Microbial transformations of non-steroid cyclic compounds. J. Wiley, [Chichester, Eng.].

44. **Kinouchi, Y., H. Ohtsu, H. Tokuda, H. Nishino, S. Matsunaga, and R. Tanaka.** 2000. Potential antitumor-promoting diterpenoids from the stem bark of *Picea glehni*. J Nat Prod **63:**817-20.

45. **Kitazume, T., N. Takaya, N. Nakayama, and H. Shoun.** 2000. *Fusarium oxysporum* fatty-acid subterminal hydroxylase (CYP505) is a membrane-bound eukaryotic counterpart of *Bacillus megaterium* cytochrome P450BM3. J. Biol. Chem. **275:**39734-39740.

46. **Kouzi, S. A., and J. D. McChesney.** 1991. Microbial models of mammalian metabolism: fungal metabolism of the diterpene sclareol by *Cunninghamella* species. J Nat Prod **54:**483-90.

47. **LaFever, R. E., B. S. Vogel, and R. Croteau.** 1994. Diterpenoid resin acid biosynthesis in conifers: enzymatic cyclization of geranylgeranyl pyrophosphate to abietadiene, the precursor of abietic acid. Arch Biochem Biophys **313:**139-49.

48. **Leppanen, H., J. V. K. Kukkonen, and A. O. J. Oikari.** 2000. Concentration of retene and resin acids in sedimenting particles collected from a bleached kraft mill effluent receiving lake. Water Research **34:**1604-1610.

49. **Levinson, A. S., B. C. Carter, and M. L. Taylor.** 1968. Microbial degradation of methyl dehydrobietate. Chem. Commun.:1344.

50. **Lewinsohn, E., M. Gijzen, T. J. Savage, and R. Croteau.** 1991. Defense mechanisms of conifers: Relationship of monoterpene cyclase activity to anatomical specialization and oleoresin monoterpene content. Plant Physiol. **96:**38-43.

51. **Lewis, D. F. V.** 2001. Guide to cytochromes P450 : structure and function. Taylor & Francis, London ; New York.

52. **Liang, P.-H., T.-P. Ko, and A. H.-J. Wang.** 2002. Structure, mechanism and function of prenyltransferases. Eur J Biochem **269:**3339-3354.

53. **Lin, L. H., L. W. Lee, S. Y. Sheu, and P. Y. Lin.** 2004. Study on the stevioside analogues of steviolbioside, steviol, and isosteviol 19-alkyl amide dimers: synthesis and cytotoxic and antibacterial activity. Chem Pharm Bull (Tokyo) **52:**1117-22.

54. **Liss, S. N., P. A. Bicho, and J. N. Saddler.** 1997. Microbiology and biodegradation of resin acids in pulp mill effluents: a minireview. Can J Microbiol **43:**599-611.

55. **Maria Perla Colombini, F. M., E. Ribechini,.** 2005. Direct exposure electron ionization mass spectrometry and gas chromatography/mass spectrometry techniques to study organic coatings on archaeological amphorae. Journal of Mass Spectrometry **40:**675-687.

56. **Martin, D., D. Tholl, J. Gershenzon, and J. Bohlmann.** 2002. Methyl jasmonate induces traumatic resin ducts, terpenoid resin biosynthesis, and terpenoid accumulation in developing xylem of Norway Spruce stems. Plant Physiol. **129:**1003-1018.

57. **Martin, V. J., and W. W. Mohn.** 2000. Genetic investigation of the catabolic pathway for degradation of abietane diterpenoids by *Pseudomonas abietaniphila* BKME-9. J Bacteriol **182:**3784-93.

58. **Martin, V. J., and W. W. Mohn.** 1999. A novel aromatic-ring-hydroxylating dioxygenase from the diterpenoid-degrading bacterium *Pseudomonas abietaniphila* BKME-9. J Bacteriol **181:**2675-82.

59. **Martin, V. J., D. J. Pitera, S. T. Withers, J. D. Newman, and J. D. Keasling.** 2003. Engineering a mevalonate pathway in *Escherichia coli* for production of terpenoids. Nat Biotechnol **21:**796-802.

60. **Martin, V. J., Z. Yu, and W. W. Mohn.** 1999. Recent advances in understanding resin acid biodegradation: microbial diversity and metabolism. Arch Microbiol **172:**131-8.

61. **Meshnick, S. R., A. Thomas, A. Ranz, C. M. Xu, and H. Z. Pan.** 1991. Artemisinin (qinghaosu): the role of intracellular hemin in its mechanism of antimalarial action. Mol Biochem Parasitol **49:**181-9.

62. **Mohn, W. W.** 1995. Bacteria obtained from a sequencing batch reactor that are capable of growth on dehydroabietic acid. Appl Environ Microbiol **61:**2145-50.

63. **Mohn, W. W., A. E. Wilson, P. Bicho, and E. R. Moore.** 1999. Physiological and phylogenetic diversity of bacteria growing on resin acids. Syst Appl Microbiol **22:**68-78.

64. **Morgan, C. A., and R. C. Wyndham.** 2002. Characterization of *tdt* genes for the degradation of tricyclic diterpenes by *Pseudomonas diterpeniphila* A19-6a. Can J Microbiol **48:**49-59.

65. **Morgan, C. A., and R. C. Wyndham.** 1996. Isolation and characterization of resin acid degrading bacteria found in effluent from a bleached kraft pulp mill. Can J Microbiol **42:**423-30.

66. **Narhi, L., and A. Fulco.** 1986. Characterization of a catalytically self-sufficient 119,000-dalton cytochrome P-450 monooxygenase induced by barbiturates in *Bacillus megaterium*. J. Biol. Chem. **261:**7160-7169.

67. **Newman, D. J., G. M. Cragg, and K. M. Snader.** 2003. Natural products as sources of new drugs over the period 1981-2002. J Nat Prod **66:**1022-37.

68. **Ohnuma, S.-i., K. Hirooka, N. Tsuruoka, M. Yano, C. Ohto, H. Nakane, and T. Nishino.** 1998. A pathway where polyprenyl diphosphate elongates in prenyltransferase. Insight into a common mechanism of chain length determination of prenyltransferases. J. Biol. Chem. **273:**26705-26713.

69. **Orden, A. A., D. A. Cifuente, E. J. Borkowski, C. E. Tonn, and M. K. Sanz.** 2005. Stereo- and regioselective hydroxylation of grindelic acid derivatives by *Aspergillus niger*. Nat Prod Res **19:**625-31.

70. **Peters, R. J., J. E. Flory, R. Jetter, M. M. Ravn, H.-J. Lee, R. M. Coates, and R. B. Croteau.** 2000. Abietadiene synthase from Grand Fir (*Abies grandis*): Characterization and mechanism of action of the "pseudomature" recombinant enzyme. Biochemistry **39:**15592-15602.

71. **Ro, D.-K., G.-I. Arimura, S. Y. W. Lau, E. Piers, and J. Bohlmann.** 2005. Loblolly pine abietadienol/abietadienal oxidase PtAO (CYP720B1) is a multifunctional, multisubstrate cytochrome P450 monooxygenase. PNAS **102:**8060-8065.

72. **Roberts, G. A., G. Grogan, A. Greter, S. L. Flitsch, and N. J. Turner.** 2002. Identification of a new class of cytochrome P450 from a *Rhodococcus* sp. J. Bacteriol. **184:**3898-3908.

73. **Rohdich, F., K. Kis, A. Bacher, and W. Eisenreich.** 2001. The non-mevalonate pathway of isoprenoids: genes, enzymes and intermediates. Curr Opin Chem Biol **5:**535-40.

74. **Rohmer, M., M. Knani, P. Simonin, B. Sutter, and H. Sahm.** 1993. Isoprenoid biosynthesis in bacteria: a novel pathway for the early steps leading to isopentenyl diphosphate. Biochem J **295 (Pt 2):**517-24.

75. **Rojas, M. C., P. Hedden, P. Gaskin, and B. Tudzynski.** 2001. The P450-1 gene of Gibberella fujikuroi encodes a multifunctional enzyme in gibberellin biosynthesis. Proc Natl Acad Sci U S A **98:**5838-43.

76. **Rosazza, J. P., and R. V. Smith.** 1979. Microbial models for drug metabolism. Adv Appl Microbiol **25:**169-208.

77. **Ruzicka, L.** 1953. The isoprene rule and the biogenesis of terpenic compounds. Experientia **9:**357-67.

78. **Seo, J.-S., H. Chong, H. S. Park, K.-O. Yoon, C. Jung, J. J. Kim, J. H. Hong, H. Kim, J.-H. Kim, J.-I. Kil, C. J. Park, H.-M. Oh, J.-S. Lee, S.-J. Jin, H.-W. Um, H.-J.**

Lee, S.-J. Oh, J. Y. Kim, H. L. Kang, S. Y. Lee, K. J. Lee, and H. S. Kang. 2005. The genome sequence of the ethanologenic bacterium *Zymomonas mobilis* ZM4. **23:**63-68.

79. **Tavendale, M. H., P. N. McFarlane, K. L. Mackie, A. L. Wilkins, and A. G. Langdon.** 1997. The fate of resin acids-1. The biotransformation and degradation of deuterium labelled dehydroabietic acid in anaerobic sediments. Chemosphere **35:**2137-2151.

80. **Tavendale, M. H., P. N. McFarlane, K. L. Mackie, A. L. Wilkins, and A. G. Langdon.** 1997. The fate of resin acids-2. The fate of resin acids and resin acid derived neutral compounds in anaerobic sediments. Chemosphere **35:**2153-2166.

81. **Tudzynski, B.** 2005. Gibberellin biosynthesis in fungi: genes, enzymes, evolution, and impact on biotechnology. Appl Microbiol Biotechnol **66:**597-611.

82. **Ulusu, N. N., D. Ercil, M. K. Sakar, and E. F. Tezcan.** 2002. Abietic acid inhibits lipoxygenase activity. Phytother Res **16:**88-90.

83. **van Beilen, J. B., R. Holtackers, D. Luscher, U. Bauer, B. Witholt, and W. A. Duetz.** 2005. Biocatalytic production of perillyl alcohol from limonene by using a novel *Mycobacterium* sp. cytochrome P450 alkane hydroxylase expressed in *Pseudomonas putida.* Appl Environ Microbiol **71:**1737-44.

84. **Vogel, B. S., M. R. Wildung, G. Vogel, and R. Croteau.** 1996. Abietadiene Synthase from Grand Fir (*Abies grandis*). cDNA isolation, characterization, and bacterial expression of a bifunctional diterpene cyclase involved in resin acid biosynthesis. J. Biol. Chem. **271:**23262-23268.

85. **Wang, K. C., and S.-i. Ohnuma.** 2000. Isoprenyl diphosphate synthases. Biochimica et Biophysica Acta (BBA) - Molecular and Cell Biology of Lipids **1529:**33-48.

86. **Warren, R., W. W. Hsiao, H. Kudo, M. Myhre, M. Dosanjh, A. Petrescu, H. Kobayashi, S. Shimizu, K. Miyauchi, E. Masai, G. Yang, J. M. Stott, J. E. Schein, H. Shin, J. Khattra, D. Smailus, Y. S. Butterfield, A. Siddiqui, R. Holt, M. A. Marra, S. J. Jones, W. W. Mohn, F. S. Brinkman, M. Fukuda, J. Davies, and L. D. Eltis.** 2004. Functional characterization of a catabolic plasmid from polychlorinated- biphenyl-degrading *Rhodococcus* sp. strain RHA1. J Bacteriol **186:**7783-95.

87. **Woodrow, C. J., R. K. Haynes, and S. Krishna.** 2005. Artemisinins. Postgrad Med J **81:**71-78.

88. **Zhang, L., and A. L. Demain.** 2005. Natural products : drug discovery and therapeutic medicine. Humana Press, Totowa, N.J.

2. A cytochrome P450 involved in the metabolism of abietane diterpenoids by *Pseudomonas abietaniphila* BKME-9[1]

2.1 Introduction

Pseudomonas abietaniphila BKME-9 contains a cluster of genes required for the catabolism of abietane diterpenoids (10, 11). Several genes of the BKME-9 diterpenoid degradation (*dit*) cluster were sequenced and characterized, and a convergent pathway for abietane diterpenoid metabolism was proposed (see Fig. 1.11)(10). As presented in the Introduction, some evidence from research on the abietane diterpenoid degrading bacterium *Pseudomonas diterpeniphila* A19-6a suggests that a P450 monooxygenase is involved in the catabolism of these compounds (13). No candidate P450 encoding genes, however, have been identified in the characterized BKME-9 *dit* cluster.

Based on the above evidence we investigated the possibility of a cytochrome P450 involvement in the initial steps in the abietane diterpenoids degradation pathway of BKME-9. To accomplish this a genomic DNA fragment contiguous to the *dit* cluster was cloned and characterized. Here we provide previously missing evidence for the existence of a P450 enzyme in the *dit* cluster and demonstrate that it is involved in diterpenoid metabolism. We also show an apparent difference in strains BKME-9 and A19-6a, as the former does not require the P450 for normal metabolism of abietic acid. We characterized the P450 using a knockout mutant, a gene-fusion transcriptional reporter, and by determining carbon monoxide (CO)- and substrate-binding spectra of the protein expressed in *E. coli*. We also provide additional evidence for the homology of diterpenoid degradation genes in both BKME-9 and A19-6a.

[1] A version of this chapter has been published as: Smith, D.J., V.J.J. Martin, and W.W. Mohn 2004. A Cytochrome P450 Involved in the Metabolism of Abietane Diterpenoids by *Pseudomonas abietaniphila* BKME-9. J Bacteriol 186:3631-9.

2.2 Methods and Materials

Bacterial Strains, plasmids, and culture conditions. The bacterial strains and plasmids used in this study are listed in Table 2.1. *Escherichia coli* was cultured on Luria-Bertani medium and *P. abietaniphila* strains was cultured on tryptic soy broth, or mineral medium supplemented with diterpenoids as previously described (12). Mutants of strain BKME-9 were cultured with 4 μg of gentamicin. Diterpenoids were supplied by Helix Biotechnologies, Richmond, Canada.

Table 2.1 Strains and plasmids used in this study

	Genotype or Description	Reference or Source
Strains		
P. abietaniphila		
BKME-9	Wild type; grows on abietane diterpenoids	(3)
P450KO	*ditQ*:: *xylE-accC1*; Gm^r	This study
P. diterpeniphila		
A19-6a	Wild type; grows on DhA	(13)
E. coli		
DH5α	*endA1 hsd*R17 (r_k^- m_k^-) *supE44 thi-1 recA1 gyrA (Nal^r) relA1 Δ(lacIZYA-argF)* U169 *deoR (Φ80dlacΔ(lacZ)M15)*	Gibco BRL
S17-1	*recA pro thi hsdR* with integrated RP4-2-TcMu::Kna::Tn7; Tra^+ Tr^r Sm^r	(17)
Plasmids		
pUC19	Cloning vector , Ap^r	(22)
pEX100T	*sacB* conjugable plasmid for gene replacement; Ap^r	(16)
pX1918G	xylE-*accC1* fusion cassette-containing plasmid; Ap^r Gm^r	(16)
pDS1	5.1-kb *EcoR* I fragment of pLC162 cloned into the *Eco*RI site of pUC19	This study
pEXP450	1482-bp *Eco*RV-*Sma*I of pDS1 cloned into the *Sma*I site of pEX100T	This study
pEXP450KO	*Pst*I *xylE-accC1* cassette of pX1918G cloned into the *Pst*I site of pEXP450	This study
pLC48	SuperCos1 cosmid library clone containing DhA degradation genes	(11)
pLC162	SuperCos1 cosmid library clone containing DhA degradation genes	(11)

The AbA used was approximately 96% pure, with another diterpenoid, most likely DhA, comprising the remainder. The PaA used was approximately 90% PaA, 7% DhA, and 3% AbA. The 7-oxo-DhA used was greater than 97% pure with trace amounts of several undetermined diterpenoids. DhA, and isopimaric acid (IpA) used in the study were greater than 99% pure.

Southern hybridization. Standard techniques of Southern hybridization analysis were followed as previously described. Briefly, SS Maximum Strength Nytran Plus was used for blotting (Schleicher and Schuell, Keene, New Hampshire). The immobilized DNA was hybridized to *tdtD* labeled with [α^{32}-P] dCTP (NEN, Boston, Mass.) using the Nick Translation System from Gibco BRL (Gaithersburg, Md.). Dr. Cam Wyndham, Institute of Biology, Carleton University Ottawa, Canada, kindly provided *tdtD* from *P. diterpeniphila* A19-6a. Labeling efficiency was recorded at 6.7 x 10^7 cpm/µl of probe solution.

After blotting the membrane was washed in 6X SSC (0.9 M NaCl, 90 mM sodium citrate, pH 7.0) for 5 min and then nucleic acids were immobilized by heating at 80° C for 90 min. Hybridization solution was prepared by combining 5 ml formamide, 3 ml 20X SSPE (3.6 mM NaCl, 200 mM $NaPO_4$ (pH 7.7), 1 mM EDTA), 0.5 ml 100X Denhart's (0.2% ficoll, 0.2% polyvinylpyrrolidone, 0.2% bovine serum albumin), 0.5 ml 2 µg/µl salmon sperm DNA. Prior to adding the probe the membrane was incubated in 5 ml of hybridization solution at 42°C in a preheated tube roller for 2 hours and then drained. The probe was boiled for 3 min and then the entire 50 µl was added to 5 ml of hybridization solution in the tube containing the membrane. After overnight hybridization at 42°C the membrane was briefly washed with 20 ml 7X SSPE/1% sodium dodecyl sulfate (SDS) followed by a second wash with 150 ml 7X SSPE/1% SDS at 42° for 1 hour. Hybridization was analyzed by using standard phosphorimager scanning and autoradiography techniques.

DNA manipulation. Plasmid DNA was isolated by the standard alkali lysis (2) or by QIAprep Spin Miniprep Kit (Qiagen, Santa Clarita, California). Restriction endonuclease (New England Biolabs [NEB], Beverly, Mass., or Gibco BRL) digestions were performed by standard procedures. DNA fragments were purified from agarose gels with QIAquick gel extraction kit (Qiagen). Plasmid pUC19 and *E. coli* DH5α were used to clone the 5.1 kbp *EcoR*I digested

fragment from pLC162 to generate pDS1. Prior to ligation *EcoR*I digested pUC19 was treated with alkaline phosphatase (Gibco) as per manufacture's instructions. Nucleic acids were then ethanol precipitated and suspended in 5 μl of ddH_2O.

Ligation reactions were conducted using T4 DNA ligase (NEB) as per manufacture's instructions. The ligase reaction mixture was incubated at 15° C over night and used to transform *E. coli* DH5α by electroporation according to the protocol supplied with the Bio-Rad (Hercules, Calif.) gene pulser. Positive transformations were selected by blue/white colony growth after over night incubation on LB agar plates supplemented with ampicillin (50 μg/ml) and 40 μl of X-gal (40 mg/ml in dimethyl formamide). Two dilutions of transformed cells were used for plating: 10 μl and 990 μl. White colonies were picked from the plates and grown overnight in 5 ml of LB broth supplemented with 50 μg/ml ampicillin. Plasmid DNA was then extracted with QIAprep Spin Miniprep columns as above, digested with *EcoR*I, and run on a 0.7 % agarose gel to identify insert and vector. The successful ligation was designated pDS1.

Successive unidirectional deletions. Successive unidirectional deletions of pDS1 DNA were prepared using the double-stranded nested deletion system from Pharmacia Biotech (Uppsala, Sweden). Support protocol provided with the system was followed as per manufacturer's recommendations. In general, pDS1 was prepared for nested deletions by extracting plasmid DNA from overnight LB grown cultures supplemented with 100 μg/ml ampicillin using QIAprep Spin Miniprep Kit eluted with 50 μl of ddH_2O. Plasmids were linearized by digesting with *Sal*I (NEB) at 37°C for 2 hours. DNA was then ethanol precipitated and suspended in ddH_2O. *Sal*I digested samples were then backfilled with thionucleotides using Klenow fragment provided with the system. The reaction mixtures were incubated in a water bath at 37°C for 30 min followed by 20-min incubation at 65°C to inactivate the Klenow fragment. Backfilled DNA samples were purified using QIAquick PCR Purification Kit (Qiagen) and suspended in 30 μl of

ddH_2O. The concentration of backfilled DNA for this sample was 380 ng/μl as determined by agarose gel electrophoresis analysis. 5'- overhanging ends susceptible for Exonuclease III digestion were prepared by *Xba*I (Gibco) digest incubated in a 37°C water bath for 90 min. Exonuclease III deletion reactions were carried out at 37°C under the following conditions; 20 μl *Xba*I digested DNA (~2 μg), 20 μl 2X Exo III buffer solution (8 μl Exo III buffer, 6μl 0.3 M NaCl and 10μl ddH_2O, and 1 μl Exonuclease III (90,000-130,000 units/ml). Twenty-four 1.6 μl aliquot, were removed from the reaction mixture at 4 min intervals and combined with 3 μl of S1 nuclease solution as described in the support protocol. After a 30 min incubation at room temperature 1 μl of S1 Stop Solution was added to each sample followed by 10-min incubation at 65°C.

Deletions were analyzed by electrophoresis on a 1% agarose gel of 2.6 μl from each aliquot. The remaining 3μl of each aliquot were used for circularization of the linearized plasmids as outline in the protocol provided with the system. Based on the extent of deletion, circularized plasmids were selected for transformation into chemically competent DH5α *E. coli* cells prepared essentially as described by Hanahan (6). Transformed DH5α cells were screened on LB agar plates using blue/white screening as described above. White colonies from each plate were used to inoculate 5 ml of LB broth supplemented with 100 μg/ml of ampicillin. Alkaline lysis mini-preps, as described above, were used to isolate plasmid DNA. Following *EcoR*I digestion plasmid sizes were analyzed by gel electrophoresis on 0.7% agarose gel. Clones of the appropriate sizes were then used to inoculate 5 ml LB broth with 100 μg/ml of ampicillin. Plasmid DNA was isolated with Qiagen Miniprep kit as described above and suspended in 50 μl of ddH_2O. 1 μl of each sample was then linearized by an *EcoR*I digest and analyzed by electrophoresis to confirm fragment size and determine DNA concentration.

Sequencing and sequence analysis. Standard M13 primers for sequencing of successive unidirectional deletion clones were supplied by the Nucleic Acid and Protein Service (NAPS) at the University of British Columbia. The forward primer used was –21M12, (5'-TGT-AAA-ACG-ACG-GCC-AGT-3') and the reverse primer used was M13R, (5'- CAG-GAA-ACA-GCT-ATG-ACC-3'). Primers used for "primer walking" of cosmid library clones were supplied by AlphaDNA (http://www.alphadna.com). AlphaDNA also supplied primers used for colony PCR of P450KO and sequencing of the PCR product. DNA sequences were determined at NAPS at the University of British Columbia using the AmpliTaq dye terminator cycle sequencing (Applied Biosystems, Forest City, CA). Conditions of the sequencing reaction were as follows; 4 µl terminator premix (NAPS), 0.25-0.5 µg of plasmid template or 1 µg of cosmid template, 3.2 pmol primer, and ddH_2O as required to 20 µl. Primer extension products were prepared by PTC-150 Minicycler with a Hot Bonnet (MJ Research, Waltham, MA) using the following program for 25 cycles; rapid thermal ramp to 96°C, 96°C for 30 seconds, rapid thermal ramp to 50°C, 50°C for 15 seconds, rapid thermal ramp to 60°C, 60°C for 4 min. Extension products were purified using Centri-Sep columns (Princeton Separation, Adelphia, NJ). A consensus nucleic acid sequence was prepared using Bioedit (Version 5.0.0), available at http://www.mbio.ncsu.edu/RNaseP/info/programs/BIOEDIT/bioedit.html). ORF finder software at http://www.ncbi.nlm.nih.gov/gorf/gorf.html was used to determine open reading frames and to conduct sequence similarity searches using BLASTP software (2.2.6) from the National Center for Biotechnology Information website. The ClustalW Multiple Alignment program included with the Bioedit software was used to align and analyze protein sequences using the default setting.

Knockout of the putative P450 by gene replacement. A knockout of *ditQ* was generated by gene replacement to yield strain P450KO. Plasmid pEXP450 was constructed by ligating a 1482 bp *Eco*RV *Sma*I blunt end fragment of pDS1 into the dephosphorylated unique *Sma*I site of

pEX100T (8) containing the *SacB* counterselectable maker and transforming Dh5α. Next, a *Pst*I-digested *xylE-accC1* transcriptional fusion antibiotic cassette of pX1918G (8) was ligated into the dephosphorylated unique *Pst*I site of pEXP450, which disrupted the P450 gene and the product was used to transform *E. coli* S17-1 to create pEXP450KO. Successful transformants were selected by growth on LB plates containing 10 μg/ml of gentamycin and the ability to cleave catechol producing a yellow colour after spraying colonies with 0.1 M potassium phosphate (pH 7.5) containing 100 mM catechol as in (8). Ligation and transformation were confirmed by *I-Sce* digest of alkaline lysed extracts of overnight culture yielding two bands on an agarose gel representing the vector and the insert. Homologous recombination of the mutated allele into strain BKME-9 was accomplished by diparental conjugation as in (5) followed by a two step selection method as previously described (11). Successful gene replacement was monitored by colony PCR (23) with primers targeted to the P450 gene (P450-404left, 5'-GCG GAC CTT GAA GGT AGC GA-3', and P450-3567right, 5'-GCA ACT TCA TGG CAG GCC TT-3') at an annealing temperature of 61°C and a 4-min extension time. In order to confirm insertion into the gene of interest the 3163 bp amplicon from the above PCR was then used in two sequencing reactions with P450-404left and P450-3567right as primers.

Growth assays and cell suspensions. Cultures of BKME-9 and P450KO were grown overnight at 28°C on mineral medium supplemented with 90 mg of DhA per litre, or with 1 g of sodium pyruvate per litre supplemented with 4 mg of gentamycin per litre. These overnight cultures were then transferred to mineral medium supplemented with 1 g sodium pyruvate per litre. After overnight growth, cells were collected by centrifugation, washed and suspended in sterile saline at an optical density at 600 nm (OD_{600}) of 0.6. These cell suspension was then used to inoculate (0.1%) 2-ml cultures in solvent-washed tubes of mineral medium supplemented with either 1 g of sodium pyruvate, 90 mg of AbA, 90 mg of DhA, 90 mg of PaA, or 95 mg of 7-oxo-DhA per litre. All cultures were then incubated on a rotary shaker at 28°C. At selected time intervals 2 to

4 replicates of 2-ml cultures of each strain were removed from the incubator. Half of the cultures were acidified with 2 drops of 1 M HCl and immediately frozen at -20°C for later analysis of abietanes by gas chromatography using a flame ionization detector (GC-FID), as previously described (12). The other half of the cultures (1 ml) was centrifuged, the pellet washed with 0.9% sterile saline, the suspension centrifuged again and the pellet frozen at -20°C. These samples were later used to determine protein concentration using the micro-bicinchoninic acid (BCA) protein assay kit (Sigma) and bovine serum albumin as the standard (18). BCA protein quantification was used to monitor growth as opposed to optical density, because resin acids precipitating in the medium prevented accurately measuring OD. Cell suspension assays were conducted as previously described (11). GC electron impact (EI) mass spectrometry (MS) of methyl ester derivatives was conducted as previously described (12) using an Agilent Technologies 6890N Network GC system equipped with an Agilent 5973 Mass Selective Detector. National Institute of Standards and Technology MS Search (2.0) was used to analyze mass spectral data.

Catechol 2,3-dioxygenase (C23O) assays. Previously it was reported that BKME-9 shows no endogenous C23O activity and that activity served as an adequate reporter for gene induction studies (10). For C23O assays, strain P450KO was grown on mineral medium supplemented with 1g per litre sodium pyruvate to an OD_{600} between 0.15 and 0.3 and then spiked with a potential inducer, 150 mg per litre DhA, 150 mg per litre AbA, 158 mg per litre 7-oxo-DhA, 150 mg per litre isopimaric acid, 37 mg per litre 12,14-dichlorodehydroabietic acid, 15.4 mg per litre biphenyl, 12.0 mg per litre naphthalene, or 17.8 mg per litre phenanthrene. These cultures were incubated until they reached an OD_{600} between 0.6 and 0.7. Cultures were then harvested, washed in 10 mM KPO_4 buffer (pH 7.5) at 4°C and suspended in the buffer at an OD_{600} of 6.0. Triplicate enzyme assays were performed on whole cells suspended at an OD_{600} of 0.1 in 1 ml of

the buffer containing 500 μM catechol. C23O activity was assayed spectrophotometrically at 30°C as the formation of 2-hydroxy semialdehyde at 375 nM ($\varepsilon = 44\ mM^{-1}\ cm^{-1}$) for 3.5 min.

Spectrophotometric assays. A 2-litre flask containing 1 litre of LB with 50 μg/ml of ampicillin was inoculated with 5 ml of an overnight culture of *E. coli* harbouring pEXP450 or pEX100T. The culture was incubated with shaking until the OD_{600} reached approximately 0.6. Expression of *ditQ* was induced by addition of 1 mM IPTG and further incubation for 18 to 24 hours. Cells were harvested by centrifugation at 8275 x g in a Sorvall SLA 3000 rotor for 15 min. The pellet was washed with 1 litre of TrisCl pH 7.4 and centrifuged as above. The pellet was then suspended in 5 ml of the buffer plus 1 mM DTT and 1 mM PMSF. The suspension was passed through a French pressure cell 2 times, and the crude lysate was centrifuged for 30 min at 25000 x g in a Sorvall SS-34 rotor. The supernatant was removed and the crude extract was used for spectrophotometric analysis, using a Cary 1E spectrophotometer and Cary UVWin Scan Application Version 2.00 software.

The reduced CO binding spectrum was obtained with 200 μl of crude extract added to 1.80 ml of the same buffer as above plus a few crystals of sodium dithionite to reduce the sample. The sample was then equally divided in two 1-ml, optically matched cuvettes. One sample was treated by bubbling carbon monoxide through the cuvette slowly for 30 sec. The second sample was used as the reference in difference spectroscopy with the carbon monoxide treated sample.

Substrate binding assays were performed in two optically matched 3-ml cuvettes, each with 300 μl of the above crude extract of *E. coli* harbouring pEX100T or pEXP450 plus 2.70 ml of buffer used above. Increasing concentrations of substrate in buffer were added to the sample cuvette and equal volumes of buffer were added to the reference cuvette. The difference spectra were determined from 350 nm to 500 nm. The binding constant, K_d, was determined using the following non-linear fitting equation:

$$\Delta A' = \Delta A_M ((\ [L_T] + [E_T] + K_d) - ((\ [L_T] + [E_T] + K_d)^2 - 4\ [L_T][E_T])^{0.5})/\ (2\ [E]_T)$$

where ΔA is the difference in absorbance between 387 and 425, ΔA_M is the maximum change in absorbance, $[L]_T$, is the total ligand concentration, and $[E]_T$ is the total enzyme concentration (4). P450 levels were calculated from the absorbance at 450 nm of the ferrous form complexed with CO using the cytochrome P450 extinction coefficient, 91 mM^{-1} cm^{-1}.

Nucleotide sequence accession number. The nucleotide sequences reported in this study were submitted to GenBank under accession no. AF119621.

2.3 Results

2.3.1 Sequencing of 10.4 kbp region containing a putative P450 gene

To determine if a gene cluster corresponding to the *tdt* cluster of *P. diterpeniphila* A19-6a is located adjacent to the *dit* cluster of BKME-9, we analyzed by Southern blot nine *Eco*RI-digested BKME-9 cosmid library clones containing *ditA1,* using the *tdtD* gene as a probe. The lanes containing fragments from cosmids pLC48 and pLC162 had single bands with high intensity of approximately 6 kbp and 5.1 kbp respectively (Fig 2.2). The 5.1 kbp fragment of pLC162 hybridizing to the *tdtD* probe was cloned and sequenced. This 5.1 kbp fragment is located approximately 2.8 kbp downstream from ORF1 of the previously characterized *dit* cluster (Fig. 2.2). The 2.8 kbp gap was sequenced from cosmid library clone pLC162 by primer walking. We also used primer walking to sequence 2.5 kbp beyond the end of the 5.1 kbp fragment opposite to the gap, using the pLC48 cosmid as a template. Thus, a total region 10.4 kbp adjacent to the *dit* cluster was sequenced.

Table 2.2 Amino acid sequence comparison of deduced DitQ ($P450_{dit}$) to proteins in the non-redundant database obtained by BLASTP search

Proteins with similar sequence (protein function)	E-values	% identity (no. of residues)	Organism	Reference	Accesion no.
TdtD (cytochrome P450)	e-178	84 (424)	*Pseudomonas diterpeniphila*	(13)	AAK95585
ERYK Cytochrome P450 113A1 (erythromycin B/D C-12 hydroxylase)	7e-22	26 (397)	*Saccharopolyspora erythraea*	(19)	P48635
CYP108 cytochrome $P450_{terp}$ (α terpineol oxidation)	1e-18	23 (428)	*Pseudomonas sp.*	(15)	P33006
CamC $P450_{cam}$ (cytochrome P450) (camphor 5-monooxygenase)	0.023	17 (415)	*Pseudomonas putida*	(20)	P00183

The region of the above 5.1-kbp fragment, presumably hybridizing to the *tdtD* probe, corresponds to an ORF designated *ditQ*. A similarity search of the non-redundant GenBank database using BLASTP (1) with the deduced amino acid sequence of *ditQ* indicates that *ditQ* codes for a putative P450 (Table 2.2). Comparison of the inferred amino acid sequence of *ditQ*

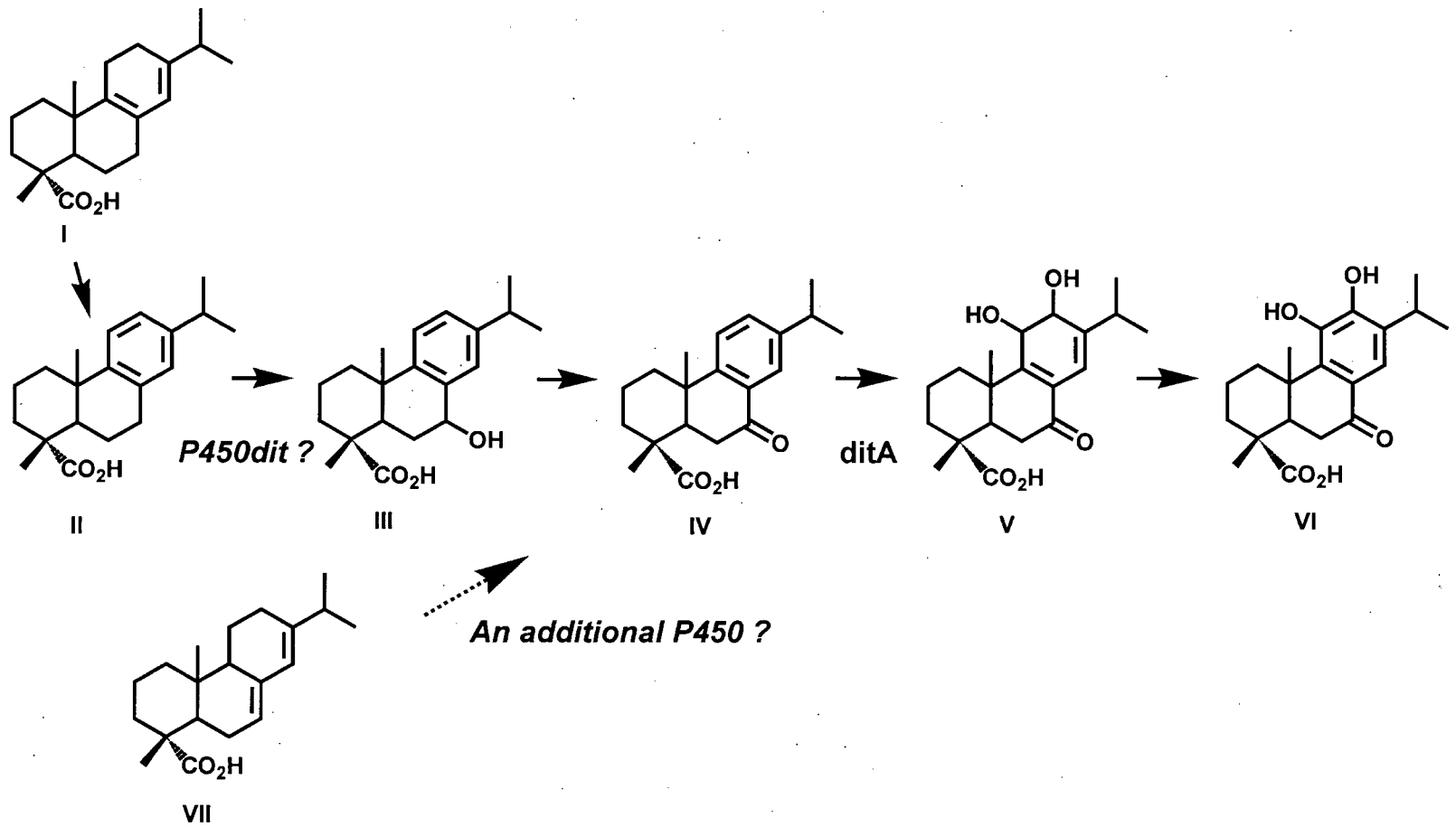

Figure. 2.1 Proposed pathway for abietane degradation by *P. abietaniphila* BKME-9.
Chemical designations: I, palustric acid; II, dehydroabietic acid; III, 7-hydroxydehydroabietic acid; IV, 7-oxodehydroabietic acid; V, 7-oxo-11,12-dihydroxy-8-13-abietadien acid; VI, 7-oxo-11,12-dihydroxydehydroabietic acid; VII, abietic acid

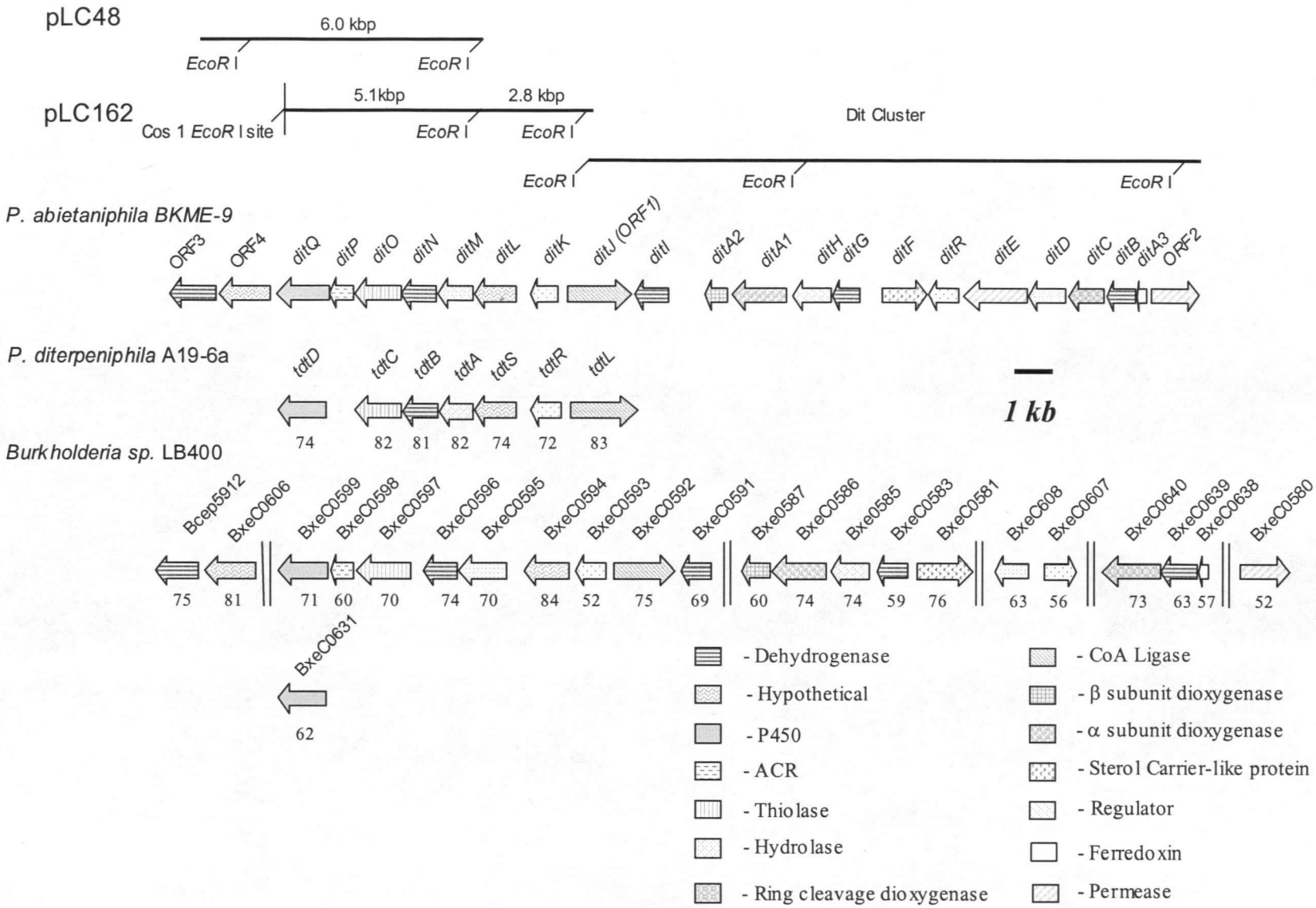

Figure 2.2 Physical map of the *dit* gene cluster of BKME-9, the *tdt* gene cluster of A19-6a and homologues from LB400. Genes are represented by arrows with patterns and colours corresponding to putative functions. Numbers below each gene represent the percent amino acid identity corresponding to the deduced protein sequence of the BKME-9 gene above. Double vertical lines indicate gaps in the genome sequence of unspecified length, which may contain additional ORFs. Horizontal lines refer to cosmid library clones used for subcloning and sequencing of BKME-9 DNA and the *dit* cluster.

to the Cluster of Orthologous Groups of protein (COGS) and Protein families database of alignments and HMMS showed similarity to P450s (Table 2.3). Alignment of the $P450_{dit}$ deduced protein with the well-characterized $P450_{cam}$ showed conservation of functional residues including the highly conserved heme-binding region with consensus sequence FG(F/H)G(P/S)H(M/L)C.

2.3.2 Sequence analysis of 10.4-kbp *dit* cluster extension

Sequence analysis of the 10.4-kbp fragment revealed nine complete ORFs and one partial ORF which are homologues of genes encoding 2 dehydrogenases, a thiolase, a hydrolase, an ancient uncharacterized conserved region, a cytochrome P450, a transcriptional regulator, a CoA ligase and 2 conserved hypothetical proteins (Fig. 2.2). The CoA ligase sequence is contiguous with the previously identified ORF1 (10) of the *dit* cluster and completes this gene sequence, now designated *ditJ* (Fig. 2.2, Tables 2.2 and 2.3). A region of the 10.4-kbp extension corresponds very closely to the *tdt* cluster (13), having the same ORF arrangement and greater than 72% identity of deduced amino acid sequences. The gene encoding DitP was identified by COG analysis as an ancient conserved region common to two or more phylogenetic branches (Table 2.3). Morgan and Wyndham (13) did not identify this coding region on the *tdt* cluster. Further analysis of the *tdt* sequence did not reveal an ORF corresponding to *ditP*.

Table 2.3 Conserved domain search and COG comparison

Gene	Deduced no. of residues	Functional assignment based on COG comparison		Conserved Domains Pfam Data base Search		
				Domain	E-value	Residues
ORF3	398	COG1960	Acyl-CoA dehydrogenases	1. Acyl-CoA dehydrogenase, N-terminal domain (pfam02771)	2.4e-6	27-145
				2. Acyl-CoA dehydrogenase, middle domain. (pfam02770)	3.4e-16	147-248
ORF4	435	No Hits		Amidohydrolase family (pfam04909)	3.4e-08	41-373
ditQ	424	COG2124	Cytochrome P450	Cytochrome P450 (pfam00067)	2.3e-24	39-421
ditP	140	COG2128	Uncharacterized ancient conserved region	No Hits		
ditO	391	COG0183	Acetyl-CoA acetyltransferase	1. Thiolase, N-terminal domain (pfam00108)	1.6e-86	1-260
				2. Thiolase, C-terminal domain. (pfam0280)	1.6e-63	265-389
ditN	301	COG1250	3-Hydroxyacyl-CoA dehydrogenase	1. 3-hydroxyacyl-CoA dehydrogenase, NAD binding domain (pfam02737)	2.3e-53	3-188
				2. 3-hydroxyacyl-CoA dehydrogenase, C-terminal domain (pfam00725)	5.8e-41	190-285
ditM	289	COG0179	2-keto-4-pentenoate hydratase/2-oxohepta-3-ene-1,7-dioic acid hydratase (catechol pathway)	Fumarylacetoacetate (FAA) hydrolase (pfam01557)	1e-45	86 254
ditL	359	No Hits		Amidohydrolase (pfam04909)	3.6e-32	1-344
ditK	249	No Hits		Bacterial regulatory proteins, tetR family (pfam00440)	2e-12	67-113
ditJ	546	COG0318	Acyl-CoA synthetases (AMP-forming)/AMP-acid ligases II	AMP-binding enzyme (pfam00501)	7.5e-105	43-459

2.3.3 Growth of *ditQ* mutant on abietanes

A *ditQ* mutant strain, P450KO, was used to investigate the function of *ditQ* in abietane diterpenoid metabolism. Characterization of the growth of P450KO on abietane diterpenoids revealed that *ditQ* is required for a growth phenotype similar to the wild type on DhA and PaA but not on AbA or 7-oxo-DhA. BKME-9 growing on AbA had a doubling time ($\pm$ standard error) of 12 ± 2.0 h and reached a protein concentration of 10 ± 0.4 µg of protein/ml for a growth yield of $0.1 \pm 0.4 \times 10^{-2}$ g of protein per g of AbA, while P450KO had a doubling time of

10 ± 4.0 h and reached a protein concentration of 11 ± 0.5 μg /ml for a growth yield of 0.1 ± 0.6 x 10^{-3} g of protein per g of AbA (Fig 2.3 A) Similarly growth of BKME-9 on 7-oxo-DhA had a doubling time of 4.5 ± 0.6 h and reached a protein concentration of 16 ± 1.0 μg/ml for a growth yield of 0.16 ± 0.01 g of protein per g of 7-oxo-DhA, while P450KO had a doubling time of 7.7 ± 0.7 h and reached a protein concentration of 12 ± 4.0 x 10^{-2} μg/ml for a growth yield of 0.13 ± 0.01 g of protein per g of 7-oxo-DhA.

The growth rates and yields of P450KO were substantially lower than those of BKME-9 on DhA or PaA. Using DhA as a carbon and energy source, BKME-9 had a doubling time of 3.6 ± 0.2 h and reached a protein concentration of 22 ± 0.5 μg/ml for a growth yield of 0.24 ± 0.88 x 10^{-2} g of protein per g of DhA; whereas, P450KO had a doubling time of 10 ± 1.7 h and a reached a protein concentration of only 10 ± 0.6 μg/ml for a growth yield of 0.11 ± 0.40 x 10^{-2} g of protein per g of DhA (Fig. 2.3B). Similarly, on PaA, BKME-9 had a doubling time of 5.6 ± 3.0 x 10^{-2} h and reached a protein concentration of ~27 ± 2.2 μg/ml for a growth yield of 0.3 ± 0.1 x 10^{-2} g of protein per g of PaA; whereas P450KO had a doubling time of 23 ± 2.8 h and reached a final protein concentration of 18 ± 1 μg/ml for a growth yield of 0.2 ± 0.8 x 10^{-2} g of protein per g of PaA. These results suggest that a P450 encoded by *ditQ* plays an important role in metabolism of DhA and PaA but not metabolism of AbA or 7-oxo-DhA.

We cannot exclude the possibility that the *xylE-accC1* insertion cassette used to create P450KO may have a polar effect on transcription of ORFs downstream of *ditQ*. But, this is unlikely given that the cassette does not contain a transcription terminator and so should allow transcription of downstream sequences. Additionally, there is a classic *rho*-independent terminator sequence located 30 bp downstream of *ditQ*. The terminator mRNA sequence forming the stem-loop is 5'ACCCGUGCCU-GAGA-AGGCGCGGGUUUUUU-3' (with underlined bases indicating the stems and hyphens indicating the loop). The 3' end of the mRNA

has poly(U) tail that is required for termination. The hairpin structure has a free energy of –20.5 kcal/mol as predicted by Kinefold (http://kinefold.u-strasbg.fr/) or –19.53 kcal/mol as predicted by RNAfold (http://rna.tbi.univie.ac.at/cgi-bin/RNAfold.cgi).

2.3.4 Abietane removal by P450KO

Abietane diterpenoid removal coincided with increases in protein concentration during growth by both BKME-9 and P450KO (Fig 2.3). Kinetics of removal of AbA and 7-oxo-DhA by P450KO were similar to removal by BKME-9. In contrast, removal of DhA and PaA by P450KO required longer incubation periods than those observed for BKME-9 (Fig. 2.3). By 24 h BKME-9 had removed 100% of the initial DhA, whereas P450KO had only removed ~12%. Similarly, BKME-9 had removed 98% of the initial PaA by 48 hours, whereas P450KO had only removed ~5% by the same time. After 90 hours P450KO had only removed 65% of the original PaA. Along with the removal of PaA by P450KO, accumulation of DhA was also observed (data not shown), suggesting that PaA is transformed to DhA by the strain. The PaA reagent is 90% pure, containing also 7% DhA and 3% AbA. In cultures of P450KO on PaA, the DhA concentration increased to a maximum at 80 hours and was reduced to an undetectable level by 100 hours. The AbA concentration did not increase and was also undetectable by 100 hours. The increase in DhA was not observed when BKME-9 grew on PaA, and in those cultures, the trace amounts of both DhA and AbA associated with the PaA reagent were removed by 50 hours. When P450KO grew on DhA, 2 putative metabolites accumulated. The same two metabolites were also found at lower concentrations when P450KO was grown on PaA. These metabolites did not accumulate when BKME-9 was grown on any resin acid tested. Mass spectral analysis by GC-MS was not sufficient to determine the structure of the metabolites.

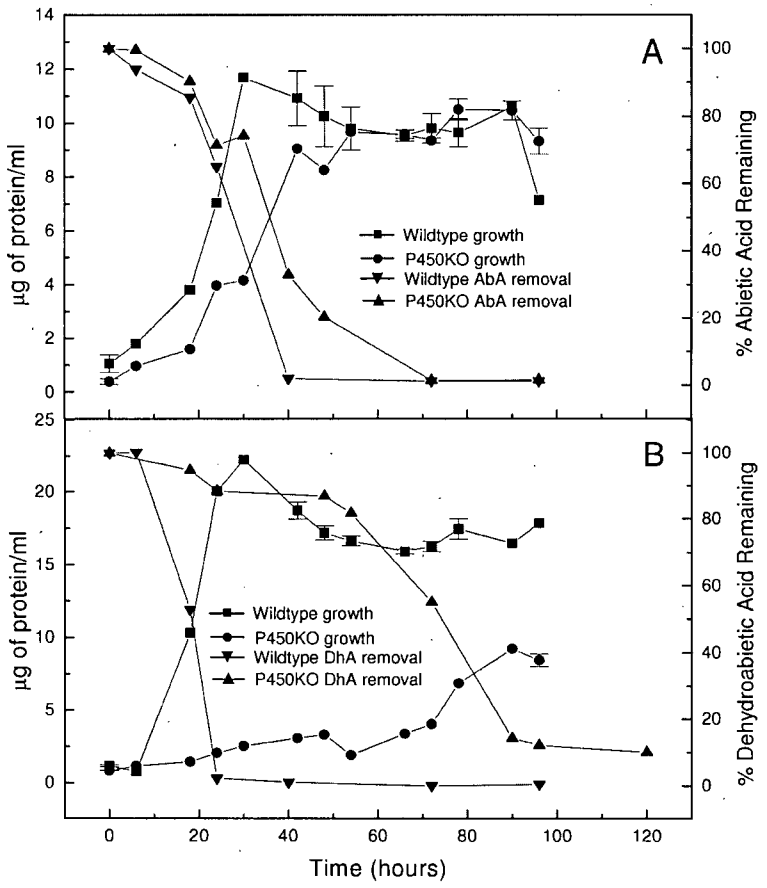

Figure 2.3 Growth and substrate removal of BKME-9 and P450KO on DhA and AbA. A. Protein growth curves of BKME-9 and *ditQ* mutant strain, P450KO, on AbA showing AbA removal. **B.** Protein growth curves of BKME-9 and the *ditQ* mutant strain on DhA showing DhA removal. Error bars indicate standard deviation of the average of 3 samples.
strain. The highest rates of removal occurred during highest rates of growth in all cases.

2.3.5 Specific induction of $P450_{dit}$ by abietane diterpenoids

The *xylE* transcriptional fusion of the *ditQ* knockout strain encodes catechol 2,3-dioxygenase (C23O), which allowed for analysis of induction of *ditQ* transcription by spectrophotometrically monitoring cleavage of catechol in suspended cells incubated with various inducers. The *ditQ* gene was induced by all 4 abietane diterpenoids tested (Fig. 2.4). In fact, a pimerane diterpenoid, isopimaric acid, and a chlorinated diterpenoid, 12,14-dichlorodehydroabietic acid, also induced *ditQ,* despite these two compounds not being growth substrates for BKME-9. However, this is not surprising considering that the same inducers were

identified for *ditA1* and *ditA3*, the genes encoding the α subunit and ferredoxin of the ring hydroxylating dioxygenase, respectively (10). As previously seen with the dioxygenase components, non-diterpenoid compounds did not induce expression of *ditQ* above the level of the pyruvate control.

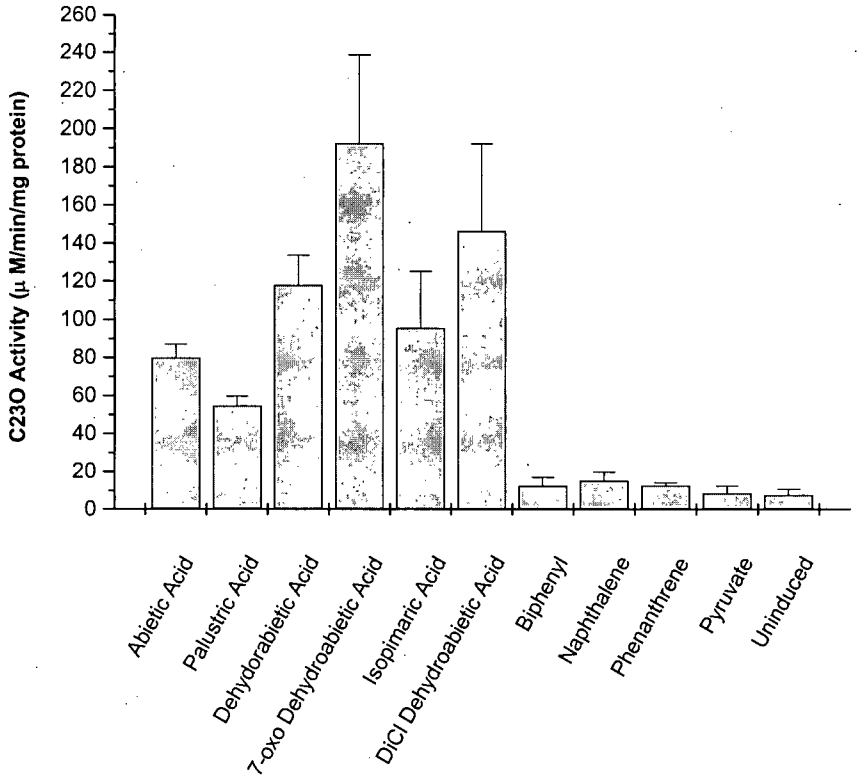

Figure 2.4 Expression of *ditQ-xylE* gene fusion product in response to various diterpenoids and aromatic compounds. C23O activity was assayed spectrophotometrically at 30°C as the formation the yellow catechol cleavage product, 2-hydroxy semialdehyde, at 375 nM (ε = 44 mM^{-1} cm^{-1}) for 3.5 min. Activity values are means ± SD (n=3) of enzyme assays.

2.3.6 $P450_{dit}$ reduced carbon monoxide and substrate binding spectra

P450s are identified by a characteristic Soret maximum at 450 nm in the CO-bound form of the reduced enzyme. The difference spectrum of reduced $P450_{dit}$ expressed in *E. coli* with and without carbon monoxide produced a Soret maximum at 450 nm (not shown). This result confirms that *ditQ* codes for a cytochrome P450.

DhA substrate binding experiments with the crude lysate of *E. coli* expressing $P450_{dit}$ yielded a type I substrate binding spectrum, which is a strong indicator that DhA is a substrate for $P450_{dit}$. Titration of $P450_{dit}$ with DhA yielded a type I substrate binding spectrum with a minimum at 387 and a maximum at 425 nm (Fig. 2.5). Type I curves result from the conversion of low spin hexacoordinated ferric heme with a Soret peak at around 417 nm to a high spin pentacoordinated ferric heme with the displacement of the distal water ligand after substrate binding (9). This results in a decrease in the Soret peak at 417 and an increase of a Soret peak at 387 nm. A plot of the difference in absorbance between 387 nm and 425 nm versus substrate concentration fitted to the binding curve equation gave an estimated K_d of 0.43 μM with a standard deviation of $\pm$ 0.03.

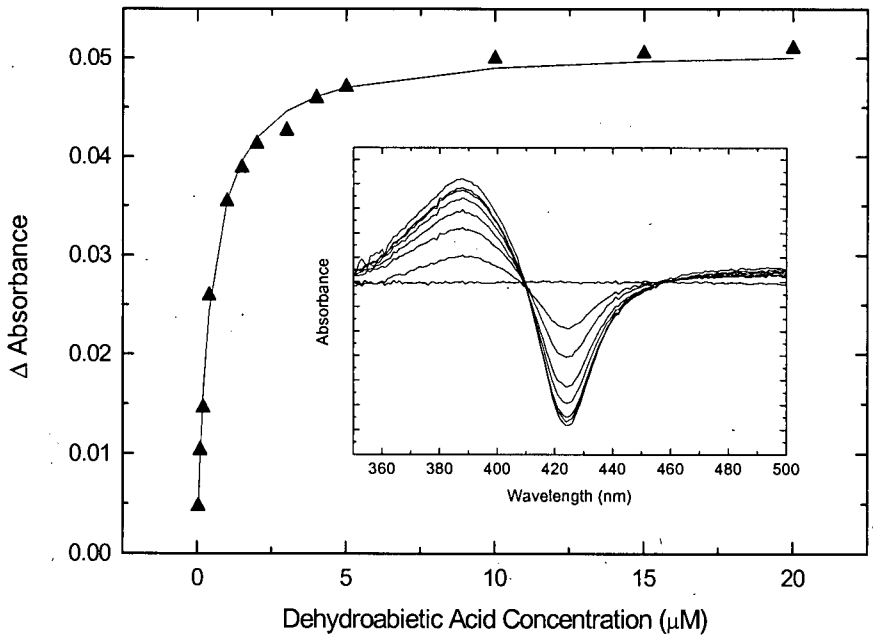

Figure 2.5 Binding spectrum for $P450_{dit}$ with DhA. Data points represent the difference in absorbance between 387 nm and 425 nm caused by increasing DhA concentration. The curve represents a best fit of the data to the binding equation in which $K_d = 0.43 \pm 0.03$ μM and $\Delta A_{max} = 0.05 \pm 6.81 \times 10^{-4}$. Inset: UV/Visible difference spectra of $P450_{dit}$ with increasing concentration of DhA.

Neither AbA nor PaA produced typical P450 substrate binding spectra, and so, are likely not substrates for $P450_{dit}$ (data not shown). Although both seemed to cause a perturbation of the heme environment, resulting in a shift of the Soret maximum, the curves produced were ambiguous, and further study is required for definitive analysis of binding using these compounds. 7-Oxo-DhA is also a growth substrate for BKME-9 but clearly did not bind to $P450_{dit}$ and is therefore not likely a substrate for $P450_{dit}$. Isopimaric acid, which is not a growth substrate for BKME-9, may bind to $P450_{dit}$ weakly but did not yield a typical binding spectrum, and therefore, is not likely a substrate of $P450_{dit}$.

2.4 Discussion

In this study we demonstrated the involvement of a newly identified cytochrome P450 in the metabolism of abietane diterpenoids by BKME-9. A gene knockout of *ditQ,* coding for $P450_{dit}$, indicates that this gene is involved in the degradation of DhA and PaA. The knockout increased the doubling times, and lowered the protein yields of the mutant growing on either DhA or PaA, in comparison to BKME-9 (Fig. 2.3). The $P450_{dit}$ mutant retained the ability to grow slowly on DhA relative to BKME-9. This is an indication that an alternate degradation pathway, not involving $P450_{dit}$, is able to metabolize DhA and PaA. Perhaps it is this same alternate pathway that is responsible for the metabolism of AbA and 7-oxo-DhA. In addition, growth of strain P450KO on PaA or DhA produced the same putative metabolites, suggesting disruption in the metabolism of these compounds at the same point in a convergent pathway. Induction analysis indicates that *ditQ* expression is inducible by a range diterpenoids (Fig. 2.4), while a substrate binding assay showed that DhA is a likely substrate for this enzyme with a relatively low K_d of 0.4 μM (Fig. 2.5).

The results of this study are not in complete agreement with those of Morgan and Wyndham (13), who reported that a *tdtD* mutant of *Pseudomonas* sp. A19-6a retained the ability to grow on DhA and AbA and exhibited similar decreases in removal rates for both substrates.

However, since abietanes were not extracted from the cells in that study, abietanes sorbed to cells but not necessarily degraded would have been considered removed. It is also possible that A19-6a differs from BKME-9 in its complement of diterpenoid degradation enzymes in a way that does not allow for metabolism of AbA in the A19-6a *tdtD* mutant.

We hypothesize that the function of $P450_{dit}$ is to hydroxylate DhA at C-7 (Fig. 2.1). In a previous study on abietane degradation by BKME-9, Martin and Mohn (10) showed that a ring-hydroxylating dioxygenase mutant, BKME-41, accumulated 7-oxo-DhA in cell suspension assays on DhA, PaA or AbA. They also showed that the substrate for the ring hydroxylating dioxygenase, DitA, required a ketone group at C-7, as DhA was not a substrate for the dioxygenase. The bacterial degradation of several natural plant products involves P450 monooxygenases that catalyze ring hydroxylation followed by oxidation of the hydroxyl group to a carbonyl. Some examples of this mechanism include the degradation of camphor involving $P450_{cam}$ (14), the degradation of limonene involving the P450, limonene-6-hydroxylase, (21) and the recently reported degradation of cineole involving $P450_{cin}$ (7). The metabolism of abietane diterpenoids appears to follow the same pattern, with $P450_{dit}$ catalyzing the hydroxylation of DhA to 7-hydroxy-DhA before a further oxidation to 7-oxo-DhA.

Since 7-oxo-DhA is a metabolic intermediate of AbA, and substrate binding assays indicate that AbA is not a substrate of $P450_{dit}$, how then is AbA transformed to 7-oxo-DhA? Possibly another pathway is used for AbA metabolism, involving another P450 which functions to hydroxylate AbA or one of its derivatives. The existence of an additional P450 that can partially complement $P450_{dit}$ could also explain how the $P450_{dit}$ mutant strain was able to grow, albeit slowly, on DhA and PaA. Further, the possibility of a second P450 is also consistent with sequence analysis of *Burkholderia* sp. LB400 (see below).

The results of this study and a previous one (10) are consistent with a mechanism of PaA degradation involving DhA as an intermediate that is subsequently hydroxylated at C-7 by

$P450_{dit}$ (Fig. 2.1). Martin and Mohn (10) showed an accumulation of DhA along with 7-oxo-DhA from PaA in a cell suspension assay of the *ditA1* mutant. In this study, we observed an increase in DhA concentration during growth of the $P450_{dit}$ mutant on PaA. The *dit* cluster contains several putative dehydrogenase genes, which could function in the formation of DhA from PaA. Substrate binding data strongly suggest that DhA is the better substrate for $P450_{dit}$; while, PaA did not produce a typical substrate binding spectrum and does not appear to be a good substrate for this enzyme. Additional work, using a more pure PaA reagent would lead to greater insight regarding this potential substrate.

This study confirms the relationship between the newly described 10.4 kbp extension of the *dit* cluster in BKME-9 and the *tdt* cluster of *Pseudomonas diterpeniphila* A19-6a. These two sequences encode highly similar proteins and share the same gene arrangement (Fig. 2.2). Sequence alignment of the deduced amino acid sequences from the *tdt* cluster with the corresponding putative homologues in the *dit* cluster showed 72% or greater amino acid identity. We hypothesize that the P450 and the putative thiolase, dehydrogenase, isomerase, hypothetical, regulator and CoA-ligase genes of the two organisms are functional homologues. Based on deduced amino acid sequence identity between TdtD and $P450_{dit}$, the latter would constitute a second member of the new P450 family proposed by Morgan and Wyndham (13). (Recently named CYP226A.)

Sequence comparison of the *dit* cluster with the recently sequenced *Burkholderia sp.* LB400 genome suggests that LB400 also contains homologues of *dit* cluster genes. With the exception of *ditE,* coding for a putative permease of the major facilitator superfamily, every protein encoded by the *dit* cluster (including the 10.4 kbp extension) has a putative homologue in a 60 kbp region of the LB400 genome (Fig. 2.2). Further, most of the genes are in small groups that have the same gene order as their putative homologues in BKME-9. An alignment of the deduced amino acid sequence shows high sequence identity between these deduced proteins of

BKME-9 and LB400. Preliminary results indicate that LB400 can grow on DhA as a sole organic substrate (unpublished data). We are currently testing the hypothesis that this 60-kbp region of the LB400 genome codes for proteins that are required for diterpenoid degradation.

Interestingly, the genome sequence of LB400 provides additional evidence for the involvement of two P450s in diterpenoid metabolism. The above 60 kbp region in the LB400 genome includes two genes coding for putative cytochromes P450, BxeC0599 and BxeC0631 (Fig. 2.2), whose deduced protein products both have a high percent identity to $P450_{dit,}$ relative to other P450 homologues in the data bases (Fig. 2.2). Possibly one of the two genes codes for a $P450_{dit}$ homologue responsible for DhA/PaA degradation while a second codes for a second P450 responsible for AbA degradation. Other genes of interest in the 60-kbp region include (i) BxeC0579 with high sequence identity to ferredoxin reductase genes, (ii) BxeC0601, a ferredoxin gene homologue with similarity to those of P450 ferredoxins, and (iii) BxeC0612, a gene putatively coding for a methyl accepting chemotaxis protein. Additionally, the most highly conserved genes shared between the *dit* cluster and the 60kbp region of LB400 are the 2 encoding hypothetical proteins. High sequence conservation suggests that the gene products may perform an essential unknown function. Mutations are currently being generated in LB400 to investigate the functions of selected genes.

Figure 2.1 shows a proposed pathway for abietane diterpenoid metabolism in BKME-9. In this convergent scheme, PaA is transformed to DhA followed by hydroxylation at C-7 and further oxidation to form 7-oxo-DhA. This agrees with a previous reports on resin acid degradation (10, 11), which showed the requirement of a carbonyl group at C-7 for DitA dioxygenase activity and showed the accumulation of 7-oxo-DhA during growth of a *ditA1* knockout mutant on AbA, DhA or PaA. In accordance with the results of this study, AbA is transformed to 7-oxo-DhA without the formation of DhA. Possibly a P450, other than $P450_{dit}$, is involved in this transformation, as suggested by the LB400 genome analysis. We are confident

that DhA is the substrate for $P450_{dit}$, however at this time we have not characterized the product of this reaction. We hypothesize that the product is 7-hydroxy-dehydroabietic acid.

2.6 References

1. **Altschul, S. F., T. L. Madden, A. A. Schaffer, J. Zhang, Z. Zhang, W. Miller, and D. J. Lipman.** 1997. Gapped BLAST and PSI-BLAST: a new generation of protein database search programs. Nucleic Acids Res **25:**3389-402.

2. **Ausubel, F. M.** 1992. Short protocols in molecular biology, 2nd ed. Green Publishing Associates ; John Wiley & Sons, New York, N.Y.

3. **Bicho, P. A., V. Martin, and J. N. Saddler.** 1995. Growth, induction, and substrate specificity of dehydroabietic acid-degrading bacteria isolated from a kraft mill effluent enrichment. Appl Environ Microbiol **61:**3245-50.

4. **Clarke, A. R.** 1996. Analysis of Ligand Binding by Enzymes, p. 199-221. *In* Enzymology Labfax. Academic Press Inc. and BIOS Scientific Publishers, San Diego.

5. **Gerhardt, P.** 1994. Methods for general and molecular bacteriology. American Society for Microbiology, Washington, D.C.

6. **Hanahan, D.** 1983. Studies on transformation of Escherichia coli with plasmids. J Mol Biol **166:**557-80.

7. **Hawkes, D. B., G. W. Adams, A. L. Burlingame, P. R. Ortiz de Montellano, and J. J. De Voss.** 2002. Cytochrome P450(cin) (CYP176A), isolation, expression, and characterization. J Biol Chem **277:**27725-32.

8. **Hoang, H. P. S. a. T. T.** 1995. An improved system for gene replacement and *xylE* fusion analysis in *Pseudomonas aeruginosa*. Gene **158:**15-22.

9. **Jefcoate, C. R.** 1978. Measurement of substrate and inhibitor binding to microsomal cytochrome P-450 by optical-difference spectroscopy. Methods Enzymol **52:**258-79.

10. **Martin, V. J., and W. W. Mohn.** 2000. Genetic investigation of the catabolic pathway for degradation of abietane diterpenoids by *Pseudomonas abietaniphila* BKME-9. J Bacteriol **182:**3784-93.

11. **Martin, V. J., and W. W. Mohn.** 1999. A novel aromatic-ring-hydroxylating dioxygenase from the diterpenoid-degrading bacterium *Pseudomonas abietaniphila* BKME-9. J Bacteriol **181:**2675-82.

12. **Mohn, W. W.** 1995. Bacteria obtained from a sequencing batch reactor that are capable of growth on dehydroabietic acid. Appl Environ Microbiol **61:**2145-50.

13. **Morgan, C. A., and R. C. Wyndham.** 2002. Characterization of tdt genes for the degradation of tricyclic diterpenes by *Pseudomonas diterpeniphila* A19-6a. Can J Microbiol **48:**49-59.

14. **Peterson, J. A., and Y. Ishimura.** 1971. Reaction mechanism of bacterial cytochrome P-450-catalyzed camphor methylene hydroxylation. Chem Biol Interact **3:**300-2.

15. **Peterson, J. A., J. Y. Lu, J. Geisselsoder, S. Graham-Lorence, C. Carmona, F. Witney, and M. C. Lorence.** 1992. Cytochrome P-450terp. Isolation and purification of the protein and cloning and sequencing of its operon. J Biol Chem **267:**14193-203.

16. **Schweizer, H. P., and T. T. Hoang.** 1995. An improved system for gene replacement and *xylE* fusion analysis in *Pseudomonas aeruginosa*. Gene **158:**15-22.

17. **Simons, R., U. Priefer, and A. Puhler.** 1983. A broad host range mobilization system for in vivo genetic engineering: transposon mutagenesis in Gram negative bacteria. Bio/Techonology **1:**784-790.

18. **Smith, P. K., R. I. Krohn, G. T. Hermanson, A. K. Mallia, F. H. Gartner, M. D. Provenzano, E. K. Fujimoto, N. M. Goeke, B. J. Olson, and D. C. Klenk.** 1985. Measurement of protein using bicinchoninic acid. Anal Biochem **150:**76-85.

19. **Stassi, D., S. Donadio, M. J. Staver, and L. Katz.** 1993. Identification of a *Saccharopolyspora erythraea* gene required for the final hydroxylation step in erythromycin biosynthesis. J Bacteriol **175:**182-9.

20. **Unger, B., I. Gunsalus, and S. Sligar.** 1986. Nucleotide sequence of the *Pseudomonas putida* cytochrome P-450cam gene and its expression in Escherichia coli. J. Biol. Chem. **261:**1158-1163.

21. **Wust, M., and R. B. Croteau.** 2002. Hydroxylation of specifically deuterated limonene enantiomers by cytochrome P450 limonene-6-hydroxylase reveals the mechanism of multiple product formation. Biochemistry **41:**1820-7.

22. **Yanisch-Perron, C., J. Vieira, and J. Messing.** 1985. Improved M13 phage cloning vectors and host strains: nucleotide sequences of the M13mp18 and pUC19 vectors. Gene **33:**103-19

23. **Zon, L. I., D. M. Dorfman, and S. H. Orkin.** 1989. The polymerase chain reaction colony miniprep. Biotechniques **7:**696-8.

3. The LB400 *dit* Cluster[1]

3.1 Introduction

Bacteria of the genus *Burkholderia* have been isolated throughout the environment and have significant interactions with both plants and animals. The ability to colonize both plant and animal tissue gives this group of bacteria interesting ecological niches. In humans, bacteria comprising the *Burkholderia cepacia* complex (Bcc) have been associated with respiratory tract infections in patients with cystic fibrosis (8). In plants, the relationship can be beneficial, preventing disease and contamination or promoting growth, nodule formation or nitrogen fixation (7), or deleterious, causing disease (28). However, the likely role for the majority of *Burkholderia* species is a non-pathogenic interaction with plant rhizospheres (8).

Burkholderia xenovorans LB400 was isolated from a PCB-contaminated landfill in New York State (15). The genome of *B. xenovorans* LB400 was recently sequenced and annotated (5). This large bacterial genome containing ~9000 coding sequences is 9.7 Mbp and is comprised of three replicons – chromosome 1 (4.87 Mbp), chromosome 2 (3.36 Mbp) and a megaplasmid (1.47 Mbp). Functional genomics of LB400 have focused on biphenyl, benzoate, and C1 metabolic pathways (10-12). During the course of research summarized in Chapter 2, a cluster of genes in LB400 encoding proteins with high sequence identity to those encoded by the *Pseudomonas abietaniphila* BKME-9 *dit* cluster was discovered. Other bacteria from the genus *Burkholderia* have been found to mineralize abietane diterpenoids (23), however, this is the first bacterium for which complete genomic information is available allowing for the first genomic investigation of abietane diterpenoid catabolism.

This chapter describes growth of LB400 on 4 abietane diterpenoids and changes in the LB400 *dit* cluster mRNA levels between cultures grown on DhA or succinate, using microarray transcriptomic analysis. The necessity of the LB400 *dit* cluster was established through mutation

[1] A version of this chapter will be submitted for publication.

of *ditA1* encoding a ring-hydroxylating dioxygenase. Using analysis of metabolites in cell suspensions, we show the similarity between the degradation of abietane diterpenoids by LB400 and BKME-9.

3.2 Methods and Materials

Table 3.1 Strains and plasmids used in this study

	Genotype or Description	Reference or Source
Strains		
Burkholderia xenovorans		
LB400	Wild type; grows on abietane diterpenoids	(15)
DitA1KO	*ditA1*::*accC1*; Gm^r	This study
Escherichia coli		
DH5α	*endA1* hsdR17 (r_k^- m_k^-) *supE44 thi*-1 *recA1 gyrA* (Nal^r) *relA1 Δ(lacIZYA-argF) U169 deoR (ϕ80dlacΔ(lacZ)M15)*	Gibco BRL
S17-1	*recA pro thi hsdR* with integrated RP4-2-TcMu::Kna::Tn7; Tra^+ Tr^r Sm^r	(31)
Plasmids		
pEX100T	*sacB* conjugable plasmid for gene replacement; Ap^r	(30)
pX1918G	*xylE-accC1* fusion cassette-containing plasmid; Ap^r Gm^r	(30)
pDS2	1.8 kbp PCR amplicon containing LB400 *ditA1* cloned into the unique *Xma*I site of pEX100T	This study
pDS3	1482-bp *EcoR*V-*Sma*I of pDS1 cloned into the *Sma*I site of pEX100T	This study

Bacterial strains, plasmids, and culture conditions. The bacterial strains and plasmids used in this study are listed in Table 3.1. *E. coli* was cultured on Luria-Bertani (LB) medium and incubated at 37°C, and *B. xenovorans* strains were cultured at 30°C on LB without NaCl or K1 mineral medium (11) supplemented with biphenyl vapors, 1 g per litre succinate, 90 mg per litre AbA, 90 mg per litre DhA, 90 mg per litre PaA, or 95 mg per litre 7-oxo-DhA. LB400 was streaked out from frozen stock on 1.5 % purified agar K1 plates, which were inverted over a petri dish lid containing biphenyl crystals and incubated for 3-4 days. DitA1KO was streaked out as above or on 1.5 % agar LB without NaCl plates containing 10 mg/ml of gentamycin and incubated for 2-3 days. Liquid cultures were incubated on a rotary shaker at 200-250 rpm.

Growth was monitored by analysis of optical density (OD) or protein concentration. Protein concentrations were determined using the micro-bicinchoninic acid (BCA) protein assay kit (Sigma) as described in Chapter 2 (pg. 48). 1 litre K1 was prepared by combining 100 ml of 10X K1 stock with 20 ml of Hunter mix and adding autoclaved distilled and 880 ml deionized H_2O (ddH_2O) for liquid medium or ddH_2O plus 1.5% purified agar (Becton Dickinson, Cockeysville, MD) for plates. 10X K1 stock was prepared by adding 31.8 g K_2HPO_4, 5 g $(NH_4)_2SO_4$, and 3.54 g $NaH_2PO_4 \cdot H_2O$ to 700 ml of ddH_2O while stirring, followed by addition of ddH_2O to a final volume of 1 litre. The solution was then equally divided and transferred to 2-1 litre bottles and autoclaved for 30 minutes. After cooling 250 μl (10 mg/ml in water) of the following vitamins, thiamine, nicotinic acid, inositol, and riboflavine were added to each 500-ml autoclaved portion. In addition 25 μl of 2 mg/ml biotin in methanol was added to each 500-ml portion. Bottles were then wrapped with aluminium foil and stored at room temperature. 1 litre Hutner mix was prepared by adding 10 g of nitrilotriacetic acid to 600 ml of ddH_2O. KOH pellets were then added slowly while stirring until all nitrilotriacetic acid had dissolved. Next 14.45 g of $MgSO_4 \cdot 7H_2O$, 3.33 g $Ca(NO_3)_2$, 9.25 mg $(NH_4)_6Mo_7O_{24} \cdot 24H_2O$, 99 mg $FeSO_4 \cdot 7H_2O$, and 50 ml of Metals 44 (see below), were combined with ddH_2O to 1 litre. The pH of the solution was adjusted to 6.6 to 6.8 and then the solution was equally divided and transferred to 3-500 ml bottles with screw caps and autoclaved for 30 minutes. Solutions were stored at room temperature. Metals 44 was prepared by combining 1g EDTA, 4.4 g of $ZnSO_4 \cdot 7H_2O$, 2 g $FeSO_4 \cdot 7H_2O$, 620 mg of $MnSO_4 \cdot H_2O$, 119 mg of $CuSO_4 \cdot 5H_2O$, 99.4 mg of $Co(NO_3)_2 \cdot 6H_2O$ and 70.8 mg of $Na_2B_4O_7 \cdot 10H_2O$ and adding ddH_2O to 400 ml, with the addition of a few drops of concentrated H_2SO_4 to dissolve, and autoclaved for 30 minutes and stored at room temperature.

LB400 from frozen stock was initially grown on biphenyl vapors as a means of selection. For cultures used in transcriptomic analysis, LB400 colonies grown on biphenyl vapors were used to

inoculate 50 ml of K1 containing 1 g per litre of succinate. After 24 hours the culture reached late log-phase (OD_{600} ~ 0.9) and cells were transferred to fresh K1 containing 1 g per litre of succinate at an initial OD_{600} of 0.001. After approximately 18 hours, this second succinate culture reached mid-log phase (OD_{600} 0.68). For analysis of succinate-grown LB400 and RNA extraction, cells from the second succinate culture were used to inoculate 2 –200-ml cultures of K1 containing 1g per litre succinate. From this point on, each 200-ml culture was treated separately and each represented a biological replicate. After 18 hours of incubation, cultures had reached mid-log phase (OD_{600} of 0.5) and cells were harvested as described below.

For analysis of DhA-grown LB400 and RNA extraction, cells from a second succinate culture (as described above) were transferred to a K1 medium containing 90 mg per litre of DhA with an initial OD_{600} of 0.01. After approximately 140 hours, the culture had reached late-log phase (OD_{600} of 0.15) and cells were transferred to a fresh K1 medium containing DhA at an initial OD of 0.001. After approximately 48 hours of incubation the culture had reached a mid- to late-log phase (OD_{600} of 0.07 to 0.1). Cells from this second DhA culture were then used to inoculate 2 –300-ml K1 cultures containing 90 mg per litre of DhA with an initial OD_{600} of 0.001. From this point on, each 300-ml culture was treated separately and each represented a biological replicate. After approximately 45 hours, each culture reached mid-log phase (OD_{600} 0.065 and 0.057) and cells were harvested.

Harvesting cells. Plate counts revealed that each succinate-grown culture contained approximately 10^8 colony-forming units (CFU)/ml while DhA-grown cultures contained approximately 10^7 CFU/ml of culture. Several aliquots of approximately 10^9 cells were collected for RNA extraction from each culture (10 ml of succinate-grown culture and 100 ml of DhA-grown culture). Cells were harvested as follows: immediately after incubation was halted, cultures were cooled on ice and an amount equal to 10% of the volume of 5% phenol in ethanol was added and mixed by inversion. Cells were harvested by centrifugation at 8800 rpm at 4°C

for 10 min. One ml of supernatant from each culture was removed and transferred to a 1.7 ml Eppendorf tube. The remainder of the supernatant was decanted, and the pellets of succinate- or DhA-grown cells were suspended in 10 or 100 µl, respectively, of the supernatant (removed in the last step) and 10 or 100 µl of RNA later (Qiagen). The cell suspensions were then transferred to 1.7 ml Eppendorf tubes, frozen in liquid nitrogen and stored at –80°C.

RNA Extraction. Each sample for RNA extraction was subdivided into 5 aliquots to optimize RNA extraction using the RNAeasy RNA extraction kit (Qiagen) as per manufacture's instructions. Nucleic acid was eluted from the column using 35 µl of RNase-free water two times. Nucleic acid content was quantified by UV spectroscopy. Following RNA extraction, samples were combined and DNA was removed by treatment with DNase I (Roche) as per manufacture's instructions for 30 min at room temperature. The sample was then phenol/chloroform extracted and centrifuged for 5 min at 6000 rpm. The water phase was recovered and 1/10 volume of 3M NaOAc (pH5.2 Sigma) was added, mixed and supplemented with 1 volume of cold (4°C) isopropanol (Sigma). After thorough mixing by inversion, the tube was centrifuged for 20 min at 4°C and the supernatant was removed. The pellet was then washed with 80% ethanol followed by a 20-min centrifugation at 4°C. The supernatant was then removed and allowed to air dry for ~5 min. The pellet was then suspended in 35 µl of nuclease-free water and heated at 50°C for 5-10 min to dissolve RNA. UV spectroscopy was used to determine RNA quantity and purity.

RNA Aminoallyl labelling. To generate cDNA with incorporated aminoallyl dUTP, 2 µg of RNA plus 2 µl of Random Hexamers (Invitrogen) (3 mg/ml) were combined and adjusted to a final volume of 15 µl with RNase-free water. The solution was mixed well and incubated at 70°C for 10 minutes and then placed immediately on ice. Next, 6 µl of 5X first strand buffer, 3 µl of 0.1 M DTT, 1.2 µl of 25X aminoallyl-dNTP mix (5 µl of 100 mM dATP, 5 µl of 100 mM dCTP,

5 µl 100 mM of dGTP, 3 µl 100 mM of dTTP, plus 2 µl 100 mM of aminoallyl-dUTP), 2 µl of SuperScript II RT (Invitrogen) (200 U/µl) and 2.8 µl of MilliQ water were combined and incubated at 42°C for 3 hours. To hydrolyze RNA, 10 µl 1 M NaOH, and 10 µl of 0.5 µl EDTA, were combined and mixed and incubated at 65°C for 15 minutes. To neutralize pH, 25 µl 1 M Tris (pH 7.4) or 10 µl of 1 M HCl was added. To remove unincorporated aa-dUTP and free amines, a modified Qiagen Qiaquick PCR purification kit protocol was used. A phosphate wash buffer and elution buffer (EB) were substituted for the Qiagen supplied buffer, because Qiagen buffers contain free amines, which compete with the Cy-dye coupling reaction. One hundred ml of phosphate buffer (5 mM KPO_4, pH 8.0, 80% ethanol) was prepared by mixing 0.5 ml 1 M KPO_4, 15.25 ml of MilliQ water, and 84.25 ml 95% ethanol. Phosphate EB was prepared by diluting 1 M KPO_4 (pH 8.5) to 4.0 mM with MilliQ water. The cDNA was eluted twice with 30 µl of phosphate EB. The sample was then dried in a speed vacuum system.

Coupling of Cy ester to aminoallyl-labeled cDNA. The cDNA was suspended in 4.5 µl of 0.1 M sodium carbonate buffer (Na_2CO_3), pH 9.0. 4.5 µl of the appropriate NHS-ester Cy dye (prepared as per manufacturer's instructions in DMSO) and incubated 1 hour in the dark at room temperature. Uncoupled dye was removed using the Qiagen Qiaquick PCR purification kit protocol and eluted twice with 30 µl of EB. The quantity of labelled cDNA and the fluorophore incorporation efficiency were determined by using UV-visible spectrophotometry. Cy3/Cy5 labelled probes were dried in a speed vac and stored at –80°C.

Hybridization. Hybridization and scanning were conducted at Michigan State University in the lab of Dr. J. Tiedje using microarray technology developed by Xeotron Technologies (14) and chips described in (10) and (5). Two biological replicates were used for hybridizations. cDNA generated from LB400 grown on DhA was labelled with Cy3 in one hybridization and Cy5 in the other and visa versa for LB400 grown on succinate. The LB400 array comprises 2 chips

containing a total of ~16000 probes. These represent ~8450 CDS's of the ~9000 in the current annotation. Briefly, hybridizations were conducted in a Xeotron M-2 microfluidic hybridization station as per manufacturer's instructions. All buffers were passed through a 0.22 micron filter (Corning Costar Corporation, Cambridge, Massachusetts) prior to hybridization to minimize particulate matter interference with the chips. Two hundred pmol of labelled cDNA per dye per chip were used for hybridization. Labelled cDNA was suspended in 100 µl of hybridization mix containing 33 µl of 18X SSPE (pH 6.6), 25 µl of 100% formamide, 4 µl of 10% Triton-X100, plus labelled cDNA and nuclease-free water to 100 µl. Samples were heated at 95°C for 3 minutes, placed immediately on ice for 1 min and then filtered through 0.22 micron filters as above. Samples were hybridized at 32°C at a flow rate of 300 µl/minute for 18 hours.

Scanning and data analysis. Microarray scanning and data analysis were conducted as previously reported (10). Briefly, microarrays were scanned using an Axon 4000B (Axon Instruments) scanner and data files were extracted using Genepix 5.0 (Axon Instruments). Data from two genomic sub-chips were merged and median signal intensity for both 635-nm (Cy5) and 532-nm (Cy3) were imported into Genespring 7.0 (Silicon Genetics) and normalized using Lowess intensity-dependent normalization. GeneSpring's one sample Student *t*-test algorithm was used to test whether the mean $\log_2$ ratio (DhA/Succinate) values of biological replicates were significantly different from zero. In general, a gene transcript was considered up-regulated when the $\log_2$ ratio was greater than one and the *p* value was less than 0.05, and, was considered down-regulated when the $\log_2$ ratio was less than 0.5 and the *p* value was less than 0.05. Values *M* [$M = \log_2(\text{Cy5/Cy3})$] versus A [$A = \log_2(\sqrt{(Cy5 \times Cy3)}$] were determined for each biological replicate according to the method of Dudoit et al. (13) and plotted to assess normalized data quality.

Cell suspensions. LB400 or DitA1KO colonies were used to inoculate 100 ml of K1 containing 1 g per litre succinate. When the OD_{600} reached between 0.4 and 0.8, cells were transferred to 100 ml of fresh K1 medium containing 1 g per litre succinate with an initial OD_{600} of 0.001 and incubated as above. When the OD_{600} reached between 0.3 and 0.4, cells were transferred to 1 litre of K1 containing 1 g per litre of succinate for an initial OD_{600} of 0.001 in a 2-litre Erlenmeyer flask. When the OD_{600} of these cultures' reached 0.4-0.6, cells were harvested by centrifugation for 10 minutes at 8800 X g, washed with K1 salts containing no vitamins or Hunter mix, and suspended at an OD of ~ 3.0 in K1 medium. The culture was then divided into 4 equal samples of approximately 50 ml each and 90 mg per litre AbA, 90 mg per litre DhA, 90 mg per litre PaA, or 95 mg per litre 7-oxo-DhA was added to each culture. Aliquots of 1.5 ml were collected at various time points and after addition of 2-3 drops of 1N HCl samples were frozen at –20°C for later analysis by gas chromatography–mass spectrometry (GCMS). Cell suspension assays were conducted in duplicated with representative curves presented in the results (Fig 3.2).

After thawing samples, an internal standard of 12,14-dichlorodehydroabietic acid was added to each 1.5-ml aliquot to a final concentration of 50 μM and samples were extracted twice with equal volumes of ethyl acetate and dried over anhydrous Na_2SO_4. Samples were derivatized using diazomethane. GC electron impact (EI) mass spectrometry of methyl ester derivatives was conducted as previously described in Chapter 1, using an Agilent Technologies 6890N Network GC system equipped with an Agilent 5973 Mass Selective Detector. National Institute of Standards and Technology MS Search (2.0) was used to analyze mass spectral data.

Disruption of *ditA1*. LB400 genomic DNA was used as the template in a PCR with primers P1 (5'-ATA GCC CGG GAA CAG TTG CGC CTA CCT GAA G-3') and P4 (5'-TTA GCC CGG GTA TAG ATC AGG TCC TCC GCA-3'), both containing 5' *Xma*I restriction site extensions (underlined), to amplify a 1797-bp fragment containing *ditA1*. The resulting amplicon was

digested with *Xma*I and then ligated to the unique dephosphorylated *Xma*I site of pEX100T, containing the *sacB* counter selectable marker, and used to transform *E. coli* DH5α. Electroporation and selection of white colonies were used as described in Chapter 2. Plasmid DNA was then extracted with QIAprep Spin Miniprep columns as above, digested with *Sph*I, and run on a 0.7 % agarose gel to identify clones containing inserts with the correct orientation. The successful ligation was designated pDS2. Next, the *xylE-accC1* transcriptional fusion antibiotic cassette of pX1918G was amplified using primer C1 (5'-TAG GCG CGC CGA GAG CAC CGC GAT CAA GGA-3') containing a 5' *Asc*I restriction site extension (underlined) and C2 (5'-CAT GAA TTC CGA ATT CCG ATC CGT CGA GA-3') containing a 5'*EcoR*I restriction site extension (underlined). The resulting 2.1-kbp amplicon and pDS2 were digested with *EcoR*I and *Asc*I. Digested pDS2 was run on a 1.0% agarose gel and a 6939-bp fragment was extracted from the gel as described in Chapter 2. The 2.1-kbp amplicon and 6.9-kbp pDS2 fragment were ligated to generate pDS3 and this was used to transform, by electroporation, mobilization strain *Escherichia coli* S17-1. Successful transformants were selected as described in Chapter 2. Homologous recombination of the mutated allele into strain LB400 was accomplished by diparental conjugation using a filter membrane essentially as described in (9). In general S17-1 containing pDS3 and LB400 were grown overnight on LB with 10 mg/ml gentamycin and LB (-NaCl), respectively. Fresh LB with 10 mg/ml gentamycin and LB (-NaCl) were inoculated (10%) with the respective overnight cultures and the new cultures were grown until the OD_{600} reached 1-1.5. One ml of the donor cells S17-1 containing pDS3 was washed 2 times with LB and suspended in 1 ml of LB. Next, 100 µl of donor cells and 100 µl of recipient cells were suspended in 0.8% sterile saline and vortexed for 10 seconds at medium speed. The mating mixture was then transferred to a 5-ml syringe and filtered with a 0.22 µM cellulose filter (Millipore GV type) in a reusable filter case. The filter was then removed with forceps and placed with the cells on the upper face on an LB (-NaCl) plate and incubated for ~ 24 hours at

30°C. The filter was then removed with forceps and washed by vortexing in 5 ml of sterile saline, which was then plated on K1 purified 1.5% agar plates supplemented with 1 g per litre pyruvate plus 10 mg/ml gentamycin, followed by a two step selection method as previously described (20) and Chapter 2. Homologous recombination was confirmed by PCR amplification of a 3350-kb fragment using primers P1 and P4 at an annealing temperature of 56.3°C and identified on an agarose gel. The lack of a 1.7-kbp band, and gentamycin resistance further confirmed the desired construct. The 3350-kbp fragment was also sequenced using primers P1 and P4, and the resulting sequence was compared to the expected insertion sequence.

3.3 Results

Table 3.2 Growth characteristics of LB400 on four abietane diterpenoids

	7-oxo-DhA n=4	DhA n=4	AbA n=3	PaA n=3
Lag phase (hours)	121 (4)	134 (6)	258 (21)	248 (5)
Doubling time (hours)	23 (4)	17 (1)	37 (2)	19 (1)
Maximum Protein Concentration (μg /ml culture)	18.3 (1.2)	25.5 (0.9)	10.9(1.3)	26.0 (1.1)
Growth Yield g of protein/ g of substrate	0.19 (0.01)	0.28 (0.01)	0.12 (0.01)	0.29 (0.01)

Initial inoculum for each culture was ~2 x 10^6 cells/ml grown to mid-log phase on succinate. Numbers in brackets indicate standard error. All growth was carried out in K1 mineral salt media with an initial abietane diterpenoids concentration of 300 μM.

3.3.1 LB400 growth on abietane diterpenoids

The genome of *B xenovorans* LB400 was found to contain a large cluster of genes with high similarity to those encoding abietane diterpenoid catabolism by *P. abietaniphila* BKME-9 (32). To determine if LB400 can catabolize diterpenoids, growth assays were conducted. LB400 grew on the abietane diterpenoids, AbA, DhA, PaA, or 7-oxo-DhA as sole sources of carbon and energy (Fig. 3.1, Table 3.2, see Fig. 3.5 for chemical structures). LB400 failed to grow on the pimerane diterpenoids, isopimaric acid and pimaric acid. Initial lag phases preceding growth on the abietanes were long and variable. The lag phase was shortest on the more soluble, aromatic compounds, 7-oxo-DhA and DhA and longer on the less-soluble, non-aromatic compounds, AbA and PaA. While the lag phase on PaA was almost double of that on DhA, the doubling times and yields were similar on the two compounds. 7-Oxo-DhA and AbA supported much lower maximum final protein concentrations and growth yields than DhA or PaA. Growth on AbA and DhA was confirmed by monitoring substrate removal and protein increase.

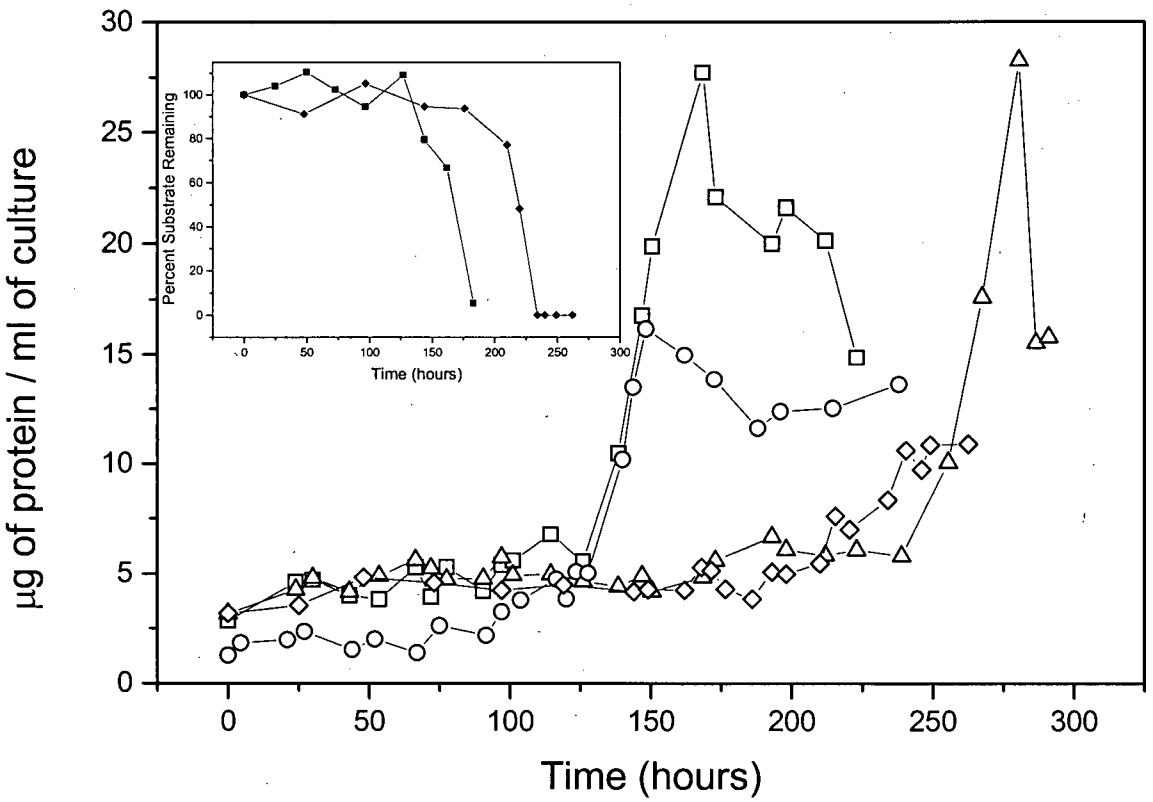

Figure 3.1 Growth curves of LB400 on four abietane diterpenoids. Initial inoculum for each culture was ~2 x 10^6 cells/ml grown to mid-log phase on succinate. Data are representative growth curves (n= 3-4). All growth was carried out in K1 mineral salt media with an initial abietane diterpenoid concentration of 300 µM. Symbols, LB400 growth on ◊ - AbA, □ – DhA, △ - PaA, and ○.- 7-oxoDhA. Inset: Substrate removal during growth. Symbols, ♦-AbA, ■ –DhA.

Rates of LB400 growth coincided with maximum rates of substrate removal, and entry into stationary phase coincided with complete removal of the substrates (Fig. 3.1).

Inocula for initial LB400 growth assays on abietane diterpenoids were grown on succinate as described in the Materials and Methods. When cells grown on DhA were transferred to fresh medium with DhA, the lag phase was reduced from over 130 hours to less than 24 hours, and the doubling time was reduced from 17 to approximately 8 hours. Further transfers on DhA resulted in minimal change in growth kinetics. A similar effect was observed with serial transfers on AbA, PaA and 7-oxo-DhA. To confirm that the LB400 *dit* cluster contains genes required for abietane degradation we generated a knockout of the gene encoding the alpha-subunit of the

ring-hydroxylating dioxygenase, *ditA1*, producing strain DitA1KO. During 400 hours of incubation DitA1KO did not grow on AbA, DhA, PaA or 7-oxo-DhA as sole organic substrates.

3.3.2 Metabolic analysis of LB400 and DitA1KO cell suspensions

Cell suspensions of LB400 removed AbA, DhA, PaA or 7-oxo-DhA completely; whereas, DitA1KO only slightly reduced concentrations of the substrates (Fig. 3.2). As previously reported (22), boiling the cells prior to incubation, nearly abolished removal of

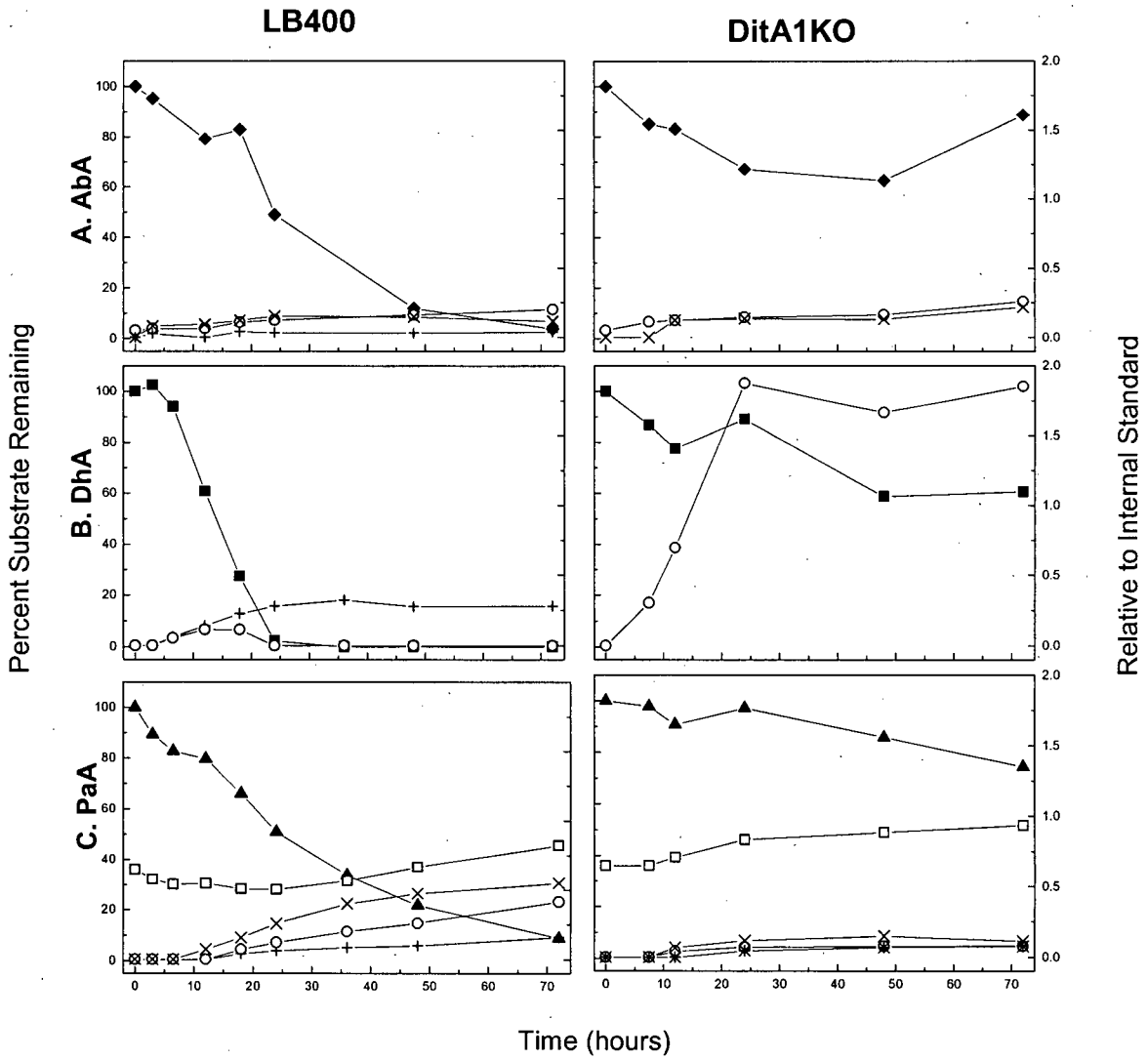

Figure 3.2 Cell suspensions of LB400 and DitA1KO with AbA, DhA, and PaA. A. AbA cell suspension, B. DhA cell suspension, C. PaA cell suspension. Left hand charts correspond to LB400 and right hand charts are DitA1KO. Open symbols indicate values corresponding to the left y-axis and open or stick symbols indicate values corresponding to the right y-axis. Symbols, ♦-AbA, ■ and □-DhA, ▲ - PaA, ○- 7-oxoDhA, +- dimethyl heptanedioic acid, and ×- Unknown I.

abietane diterpenoids; however, some initial removal (< 20%) was detected. In these cases no metabolites were formed, therefore removal was likely the result of sorption of diterpenoids to culture tubes or to the cell debris.

7-Oxo-DhA was detected in both LB400 and DitA1KO cell suspensions. LB400 transiently accumulated small amounts of 7-oxo-DhA during incubations with AbA, DhA, or PaA (Fig 3.2). All 7-oxo-DhA was completely removed within 144 hours by LB400 in all cases (not shown). DitA1KO increased 7-oxo-DhA concentrations during incubations with AbA, PaA, and particularly with DhA, but did not remove it, even after 144 hours of incubation. A second peak, observed only in LB400 cell suspensions, was identified as 2,4-dimethyl heptanedioic acid (DMHDA) by a NIST library search. LB400 accumulated small amounts of DMHDA in all cases and did not remove the accumulated DMHDA by 144 hours. Other metabolites were detected in both LB400 and DitA1KO cell suspensions on AbA, DhA, or PaA.

A peak with a retention time relative to the internal standard DiCl DhA of 0.96 (Unknown I) accumulated in both LB400 and DitA1KO cell suspensions with AbA and PaA but not on DhA. Unknown I could not be identified using a NIST library search of the MS spectrum. The 5 largest peaks of the MS spectrum are 255, 330, 256, 163, and 271 with the molecular ion at 330. Comparison of the mass spectrum of 7oxo-DhA methyl ester (MW 328) with that of the Unknown I (m/z 330) showed similar fragmentation patterns differing by an m/z of 2 (not shown), suggesting structural similarity. Major MS peaks from Unknown I correspond to loss of the methyl group of the methyl ester ($-CH_3$) (315/313), the carboxyl group (–COO) (271/269) and the ketone (-O) (255/253).

In PaA cell suspensions (Fig 3.2 C), DhA present as a contaminant in the initial substrate mixture decreased slightly during incubation with LB400 for 6 hours, but after this time, the DhA concentration increased and reached a maximum level at 72 hours. By 96 hours all accumulated DhA was removed by LB400 (not shown). In PaA cell suspensions, DitA1KO

increased the DhA concentration without an initial detected decrease for 72 hours. The DhA concentration then remained steady for at least 144 hours. The DhA concentration did not increase during incubation of boiled cell controls for 144 hours, indicating that this transformation from PaA to DhA is enzymatic. In 7-oxo-DhA cell suspensions, the substrate was removed within 24 hours by LB400 and not removed by the DitA1KO; however, the 7-oxo-DhA concentration did initially decrease (data not shown).

3.3.3 Transcriptomic analysis

Changes in gene regulation between LB400 growing exponentially on DhA or succinate were monitored by analysis of differences in mRNA levels using microarray transcriptomic analysis. Normalized data quality was evaluated using M-versus-A plot of the combined genomic chip set (Fig. 3.3), which indicated the absence of signal intensity-dependent bias.

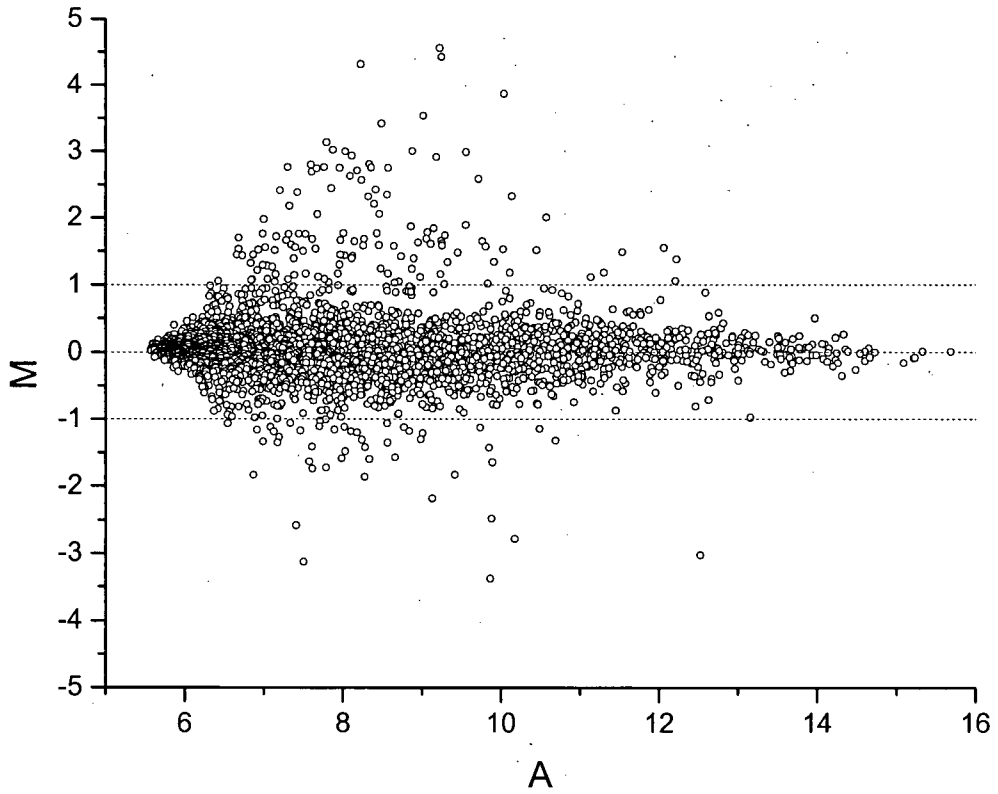

Figure 3.3 Plots of M versus A of the combined genomic chip set after Lowess intensity dependent normalization. $M = \log_2(\text{DhA signal intensity}/\text{Succinate signal intensity})$, $A = \log_2(\sqrt{\text{DhA signal intensity} \times \text{Succinate signal intensity}})$

Comparison of raw and normalized signal intensity revealed that although the growth rate of LB400 on succinate was substantially higher than that on DhA, RNA expression levels for several housekeeping genes showed only minor variations and therefore did not have an effect on overall transcriptomic analysis.

3.3.3.1 *Dit* cluster

Of the 72 genes from BxeC0578 to BxeC0649, 43 are up regulated, with a > 2 fold increase ($p < 0.05$) in expression, during growth on DhA versus on succinate (Fig. 3.4). This cluster, found on the LB400 megaplasmid, has been named the LB400 *dit* cluster for diterpenoid degradation encoding genes. (Fig. 3.4, Table 3.3). Based on similar expression levels, the same gene orientation and proximity, it is possible to predict several putative mRNA transcripts up-regulated during growth on DhA including, BxeC0583-BxeC0585, BxeC0586-BxeC0587, BxeC0590, BxeC0591, BxeC0592, BxeC0594-BxeC0597, BxeC0599, BxeC0600-BxeC0606, BxeC0609-BxeC0610, BxeC0616-BxeC0620, BxeC0621-BxeC0623, BxeC0624-BxeC0627, BxeC0638-BxeC0640, BxeC0641-BxeC0648. The most highly induced genes during growth on DhA versus succinate were BxeC0605 (encoding a putative acyl CoA dehydrogenase), BxeC0606 (encoding a conserved hypothetical protein), BxeC0642 (encoding a putative dehydrogenase), and BxeC0643 (encoding a putative enoyl CoA hydratase/isomerase).

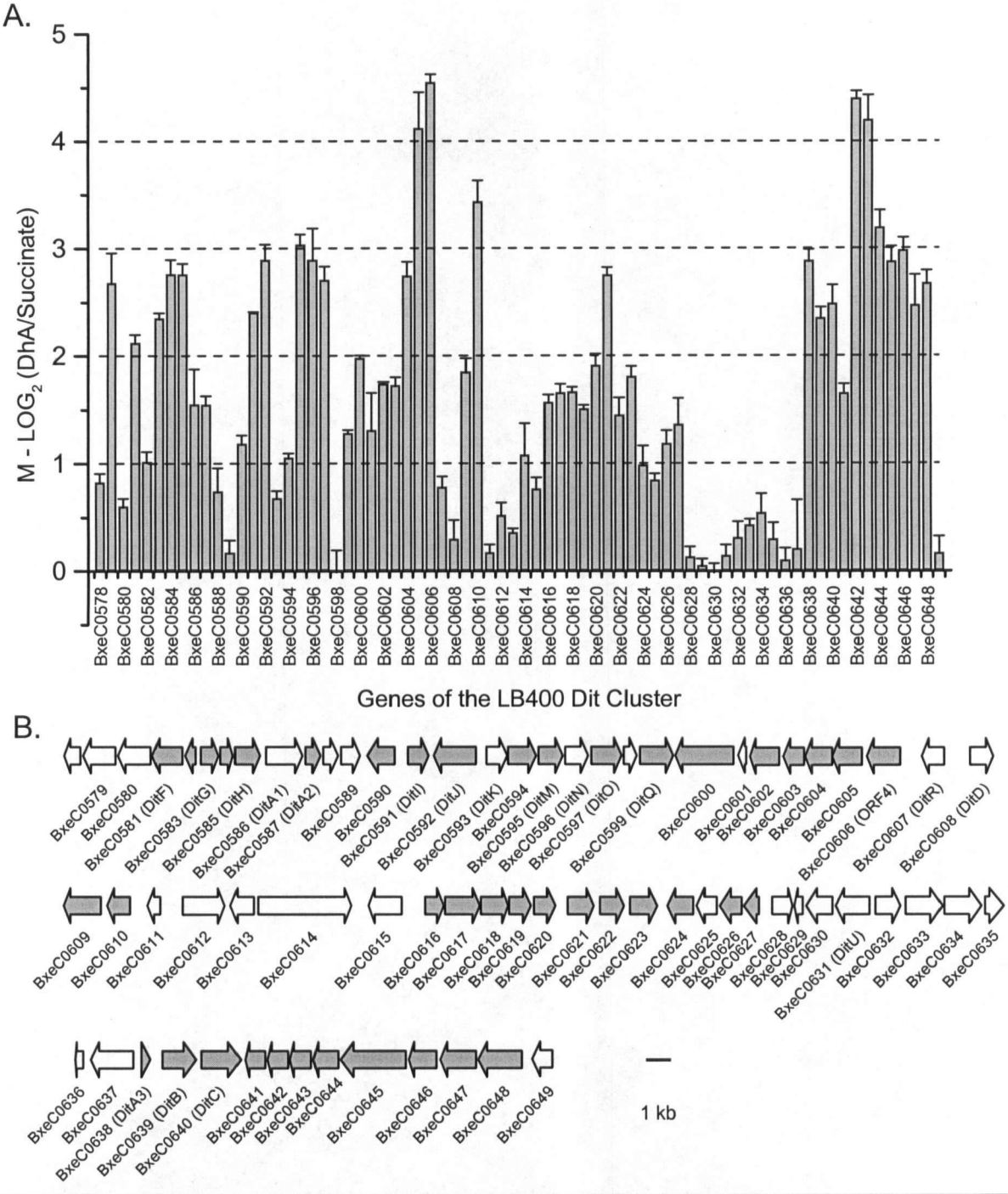

Figure 3.4 A. Plot shows M values (LOG2(DhA/Succinate) for signal intensities for genes of the LB400 *dit* cluster. Error bars indicate standard error. **B. Physical map of the LB400 *dit* cluster of genes.** The 3 rows of arrows represent one contiguous cluster of genes and show the
330 orientation of each gene. Grey arrows represent genes with > 2-fold up-regulation during growth on DhA ($p < 0.05$) compared to growth on succinate.

Table 3.3 *Dit* cluster annotation and gene expression on DhA

Gene ID	Gene Name	Product description	COG Functional Group	Fold up-regulation on DhA	*p*-Value
BxeC0578		Putative Transcriptional Regulator of the TetR/AcrR Family	K	1.77	0.002
BxEC0579		Putative Pyridine nucleotide-disulphide oxidoreductase	R	6.40	0.066
BxeC0580	ORF2	Putative Transporter of the Major Facilitator Superfamily	GEPR	1.52	0.004
BxeC0581	ditF	Conserved hypothetical	R	4.35	1E-04
BxeC0582		Conserved hypothetical	I	2.03	0.002
BxeC0583	ditG	Putative dehydrogenase	QR	5.10	2E-05
BxeC0584		Putative Hemerythrin	P	6.78	2E-04
BxeC0585	ditH	Putative Fumarylacetoacetate Hydrolase	Q	6.76	1E-04
BxeC0586	ditA1	Ring-hydroxylating dioxygenase alpha subunit	PR	2.93	0.131
BxeC0587	ditA2	Ring-hydroxylating dioxygenase beta subunit	PR	2.93	3E-04
BxeC0588		Putative Glyoxalase Family Protein	E	1.68	0.040
BxeC0589		Putative Short Chain Dehydrogenase	QR	1.13	0.23
BxeC0590		Conserved hypothetical	No COG	2.28	7e-04
BxeC0591	ditI	Putative Short Chain Dehydrogenase	QR	5.31	3e-04
BxeC0592	ditJ	Putative CoA Ligase	IQ	7.43	3e-04
BxeC0593	ditK	PutativeTranscriptional Regulator, TetR family	K	1.60	0.002
BxeC0594		Conserved hypothetical	R	2.08	1E-04
BxeC0595	ditM	Putative Fumarylacetoacetate Hydrolase	Q	8.20	0.020
BxeC0596	ditN	Putative 3-hydroxyacyl CoA Dehydrogenase	I	7.43	0.064
BxeC0597	ditO	Putative Thiolase	I	6.53	0.029
BxeC0598	ditP	Conserved hypothetical	No COG	0.99	0.955
BxeC0599	ditQ	Cytochrome P450	Q	2.43	3E-05
BxeC0600		Putative CaiB/BaiF family protein	C	3.95	0.008
BxeC0601		Putative Ferredoxin	C	2.48	0.163
BxeC0602		Putative Acyl CoA Dehydrogenase	I	3.35	0.006
BxeC0603		Putative Enoyl CoA Hydratase	I	3.31	2E-04
BxeC0604		Putative Acyl CoA Dehydrogenase	I	6.70	0.030
BxeC0605		Putative Acyl CoA Dehydrogenase	I	17.4	0.001
BxeC0606		Conserved hypothetical	No COG	23.4	9E-06
BxeC0607	ditR	Transcriptional Regulator (IcLR family)	K	1.72	0.004
BxeC0608	ditD	Putative Fumarylacetoacetate Hydrolase	Q	1.23	0.182
BxeC0609		Putative MFS transporter	GEPR	3.61	6E-04
BxeC0610		Putative short chain dehydrogenase	QR	10.8	4E-04
BxeC0611		Hypothetical	No COG	1.13	0.255
BxeC0612		Putative Methyl-Accepting Chemotaxis Protein	N	1.43	0.022
BxeC0613		Putative Transcriptional Regulator of LysR Family	K	1.286	0.002
BxeC0614		Putative Oxidoreductase	C	2.11	0.169
BxeC0615		Putative Transporter of the Major Facilitator Superfamily	E	1.70	0.005
BxeC0616		Putative Dehydrogenase	QR	2.98	2E-05
BxeC0617		Putative Acyl CoA Dehydrogenase	I	3.16	2E-04
BxeC0618		Putative Phosphotransferase	R	3.17	3E-05
BxeC0619		Putative Short chain dehydrogenase	QR	2.85	2E-05
BxeC0620		Putative Dehydrogenase	QR	3.76	3E-04
BxeC0621		Conserved hypothetical	No COG	6.73	4E-05
BxeC0622		Putative Rieske Iron Sulphur Protein	PR	2.73	0.003

Gene ID	Gene Name	Product description	COG Functional Group	Fold up-regulation on DhA	*p*-Value
BxeC0623		Conserved hypothetical	PR	3.50	3E-04
BxeC0624		Conserved hypothetical	I	1.98	0.012
BxeC0625		Conserved hypothetical	Q	1.78	1E-03
BxeC0626		Putative Methyl Transferase	H	2.28	0.002
BxeC0627		Conserved hypothetical	E	2.57	0.011
BxeC0628		Putative Transcriptional Regulator of TetR/AcrR Family	K	1.10	0.251
BxeC0629		Conserved hypothetical	No COG	1.04	0.458
BxeC0630		Conserved hypothetical	No COG	0.99	0.857
BxeC0631	ditU	Cytochrome P450	Q	1.11	0.241
BxeC0632		Putative AraC type transcriptional regulator	K	1.24	0.123
BxeC0633		Conserved hypothetical	No COG	1.34	0.004
BxeC0634		Conserved hypothetical	No COG	1.46	0.201
BxeC0635		Putative Dehydrogenase	QR	1.23	0.135
BxeC0636		Putative Transcriptional Regulator of the TetR/AcrR Family	K	1.07	0.442
BxeC0637		Conserved hypothetical	Q	1.16	0.729
BxeC0588		Hypothetical	No COG	ND	ND
BxeC0638	ditA3	Ferredoxin	C	7.38	1E-04
BxeC0639	ditB	Putative Dehydrogenase	QR	5.10	2E-04
BxeC0640	ditC	Aromatic Ring Cleavage Dioxygenase	No COG	5.60	7E-04
BxeC0641		Conserved hypothetical	R(I)	3.15	3E-04
BxeC0642		Putative Dehydrogenase	QR	21.2	2E-09
BxeC0643		Putative Enoyl CoA Hydratase/Isomerase	I	18.4	0.035
BxeC0644		Conserved hypothetical	E	9.15	0.032
BxeC0645		Putative Transporter of the RND Superfamily	R	7.34	2E-04
BxeC0646		Conserved hypothetical	No COG	7.88	1E-04
BxeC0647		Conserved hypothetical	No COG	5.54	0.003
BxeC0648		Conserved hypothetical	No COG	6.38	2E-04
BxeC0649		Putative Transcriptional Regulator of the TetR/AcrR Family	K	1.12	0.358

3.3.3.2 Global analysis - COG distribution

3.3.3.2.1 Up-regulated genes

There were 97 up-regulated genes with greater than 2-fold increase in signal intensity ($p < 0.05$) on DhA compared to on succinate (Table 3.4, Supplementary Table 3.1 pg. 98). All genes encoding proteins of the secondary metabolite biosynthesis, transport, and catabolism COG functional group (COG Q) are encoded in the *dit* cluster (Fig. 3.4, Table 3.3). The COG functional group containing the greatest number of up-regulated genes (16) was involved in lipid metabolism (COG I), ten of which are encoded by the *dit* cluster.

Table 3.4 Summary of transcriptional analysis based on COG protein classification

COG	Description	Up-regulated genes (97 total)	Down-regulated genes (39 total)
Information Storage and Transport			
K	Transcription	1	3
L	DNA replication, recombination and repair	1	1
Cellular Processes			
M	Cell envelope biogenesis, outer membrane	4	1
N	Cell motility and secretion	0	4
T	Signal transduction mechanisms	0	4
Metabolism			
C	Energy Production and Conversion	8	5
E	Amino acid transport and metabolism	8	3
F	Nucleotide transport and metabolism	0	1
G	Carbohydrate transport and metabolism	3	1
H	Coenzyme metabolism	2	1
I	Lipid metabolism	16	0
P	Inorganic ion transport and metabolism	11	2
Q	Secondary metabolite biosynthesis, transport, and catabolism	11	0
Poorly Characterized			
R	General function prediction only	8	5
S	Function unknown	1	0
None			
	No match	23	8

Values are the number of up- or down-regulated [> 2X change in expression (t-test, p-value < 0.05)] genes based on transcriptional analysis of DhA-grown cells compared to succinate-grown cells.

Genes up-regulated on DhA involved in energy production and conversion (COG C) include genes BxeB2301 and BxeB2302, which are embedded in a cluster of genes involved in citrate/aconitate metabolism. On DhA, gene BxeB2301, encoding an aconitate hydratase, was up-regulated 3.1-fold ($p = 0.019$) and BxeB2302, encoding a 2-methyl citrate synthase, was up-regulated greater than 10-fold ($p = 0.042$). Gene BxeB2300 in this citrate/aconitate metabolism cluster was also up-regulated but is included in the COG S group of unknown functions. Two clusters of genes up-regulated on DhA encode several proteins putatively involved in inorganic ion transport and metabolism (COG P). Genes BxeA2467, BxeA2469 and BxeA2470 (COG P) are putatively involved in sulphate uptake. Genes BxeA3659 (COG H), BxeA3660 (COG P), BxeA3663 (no COG), BxeA3664 (COG P), and BxeA3671 (COG R) encode proteins putatively involved in sulphate metabolism. The relationship between sulfate and abietane diterpenoid

metabolism is unclear. Another COG P protein, BxeA3458, is a putative catalase, which likely is up-regulated to detoxify byproducts of uncoupled oxygenase activity. The other up-regulated genes in the COG P group are involved in phosphate, iron, or oxygen metabolism.

Four of the eight up-regulated genes encoding proteins involved in amino acid transport and metabolism (COG E) are located in a single cluster of genes, BxeB2702, BxeB2704, BxeB2705, and BxeB2706. Also included in this cluster is a COG C group member, BxeB2708, encoding a putative class II pyridine nucleotide-disulphide oxidoreductase. Genes BxeB2702-BxeB2705 encode a putative ABC transport system. Genes BxeB2705-BxeB2706 have similarity to those encoding A and B subunits of an opine oxidase. Genes BxeB2702-BxeB2709 are conserved in *Bradyrhizobium japonicum,* with deduced amino acid identity of 48% to 56% and identical gene order. In combination, the transport genes and the A and B subunit of the opine oxidase could function in the import and oxidation of opines. Opine oxidase causes the oxidative cleavage of opines to pyruvate or 2-ketoglurate and L-arginine (38). Opines are plant-produced amino acids resulting from infection of *Agrobacterium tumefaciens* in plant rhizospheres. The only up-regulated gene with a product involved in transcription (COG K) is BxeB1739, a putative AraC family transcriptional regulator. Two genes downstream of this gene, BxeB1741 and BxeB1742, and 1 gene directly upstream, BxeB1738, were also up-regulated. Both BxeB1741 and BxeB1742 encode putative proteins involved in dimethyl sulfoxide (DMSO) reductase activity, while BxeB1738 encodes a hypothetical protein.

3.3.3.2.2 Down-regulated genes

There were 39 down-regulated genes, with > 2 fold decrease in signal intensity ($p < 0.05$) on DhA compared to on succinate (Supplementary Table 3.2 pg. 101). None of the down-regulated genes are contained in the *dit* cluster. Four signal transduction (COG T) proteins are encoded by genes that are down-regulated, compared to no up-regulated genes in this group. Two of these genes, BxeA4195 and BxeA4196, are adjacent and immediately downstream of a

down-regulated gene encoding a putative C4-dicarboxylate transport protein BxeA4197 (COG C) possibly involved in succinate transport. Other COG C genes include, BxeB1810 encoding a putative oxygen-dependent terminal cytochrome bd oxidase subunit 1, BxeA0283 encoding a putative malate dehydrogenase which catalyzes the oxidative decarboxylation of malate to pyruvate, and BxeA3313, encoding a putative cytochrome c. Overall, the down-regulated genes might indicate slower metabolism compared to metabolism during relatively rapid growth on succinate. Additionally, four cell motility and secretion proteins (COG N) encoded by genes BxeA0132, BxeA0132, BxeA0143, and BxeA0157, are down-regulated.

3.4 Discussion

This report presents the first genomic analysis of bacterial abietane diterpenoid catabolism. Based on greater than 60% deduced amino acid sequence identity with 17 of the 23 proteins encoded by the *P. abietaniphila* BKME-9 *dit* cluster (32), and transcriptional analysis of up-regulated genes, we have identified an 80.5-kb cluster of genes from BxeC0578 to BxeC0649 in LB400 involved in abietane diterpenoid catabolism (Fig. 3.4). We have designated this region of the genome the LB400 *dit* cluster. We also identified several smaller clusters of genes outside the *dit* cluster, which may be important for abietane diterpenoid degradation. This greatly increases the number of genes known to be associated with diterpenoid degradation and will facilitate further understanding of this complex catabolic process. A knockout of a key gene coding for the alpha subunit of the ring-hydroxylating dioxygenase, *ditA1*, confirmed the necessity of *dit* cluster genes in the degradation of abietane diterpenoids. Metabolites identified in cell suspensions indicate a degradation pathway similar to the proposed convergent pathway of BKME-9 (19, 20).

3.4.1 Competitiveness of LB400

Several bacteria with abietane degradation capabilities have been isolated (reviewed in (23) and (25)). Typically isolates were enriched for degradation of abietane diterpenoids from environmental samples such as pulp and paper mill effluent, forest soil, or batch sequencing reactors. The isolates, members of the community growing relatively fast on diterpenoids under the enrichment conditions, were then partially characterized genetically and biochemically. In this study, we took a different approach by first identifying homologues of genes required for abietane diterpenoid degradation from the genome sequence of LB400, and then assessing growth on those compounds. LB400 has a longer doubling time and lag phase than other characterized diterpenoid degrading bacteria (23, 32) , but it affords a much more comprehensive analysis of the degradative process than in other bacteria. It is possible that a bacterium such as LB400 would have been missed using enrichment cultures because of its long lag phase and long doubling time compared with other isolates. Growth yields of LB400 on DhA, however, were similar to those of *Sphingomonas* sp. DhA-33, *Zoogloea* sp. DhA-35 and *P. abietaniphila* BKME-9 (23, 32).

It is interesting to note that when LB400 grown on succinate is transferred to medium with different diterpenoids, the lag phase correlates with solubility of the compounds. At neutral pH, the solubilities of AbA and DhA are 3-5 mg/ per litre and 4-6 mg per litre respectively (18). The solubilities of 7-oxo-DhA and PaA are not available. However, based on turbidity of uninoculated culture medium containing 300 μM of each individual compound, 7-oxo-DhA is the most, and PaA is the least soluble. Thus, bioavailability may limit induction of diterpenoid degradation. In agreement with this interpretation, after transfer of a culture grown on a particular resin acid to fresh medium containing the same resin acid, substrate transformation begins after a shorter lag phase than in the initial culture probably because genes required for degradation are still up-regulated. Therefore, after induction, under conditions where abietane

diterpenoids are continuously available to the cells, such as wastewater treatment systems or perhaps some plant-associated environments, LB400 would grow at similar rates as other abietane diterpenoid degrading bacteria and potentially be competitive with them.

3.4.2 The *dit* clusters

As reported previously, the 72 genes of the LB400 *dit* cluster contain homologues of all 22 genes of the previously characterized BKME-9 *dit* cluster (32) and 7 genes of the previously characterized *Pseudomonas diterpeniphila* A19-6a *tdt* cluster (24), with the sole exception of *ditE* from BKME-9, encoding a putative permease of the major facilitator superfamily. Of the 52 genes that are included in the LB400 *dit* cluster and not found in the BKME-9 *dit* cluster, 30 were up-regulated during growth on DhA, indicating that these genes are functional members of the LB400 *dit* cluster. The newly described genes of the LB400 *dit* cluster encode proteins putatively involved in beta-oxidation, transport, general catabolism, and several conserved hypothetical proteins.

Through gene knockout analysis, several genes of the BKME-9 *dit* cluster (19) and A19-6a *tdt* cluster (24) were shown to be required for abietane diterpenoid metabolism, including *ditA1*. A BKME-9 strain with a Tn5 insertion in *ditA1* lost the ability to grow on DhA (20), which is in agreement with results obtained with the LB400 mutant strain DitA1KO. Other homologues of genes shown to be required for abietane diterpenoids metabolism in BKME-9 and A19-6a were up-regulated during growth on LB400 including, BxeC0581 (*ditF*, encoding a conserved hypothetical protein), BxeC0591 (*ditI*, encoding a putative short chain dehydrogenase), BxeC0585 (*ditH,* encoding a putative hydrolase), BxeC0638 (*ditA3* encoding a ferredoxin), and BxeC0640 (*ditC,* encoding a meta cleavage dioxygenase) from BKME-9 and BxeC0592 (*tdtL,* encoding a putative CoA ligase) from A19-6a.

Previously we showed that the gene in BKME-9 encoding the P450 monooxygenase, *ditQ*, was not required for growth on certain abietane diterpenoids (32). Growth of a BKME-9

ditQ mutant on AbA and 7-oxo-DhA was similar to that of the wild type, whereas growth on DhA and PaA was severely impaired. The *ditQ* orthologue in LB400 was up-regulated on DhA, which supports its involvement in DhA metabolism. We previously suggested that a paralogue of *ditQ* in BKME-9 might complement the *ditQ* gene knockout, allowing for limited growth of the knockout strain on DhA. In the LB400 *dit* cluster, we found a *ditQ* paralogue, *ditU,* which encodes a second P450. However, *ditU* was not up-regulated on DhA, and therefore likely would not complement *ditQ*. This suggests that gene regulation may differ between BKME-9 and LB400. This is supported by the different gene arrangement in the two organisms and the fact that homologues in the BKME-9 and LB400 *dit* clusters with the lowest amino acid identity are genes involved in transcriptional regulation. This also suggests that the substrate ranges of the P450s in the two bacteria may differ. Knockouts of both *ditQ* and *ditU* in LB400 are discussed in the next chapter.

3.4.3 Catabolic transposon

The genomes of *Burkholderia* spp., including LB400, are rich in insertion sequences (17). Catabolic transposons have a wide variety of sizes and have been reported to be as large as 90 kb in length (34). The LB400 megaplasmid contains several transposases including a group flanking the *dit* cluster BxeC0485-BxeC0490 and BxeC0519 and BxeC0670-BxeC0672, while no genes encoding transposases have been identified within the *dit* cluster. In addition, the GC content of the LB400 *dit* cluster is 64.9% versus 61.7% for the megaplasmid and 62.6% for the total genome. Chain et al. (5) reported the presence of the *dit* cluster of genes in two additional *B. xenovorans* strains, LMG21720 and LMG16224. Interestingly one of these strains did not contain a megaplasmid, implying that the *dit* cluster was encoded on chromosome 1 or 2 of that strain. This further implies that the *dit* cluster is mobile and raises the possibility that the LB400 *dit* cluster is part of a catabolic transposon. Interestingly, a cluster of genes with high sequence identity and similar gene arrangement to that of the LB400 and BKME-9 *dit* clusters was

identified on the recently sequenced genome of *Pseudomonas aeruginosa* 2192 (*Pseudomonas aeruginosa 2192* Sequencing Project, Broad Institute of Harvard and MIT (http://www.broad.mit.edu)), suggesting broad distribution of the *dit* cluster among Proteobacterial genomes. To date, however, there is no evidence that *P. aeruginosa* 2192 can grow on abietane diterpenoids.

3.4.4 Uptake of diterpenoids

The mechanism of uptake of abietane diterpenoids is unknown, however several putative transport proteins were up-regulated during growth on DhA. Interestingly, one gene of the BKME-9 characterized *dit* cluster which does not have a homologue in the LB400 *dit* cluster is *ditE,* encoding a putative permease. This suggests the strains may differ in the mechanism of uptake of diterpenoids. Two LB400 ABC transport systems, not encoded in the *dit* cluster, were up-regulated during growth on DhA, one associated with sulfate uptake and the other associated with opine uptake. It is possible that one or both of these transport systems is involved in abietane diterpenoid uptake; however, it is more likely that one of the putative transport proteins identified in the *dit* cluster is responsible for this activity. The genes of the *dit* cluster code for four putative permeases, 3 putative members of the major facilitator superfamily (MFS), and one putative member of the Resistance Nodulation (RND) Cell Division Superfamily. One of the MFS permeases, BxeC0609, and the putative RND permease BxeC0645, were up-regulated during growth on DhA (See Fig. 3.4).

Based on COG comparison, and a Transport Classification Data Base (TCDB) BLAST search analysis, gene BxeC0645 is a member of the RND Superfamily. This gene encodes a protein of 835 amino acids with 12 predicted transmembrane segments (TMS) and 2 large hydrophilic extracytoplasmic domains between TMS 1 and 2 and between TMS 7 and 8. Members of this family are found across diverse phyla and participate in a wide range of transport activities (36). A Prosite search of the protein encoded by BxeC0645 identified a 5

TMS sterol sensing domain from TMS 2 to TMS 6 (residues 278-400). This domain consists of ~180 amino acids that form five predicted membrane-spanning helices with short intervening loops. Recent work in vitro has shown direct binding of cholesterol to an 8 TMS containing the sterol sensing domain of a hamster protein involved in lipid homeostasis (29). Recently another member of the RND family also containing a sterol-sensing domain, NPC1L1, was found to be responsible for intestinal cholesterol absorption in mice (1). NPC1L1 is predominately expressed in the epithelial layer bordering the luminal space. Given the structural similarity between steroids and DhA, these findings raise the possibility that BxeC0645 encodes a diterpenoid transport protein responsible for uptake of abietane diterpenoids. Genes BxeC0646-BxeC0648, downstream of BxeC0645, were also up-regulated during growth on DhA and encode conserved hypothetical proteins containing signal peptides, which may also participate in an abietane diterpenoid transport system.

3.4.5 Diterpenoid metabolism

Results with cell suspensions of LB400 and DitA1KO show that the abietane diterpenoid catabolic pathway of LB400 is similar to the proposed pathway for BKME-9 (32), and differs from those proposed for *Arthrobacter* sp. and *Flavobacterium resinovorum* (as reviewed in (16)) (Fig. 3.5). The former involves a 7-oxo-DhA derivative, while the latter proceeds through a 3-oxo-DhA derivative and decarboxylation. Previously, we proposed that in BKME-9, DhA, AbA, and PaA are hydroxylated at C7 by the DitQ P450 monooxygenase, leading to 7-hydroxy-DhA. This metabolite was identified in the supernatant of *Alcaligenes eutrophus* growing on DhA (2). Oxidation of the C7 alcohol to a C7 ketone via the activity of an as yet unidentified dehydrogenase would lead to the formation of 7-oxo-DhA. 7-Oxo-DhA has been reported to be a substrate for the BKME-9 DitA ring-hydroxylating dioxygenase (20). In both BKME-9 and LB400, 7-oxo-DhA was removed by the wild type, but *ditA1* mutants of both organisms

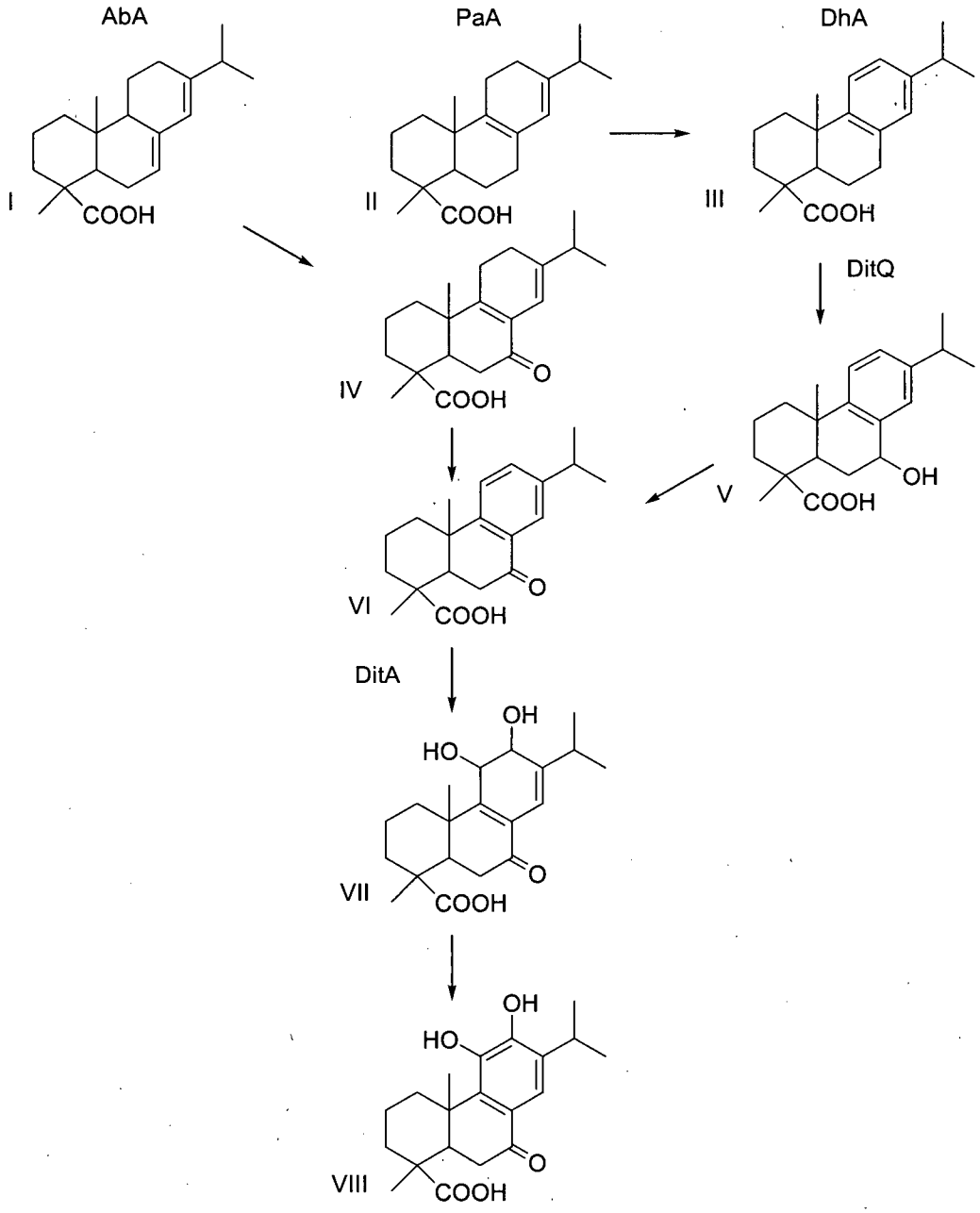

Figure 3.5 Proposed convergent pathway for abietane diterpenoid degradation by LB400. I, abietic acid; II, palustric acid; III, dehydroabietic acid; IV, 7-oxo-palustric acid; V, 7-hydroxy-dehydroabietic acid; VI, 7-oxo-dehydroabietic acid; VII, 7-oxo-11,12-dihydroxy-8,13-abieadien acid; VIII,7-oxo-11,12-dihydroxydehydroabietic acid.

failed to remove 7-oxo-DhA in cell suspensions with DhA, AbA and PaA or 7-oxo-DhA, indicating that DitA systems in both organisms likely play a similar role in DhA metabolism.

Formation of 7-oxo-DhA during AbA and PaA metabolism may proceed through a 7-oxo-PaA intermediate (Fig. 3.5). The unknown substance I that was detected in both LB400 and

DitA1KO cell suspensions with AbA or PaA was tentatively identified as 7-oxo-PaA (Fig 3.5, IV). 7-oxo-PaA could potentially be an oxidized product of both AbA and PaA degradation. The same metabolite was also detected in cell suspensions of a BKME-9 *ditA1* mutant incubated with PaA (19). These results are consistent with Unknown I being 7-oxo-PaA and confirm the common pathway used by both BKME-9 and LB400.

Previously, we reported the transformation by BKME-9 of PaA to DhA, involving aromatisation of the C ring (32). Increases of DhA concentration in both LB400 and DitA1KO cell suspensions indicate that LB400 also catalyzes this transformation. Accumulation and removal of 7-oxo-DhA by LB400 incubated with PaA further suggests that catabolism of the accumulated DhA follows the same initial pathway as in cells with DhA as the substrate (Fig. 3.5). However, the flux of PaA through this pathway is uncertain, and an additional pathway may exist. If Unknown I is 7-oxo-PaA, this would indicate that PaA can follow two routes of catalysis, either oxygenation of C7 prior to aromatisation of the C-ring or aromatisation of the C-ring prior to oxygenation of C7.

3.4.6 A putative oxygenase-driven electron transport system

In several cases, genes encoding the ferredoxin and ferredoxin reductase components of oxygenase electron transport systems are located immediately downstream of the catalytic subunit genes. This type of gene organization is seen in the LB400 biphenyl ring-hydroxylating dioxygenase, encoded by BxeC1197 and BxeC1196 (respectively encoding BphA and BphE, the alpha and beta subunits of the biphenyl ring-hydroxylating dioxygenase), BxeC1194 (encoding BphF, the ferredoxin), and BxeC1193 (encoding BphG, a ferredoxin reductase)(11). This is not the case, however, for *dit* cluster oxygenase genes. The alpha and beta subunit genes of the DitA ring-hydroxylating dioxygenase are adjacent (BxeC0586, BxeC0587); however, no ferredoxin or ferredoxin reductase genes are located near these subunit genes. Martin and Mohn (20) were able to express catalytically active DitA in *E. coli* using the *ditA1*, *ditA2* and *ditA3* of BKME-9. The

ditA3 gene codes for a 3Fe-4S ferredoxin, which is approximately 9.2 kb upstream of the alpha and beta subunits of BKME-9. No heterologous expression of a ferredoxin reductase was required; therefore, catalysis likely occurred through a surrogate ferredoxin reductase from *E. coli* (20).

The LB400 *dit* cluster contains two genes that encode ferredoxins: BxeC0601, and BxeC0638. Sequence analysis revealed that BxeC0638 encodes a 3Fe-4S ferredoxin that shares 56.7% amino acid identity with BKME-9 ditA3. By contrast BxeC0601 codes for a plant–type 2Fe-2S ferredoxin. Typically, ring-hydroxylating dioxygenases utilize 2Fe-2S type ferredoxins, however, a knockout of *ditA3,* a 3Fe-4S ferredoxin, showed that it was required for growth on abietane diterpenoids by BKME-9 (19). This combined with *ditA3* participation in the expression of DitA activity in *E. coli* support its proposed role in the DitA dioxygenase electron transport system in BKME-9. Overall sequence identity and putative structural similarities support the same role in LB400 for the 3Fe-4S-type ferredoxin encoded by BxeC0638.

A ferredoxin reductase homologue was identified in BKME-9 through Tn5 transposon mutagenesis (21). The mutant lost the ability to grow on DhA. Sequencing of the flanking regions of the transposon revealed part of an ORF with similarity to a ferredoxin reductase gene. The location of this transposon insertion, relative to the BKME-9 *dit* cluster, was not determined. The deduced 119 base amino acid sequence obtained from the sequence of the flanking regions of the Tn5 insert shares 65% amino acid identity with residues 261-380 of the deduced amino acid product of BxeC0579 of the LB400 *dit* cluster. During growth on DhA, BxeC0579 was up-regulated 6.4-fold ($p = 0.066$). The protein encoded by BxeC0579 shares 51% amino acid sequence identity with ThcD from *Rhodococcus erythropolis* (26) and 50% with EthA from *Rhodococcus ruber* (6), which serve as ferredoxin reductases in P450 systems involved in the degradation of S-ethyl dipropylcarbamothioate and ethyl tert-butyl ether, respectively. We speculate that BxeC0579 encodes a ferredoxin reductase that functions in DitA electron

transport. The transcriptomic analysis did not show up-regulation of any other ferredoxin reductase gene during growth on DhA, indicating that the ferredoxin reductase encoded by BxeC0579 may additionally function in electron transport for the P450 monooxygenase encoded by *ditQ*, which was also up-regulated on DhA. An electron transport system shared between monooxygenase and dioxygenase systems involved in a catabolic pathway for naphthalene has been reported for *Ralstonia* sp. U2 (39).

3.4.7 Role of lipid metabolism genes

Mineralization of abietane diterpenoids likely involves CoA-dependent metabolism. As mentioned previously, Morgan et al. (24) showed that *tdtL,* a homologue of BxeC0592, encoding a putative CoA ligase, was required for growth of *P. diterpeniphila* A19-6a on AbA or DhA. During growth of LB400 on DhA, BxeC0592 was up-regulated, along with two clusters of genes that encode enzymes putatively catalyzing beta-oxidation-like reactions, BxeC0594 to BxeC0597 and BxeC0600 to BxeC0606. The BxeC0594 to BxeC0597 cluster shares high sequence identity and gene arrangement in common with regions in both the BKME-9 *dit* and A19-6a *tdt* clusters, whereas the BxeC0600 to BxeC0606 cluster is newly identified in the LB400 *dit* cluster. Cleavage of the abietane diterpenoid rings followed by hydrolysis would result in branched short chain alkenes with acid, alcohol and ketone substituents, compounds expected to be degraded in the same manner as fatty acids. Possible products of a beta-oxidation-like reaction will require further transformation to TCA intermediates for complete catabolism. Based on transcriptional analysis, propionyl-CoA may be an intermediate in abietane diterpenoid degradation. The DhA up-regulated genes, BxeB2301, BxeB2302, and BxeB1203 encode enzymes that catalyze all steps required in the propionyl-CoA catabolic pathway. The induction of these genes during growth on DhA suggests that beta-oxidation processes during degradation of DhA produce propionyl-CoA that is transformed to pyruvate and enters the TCA cycle.

In conclusion, this chapter presents the first genomic study of a bacterium during growth on an abietane diterpenoid. Through the transcriptomic analysis, we were able to characterize the LB400 *dit* cluster during growth on DhA. A mutation of the DitA ring-hydroxylating dioxygenase showed that this gene, and presumably also the others of the *dit* cluster are required for catabolism of abietane diterpenoids. A convergent pathway similar to that seen in BKME-9 and utilizing 7-oxo-DhA as a central intermediate was presented. In the following chapter, the focus will return to the initial steps of abietane diterpenoid metabolism, which putatively leads to formation of 7-oxo-DhA.

625 **Supplementary Table 3.1 Up-regulated genes outside of the *dit* cluster**

Gene ID	Gene Annotation	COG Functional Groups	Fold Up-regulated on DhA	P-Value
CoA and Transport Cluster I				
BxeC0694	Hypothetical Protein	No CoG	2.314	0.00941
BxeC0698	Putative Porin Protein	M	2.6	0.000313
BxeC0700	Putative Enoyl CoA hydratase/isomerase family protein	I	2.249	0.049
BxeC0701	Putative Acyl CoA dehydrogenase	I	2.431	0.00107
Transposase				
BxeC0821	Putative Transposase	NO CoG	3.337	0.00814
Mannose Metabolism Cluster				
BxeC1071	Putative NUDIX hydrolase (gmm)	LR	2.966	0.0051
BxeC1073	Hypothetical protein	No CoG	2.236	0.000902
BxeC1085	Putative GDP Mannoase dehydratase (gmd)	M	2.011	0.00447
BxeC1090	Putative Mannose 6-phosphate isomerase (manA	M	2.393	0.0481
BxeC1103	Hypothetical Protien	No CoG	3.176	0.0168
BxeC1104	Conserved Hypothetical	No CoG	2.751	0.000533
Porin				
BxeC1231	Putative Outer membrane protein	M	2.128	0.000326
CoA Metabolism II Cluster				
BxeB0961	Putative CoA carboxyltransferase (propionyl –CoA carboxylase)	I	6.65	1.39E-06
BxeB0963	Putative Biotin Carboxylase	I	2.981	0.0144
2-methyl citrate lyase				
BxeB1203	Putative Isocitrate lyase and phosphorylmutase family protein	G	4.041	0.0277
Phosphoglucomutase				
BxeB1518	Putative Phosphoglucomutase/phosphomannomutase (ManB)	G	2.254	0.000574
DMSO Reductase Cluster				
BxeB1738	Hypothetical Protien		2.116	0.000546
BxeB1739	Putative AraC transcriptional regulator	K	2.937	0.0197

BxeB1741	DMSO reducatase anchor subunit C	R	2.336	0.0116
BxeB1742	Putative Fe-S containing protein-(similar to DMSO subunit B)	C	2.001	0.0018
BxeB2212	Putative Pyridoxamine 5'-phosphate oxidase family protein	R	3.057	0.00482
Aconitate/Citrate Cluster I				
BxeB2300	Conserved Hypothetical	S	2.914	0.0015
BxeB2301	Aconitate hydratase	C (4, 5)	3.102	0.0187
BxeB2302	2-methyl citrate synthase	C (36)	10.76	0.0421
Porin				
BxeB2364	Putative Outer Membrane Protein	No COG	2.885	0.00436
ABC Transport Cluster				
BxeB2702	Bacterial extracellular solute-binding protein	E	5.123	6.12E-05
BxeB2704	ABC transporter permease component	E/P	5.667	0.000126
BxeB2705	ABC transporter permease component	E/P	3.221	0.000974
BxeB2706	FAD dependent oxidoreductase	E	2.924	0.000862
BxeB2708	Putative Pyridine nucleotide-disulphide oxidoreductase, class-II	C/R	2.936	0.00116
Methyl Citrate Synthase				
BxeB2900	2-methyl citrate synthease	C	2.317	0.0069
ABC Transport Protein				
BxeA0019	ABC-type, periplasmic component	E	2.635	0.00397
CoA-ligase				
BxeA0042	Putative AMP dependent synthease and ligase	IQ	2.249	0.000314
Polyphosphate Kinase				
BxeA1237	Putative polyphosphate kinase	P	2.069	7.11E-05
CoA Tranferase				
BxeA1367	3-oxoacid CoA Transferase beta subunit	I (28, 34)	2.097	0.000444
Isocitrate Lysase				
BxeA1651	Putative Isocitrate Lysase	C (38)	2.759	0.000234

Sulfate Transport Cluster				
BxeA2467	Putative ABC-type sulfate/molybdate transport systems, ATPase component	P	2.315	0.0332
BxeA2469	Putative ABC-type sulfate/molybdate transport systems, permease components	P	2.824	0.00153
BxeA2470	Putative ABC-type sulfate transport system, periplasmic component- sulfate binding protein	P	4.795	0.00114
Catalase				
BxeA3458	Putative catalase	P	2.128	0.0018
Sulfate Metabolism Cluster				
BxeA3659	Putative Uroporphyrin-III C-methyltransferase	H	3.428	0.00342
BxeA3660	Putative GTPases - Sulfate adenylate transferase subunit 1 (SelB)	P	3.141	0.00176
BxeA3663	Conserved hypothetical	No COG	3.435	0.0424
BxeA3664	Putative Sulfite reductase hemoprotein beta-component	P	2.666	0.018
BxeA3671	Putative oxidoreductase, Gfo/Idh/MocA family	R	2.619	0.00668
Hypothetical				
BxeB1651	Conserved Hypothetical Protein	No COG	2.742	0.00215
BxeB2794	Conserved hypothetical	No COG	3.506	1.78E-05
BxeB2795	Conserved hypothetical	No COG	3.113	0.000485
BxeA3322	Conserved Hypothetical protein	No COG	2.046	0.00122
BxeA3394	Conserved Hypothetical protein	No COG	7.833	4.47E-05
BxeA3475	Conserved hypothetical	No COG	2.624	0.000262
BxeA4260	Conserved Hypothetical	E/R	2.042	0.00532
BxeA0586	Conserved hypothetical	No COG	2.605	0.00241
BxeA0268	Hypothetical Protein	No COG	2.779	0.0414

Supplementary Table 3.2 Down-regulated genes

Gene ID	Gene Annotation	COG Functional Group	Fold up-regulation on DhA	P-value
BxeC033	Putative ATPase	R	0.433	0.00669
BxeB0477	Putative Protein Phosphatase	T	0.448	0.0096
BxeB0695	Putative GntR Bacterial Regulator	KE	0.518	0.00105
BxeB0773	Putative FAD/FMN containing oxidoreductase	C	0.403	0.00319
BxeB0871	Putative MFS Transporter	P	0.548	0.00474
BxeB0922	Putative Sulfite/Nitrite Reductase	P	0.503	0.0131
BxeB1250	Putatvie methionie synthase cobalamin independent	E	0.122	0.000638
BxeB1493	Putative hydrolase (HAD superfamily)	R	0.443	0.0149
BxeB1810	Putative Cytochrome bd type	C	0.168	0.0129
BxeB1813	Putative Response Regulatory Protein	TK	0.473	0.00212
BxeB2567	Putative GntR Bacterial Regulator	K	0.258	0.00172
BxeB2600	Hypothetical protein	No COG	0.321	0.00274
BxeB2662	Hypothetical protein	F	0.484	0.0144
BxeB2786	Putative OmpC	M	0.0967	0.00733
BxeB2858	Putative Protein Phosphatase	No COG	0.398	0.0332
BxeB0923	Hypothetical Protein	No COG	0.323	0.0283
BxeB0921	Hypothetical Protein	No COG	0.296	0.00162
BxeA0132	Putative Flagellar GTP binding protein	N	0.549	0.000949
BxeA0141	Putative flagellar Basal Body protein	N	0.351	0.00439
BxeA0143	Putative Flagellar Hook protein	N	0.36	0.0136
BxeA0157	Putative Flagellar Motor Switch protein	N	0.436	0.0426
BxeA0178	Putative S-adenosylhomocysteine hydrolase	H	0.37	6.48E-05
BxeA0277	N-acetyl-gamma-glutamyl-phosphate reductase		0.37	0.0128
BxeA0283	Putative Malic Enzyme	C	0.495	0.000356
BxeA1538	Hypothetical Protein	No COG	0.446	4.70E-05
BxeA2843	Hypothetical Protein	No COG	0.395	0.000216
BxeA2986	Putatvie acetyltransferase, GNAT family	KR	0.269	0.00529
BxeA3155	Putative Phospholipase	R	0.175	0.00158
BxeA3313	Putative Cytochrome C	C	0.335	0.00627
BxeA3972	Putative DNA gyrase modulator	R	0.14	0.000104
BxeA3984	Putative ferritin DPS-family DNA binding protein	L	0.42	0.000451
BxeA4109	Putative membrane protein	R	0.446	0.00126
BxeA4195	Putative Transport transcriptional regualtory protein	T	0.499	0.00903
BxeA4196	Putative Signal Transduction Histadine Kinase	T	0.525	0.0239
BxeA4197	C4 –Dicarboxylate Symporter	C	0.33	0.00453
BxeA4365	Putative MFS Transporter	GEPR	0.534	0.00223
BxeA4445	Putative Amino Acid Transporter	E	0.43	0.0276
BxeA0219	Hypothetical Protein	No COG	0.449	0.0445
BxeA2598	Hypothetical Protien	No COG	0.39	0.0116

3.5 References

1. **Altmann, S. W., H. R. Davis, Jr, L.-J. Zhu, X. Yao, L. M. Hoos, G. Tetzloff, S. P. N. Iyer, M. Maguire, and A. Golovko**. 2004. Niemann-Pick C1 Like 1 protein is critical for intestinal cholesterol absorption. Science **303**:1201-1204.

2. **Biellmann, J. F., G. Branlant, M. Gero-Robert, and M. Poiret**. 1973. Degradation bacterienne de l'acide dehydroabietique par un Pseudomonas et une Alcaligenes. Tetrahedron **29**:1237-1241.

3. **Bramer, C. O., L. F. Silva, J. G. C. Gomez, H. Priefert, and A. Steinbuchel.** 2002. Identification of the 2-methylcitrate pathway involved in the catabolism of propionate in the polyhydroxyalkanoate-producing strain *Burkholderia sacchari* IPT101T and analysis of a mutant accumulating a copolyester with higher 3-hydroxyvalerate content. Appl. Environ. Microbiol. **68**:271-279.

4. **Bramer, C. O., and A. Steinbuchel.** 2001. The methylcitric acid pathway in *Ralstonia eutropha*: new genes identified involved in propionate metabolism. Microbiology **147**:2203-2214.

5. **Chain, P. S. G., V. J. Denef, K. Konstantinidis, L. M. Vergez, L. Agulló, V. L. Reyes, L. Hauser, M. Córdova, L. Gómez, M. González, M. Land, V. Lao, F. Larimer, J. J. LiPuma, E. Mahenthiralingam, S. A. Malfatti, C. J. Marx, J. J. Parnell, A. Ramette, P. Richardson, M. Seeger, D. Smith, T. Spilker, S. W., T. V. Tsoi, L. E. Ulrich, I. B. ZhulinIgor, and J. M. Tiedje**. 2006. *Burkholderia xenovorans* LB400 harbors a multi-replicon, 9.7 M bp genome shaped for versatility. Submitted to PNAS.

6. **Chauvaux, S., F. Chevalier, C. Le Dantec, F. Fayolle, I. Miras, F. Kunst, and P. Beguin**. 2001. Cloning of a genetically unstable cytochrome P-450 gene cluster involved in degradation of the pollutant ethyl tert-butyl ether by *Rhodococcus ruber*. J. Bacteriol. **183**:6551-6557.

7. **Chen, W.-M., L. Moulin, C. Bontemps, P. Vandamme, G. Bena, and C. Boivin-Masson.** 2003. Legume symbiotic nitrogen fixation by β-Proteobacteria is widespread in Nature. J. Bacteriol. **185**:7266-7272.

8. **Coenye, T., and P. Vandamme.** 2003. Diversity and significance of *Burkholderia* species occupying diverse ecological niches. Environmental Microbiology **5**:719-729.

9. **de Lorenzo, V., and K. N. Timmis.** 1994. Analysis and construction of stable phenotypes in gram-negative bacteria with Tn5- and Tn10-derived minitransposons. Methods Enzymol **235**:386-405.

10. **Denef, V. J., J. A. Klappenbach, M. A. Patrauchan, C. Florizone, J. L. M. Rodrigues, T. V. Tsoi, W. Verstraete, L. D. Eltis, and J. M. Tiedje.** 2006. Genetic and genomic insights into the role of benzoate-catabolic pathway redundancy in *Burkholderia xenovorans* LB400. Appl. Environ. Microbiol. **72**:585-595.

11. **Denef, V. J., J. Park, T. V. Tsoi, J.-M. Rouillard, H. Zhang, J. A. Wibbenmeyer, W. Verstraete, E. Gulari, S. A. Hashsham, and J. M. Tiedje.** 2004. Biphenyl and benzoate metabolism in a genomic context: outlining genome-wide metabolic networks in *Burkholderia xenovorans* LB400. Appl. Environ. Microbiol. **70**:4961-4970.

12. **Denef, V. J., M. A. Patrauchan, C. Florizone, J. Park, T. V. Tsoi, W. Verstraete, J. M. Tiedje, and L. D. Eltis**. 2005. Growth substrate- and phase-specific expression of biphenyl, benzoate, and C1 metabolic pathways in *Burkholderia xenovorans* LB400. J. Bacteriol. **187**:7996-8005.

13. **Dudoit, S., Y. H. Yang, J. C. Callow, and T. P. Speed.** 2002. Statistical methods for identifying differentially expressed genes in replicated cDNA microarray experiments. Statistica Sinica **12**:111-139.

14. **Gao, X., E. LeProust, H. Zhang, O. Srivannavit, E. Gulari, P. Yu, C. Nishiguchi, Q. Xiang, and X. Zhou.** 2001. A flexible light-directed DNA chip synthesis gated by deprotection using solution photogenerated acids. Nucl. Acids Res. **29**:4744-4750.

15. **Goris, J., P. De Vos, J. Caballero-Mellado, J. Park, E. Falsen, J. F. Quensen, 3rd, J. M. Tiedje, and P. Vandamme.** 2004. Classification of the biphenyl- and polychlorinated biphenyl-degrading strain LB400T and relatives as *Burkholderia xenovorans* sp. nov. Int J Syst Evol Microbiol **54**:1677-81.

16. **Kieslich, K.** 1976. Microbial transformations of non-steroid cyclic compounds. J. Wiley, Chichester, Eng..

17. **Lessie, T. G., W. Hendrickson, B. D. Manning, and R. Devereux.** 1996. Genomic complexity and plasticity of *Burkholderia cepacia*. FEMS Microbiol Lett **144**:117-28.

18. **Liss, S. N., P. A. Bicho, and J. N. Saddler.** 1997. Microbiology and biodegradation of resin acids in pulp mill effluents: a minireview. Can J Microbiol **43**:599-611.

19. **Martin, V. J., and W. W. Mohn.** 2000. Genetic investigation of the catabolic pathway for degradation of abietane diterpenoids by *Pseudomonas abietaniphila* BKME-9. J Bacteriol **182**:3784-93.

20. **Martin, V. J., and W. W. Mohn.** 1999. A novel aromatic-ring-hydroxylating dioxygenase from the diterpenoid-degrading bacterium *Pseudomonas abietaniphila* BKME-9. J Bacteriol **181:**2675-82.

21. **Martin, V. J. J.** 1999. Molecular Genetic Investigation of the Abietane Diterpenoid Degradation Pathway of *Pseudomonas abietaniphila*BKME-9. Doctor of Philosophy. University of British Columbia, Vancouver.

22. **Mohn, W. W.** 1995. Bacteria obtained from a sequencing batch reactor that are capable of growth on dehydroabietic acid. Appl Environ Microbiol **61**:2145-50.

23. **Mohn, W. W., A. E. Wilson, P. Bicho, and E. R. Moore.** 1999. Physiological and phylogenetic diversity of bacteria growing on resin acids. Syst Appl Microbiol **22**:68-78.

24. **Morgan, C. A., and R. C. Wyndham.** 2002. Characterization of *tdt* genes for the degradation of tricyclic diterpenes by *Pseudomonas diterpeniphila* A19-6a. Can J Microbiol **48**:49-59.

25. **Morgan, C. A., and R. C. Wyndham.** 1996. Isolation and characterization of resin acid degrading bacteria found in effluent from a bleached kraft pulp mill. Can J Microbiol **42**:423-30.

26. **Nagy, I., G. Schoofs, F. Compernolle, P. Proost, J. Vanderleyden, and R. de Mot.** 1995. Degradation of the thiocarbamate herbicide EPTC (S-ethyl dipropylcarbamothioate) and biosafening by *Rhodococcus sp.* strain NI86/21 involve an inducible cytochrome P-450 system and aldehyde dehydrogenase. J. Bacteriol. **177:**676-687.

27. **Parales, R. E., and C. S. Harwood.** 1992. Characterization of the genes encoding beta-ketoadipate: succinyl-coenzyme A transferase in *Pseudomonas putida*. J Bacteriol **174**:4657-66.

28. **Partida-Martinez, L. P., and C. Hertweck**. 2005. Pathogenic fungus harbours endosymbiotic bacteria for toxin production. **437**:884-888.

29. **Radhakrishnan, A., L.-P. Sun, H. J. Kwon, M. S. Brown, and J. L. Goldstein**. 2004. Direct binding of cholesterol to the purified membrane region of SCAP: Mechanism for a sterol-sensing domain. Molecular Cell **15**:259-268.

30. **Schweizer, H. P., and T. T. Hoang.** 1995. An improved system for gene replacement and xylE fusion analysis in *Pseudomonas aeruginosa*. Gene **158**:15-22.

31. **Simons, R., U. Priefer, and A. Puhler.** 1983. A broad host range mobilization system for in vivo genetic engineering: transposon mutagenesis in Gram negative bacteria. Bio/Techonology **1**:784-790.

32. **Smith, D. J., V. J. Martin, and W. W. Mohn.** 2004. A cytochrome P450 involved in the metabolism of abietane diterpenoids by *Pseudomonas abietaniphila* BKME-9. J Bacteriol **186**:3631-9.

33. **Steinmann, D., R. Koplin, A. Puhler, and K. Niehaus**. 1997. *Xanthomonas campestris* pv. campestris *lpsI* and *lpsJ* genes encoding putative proteins with sequence similarity to the α and β-subunits of 3-oxoacid CoA-transferases are involved in LPS biosynthesis. Archives of Microbiology **168**:441-447.

34. **Tan, H.-M**. 1999. Bacterial catabolic transposons. Applied Microbiology and Biotechnology **51**:1-12.

35. **Textor, S., V. F. Wendisch, A. A. D. Graaf, U. Muller, M. I. Linder, D. Linder, and W. Buckel.** 1997. Propionate oxidation in *Escherichia coli*: evidence for operation of a methylcitrate cycle in bacteria. Archives of Microbiology **168**:428-436.

36. **Tseng, T. T., K. S. Gratwick, J. Kollman, D. Park, D. H. Nies, A. Goffeau, and M. H. Saier, Jr.** 1999. The RND permease superfamily: an ancient, ubiquitous and diverse family that includes human disease and development proteins. J Mol Microbiol Biotechnol **1**:107-25.

37. **Wang, Z.-X., C. O. Bramer, and A. Steinbuchel**. 2003. The glyoxylate bypass of *Ralstonia eutropha*. FEMS Microbiology Letters **228**:63-71.

38. **Zanker, H., G. Lurz, U. Langridge, P. Langridge, D. Kreusch, and J. Schroder.** 1994. Octopine and nopaline oxidases from Ti plasmids of *Agrobacterium tumefaciens*: molecular analysis, relationship, and functional characterization. J. Bacteriol. **176**:4511-4517.

39. **Zhou, N.-Y., J. Al-Dulayymi, M. S. Baird, and P. A. Williams.** 2002. Salicylate 5-hydroxylase from *Ralstonia* sp. Strain U2: a monooxygenase with close relationships to and shared electron transport proteins with naphthalene dioxygenase. J. Bacteriol. **184**:1547-1555.

4. DitQ and DitU[1]

4.1 Introduction

The involvement of DitQ in the initial steps of the catabolism of abietane diterpenoids by BKME-9 was examined in Chapter 2. While a knockout of *ditQ* in BKME-9 led to impaired growth on DhA and PaA, it affected growth on AbA or 7-oxo-DhA minimally. Substrate binding of DhA to DitQ supported its role in DhA catabolism; however, binding assays with other substrates were inconclusive. These findings raised the possibility of a second monooxygenase that was able to partially complement the *ditQ* knockout in the metabolism of DhA and PaA and possibly responsible for the transformation of AbA. This hypothesis was supported by the *dit* cluster of LB400, which contains two genes encoding cytochromes P450 sharing greater than 60% amino acid identity with DitQ–BKME-9. As noted in Chapter 3, transcriptomic analysis of LB400 cells confirmed that *ditQ* (encoding CYP226A1) was up-regulated during growth on DhA while the second putative P450 encoding gene, *ditU* (encoding CYP226A2), was not.

This chapter describes the use of 2D gel-based proteomics to characterize the expression of proteins during growth of *Burkholderia xenovorans* LB400 on each of DhA and AbA. This analysis was aimed at gaining a clearer understanding of the initial steps of abietane diterpenoid catabolism and the involvement of two cytochromes P450, DitQ and DitU. The results revealed a key difference in the catabolism of DhA and AbA by LB400: the differential expression of DitU. DitQ is expressed during growth on both DhA and AbA, whereas DitU is only expressed during growth on AbA. Phenotypic studies of the knockouts containing an insertional mutation of *ditQ* or *ditU* showed that *ditQ* is required for growth on DhA and substrate transformation, both DhA and PaA but not 7-oxo-DhA. An in vitro P450 assay confirmed that DhA is a substrate whereas *ditU* is required for AbA catabolism. Substrate binding assays revealed that DitQ binds for DitQ and transforms DhA to 7-hydroxy-DhA.

[1] A version of this chapter will be submitted for publication.

4.2 Materials and Methods

Bacterial strains, plasmids, and culture conditions. The bacterial strains and plasmids used in this study are listed in Table 4.1. *E. coli* was cultured on Luria-Bertani (LB) medium and incubated at 37°C and *B. xenovorans* strains were cultured on LB without NaCl, or K1 mineral medium (see Chapter 3 for details) supplemented with 1 g per litre succinate, 90 mg per litre AbA, 90 mg per litre DhA, 90 mg per litre PaA, or 95 mg per litre 7-oxo-DhA. All *B. xenovorans* strain incubations were conducted at 30°C. All liquid cultures were incubated on a rotary shaker at 200-250 rpm.

Table 4.1 Bacterial strains and plasmids used in this study

	Genotype or Description	Reference or Source
Strains		
Burkholderia xenovorans		
LB400	Wild type; grows on abietane diterpenoids	(9)
DitQKO	*ditQ*:: *xylE-accC1*; Gm^r	This study
DitUKO	*ditU*:: *xylE-accC1*; Gm^r	This study
Escherichia coli		
DH5α	*end*A1 *hsd*R17 (r_k^- m_k^-) *supE44 thi-1 recA1 gyrA (Nal^r) relA1* Δ*(lacIZYA-argF)* U169 *deoR* (ϕ*80dlac*Δ*(lacZ)M15)*	Gibco BRL
S17-1	*recA pro thi hsdR* with integrated RP4-2-TcMu::Kna::Tn7; Tra^+ Tr^r Sm^r	(26)
Plasmids		
pEX18AP	*sacB* conjugable plasmid for gene replacement; Ap^r	(23)
pX1918G	*xyl*E-Gm^r fusion cassette-containing plasmid; Ap^r Gm^r	(23)
pEX5906	1.3 kbp PCR amplicon containing LB400 *ditQ* cloned into the *Xba*I *Hind*III of the multiple cloning site of pEX18AP	This study
pEX5906KO	PCR amplified *xylE-Gm^r* fusion cassette of pX1918G cloned into *Kas*I *Noc*I site of pEX5906	This study
pEX5938	1.6 kbp PCR amplicon containing LB400 *ditU* cloned into the *EcoR*I *BamH*I of the multiple cloning site of pEX18AP	This study
pEX5938KO	*Xma*I digested fragment of pX1918G containing the *xylE-accC1* fusion cassette cloned into the unique *Xma*I site of peX5938 disrupting *ditU*	This study

DNA Manipulation

DitQKO. Primers HISLEFT5906 and HISRIGHT5906 (Table 4.2) were used to amplify a 1312 bp fragment including *ditQ* from LB400 genomic DNA. The *Nhe*I and *Hind*III digested amplicon was ligated into *Xba*I and *Hind*III digested pEX18AP (11) and used to transform

DH5α to produce pEX5906. Next, the x*ylE—accC1* transcriptional fusion antibiotic cassette of pX1918G was amplified using primers XyLE5906L and XyLE5906R and ligated into the *Kas*I and *Noc*I digested pEX5906, which disrupted *ditQ*. The ligation product was used to transform S17-1 to produce pEX5906KO.

Table 4.2 Oligonucleotide primers used in PCR

Oligo nucleotide	Sequence[a]	Restriction Site
HISLEFT5906	5'-CGC GCG CTA GCA TGG AGA CCG GAA TGA CCA-3'	*Nhe*I
HISRIGHT5906	5'-GCG CGA AGC TTG TCG ACG GAC TAC CGC TCA-3'	*Hind*III
XyLE5906L	5'-GAT CCC ATG GAC CGT GAT CGG CGA ACT GGA-3'	*Nco*I
XyLE5906R	5'- ATA TGG CGC CCTCGG CCA CCG TCA TCT TCC-3'	*Kas*I
KOLBcep5938	5'-CGC GGA TCC TGG TGA GTT GCA GGC CGT A-3'	*BamH*I
KORBcep5938	5'-CCG GAA TTC ACG CCG TTA AGC TGC ACG A–3'	*EcoR*I
HISLEFT5938	5'-CGC GCA AGC TTT GGT GAG TTG CAG GCC GTA-3'	*Hind*III
HISRIGHT5938	5'-CGC GCG CTA GCA TGA GCA CCA CCC TCG AAA-3'	*Nhe*I

[a] Restriction sites are underlined.

DitUKO. Primer KOLBcep5938 and KORBcep5938 were used in an LB400 colony PCR (annealing temp. 58.9°C) to amplify a 1609 bp fragment including *ditU*. A *BamH*I and *EcoR*I digest of the amplified fragment was ligated into the *EcoR*I and *BamH*I digested pEX18AP to produce pEX5938. Next, an *Xma*I digested *xylE*-Gm^r transcriptional fusion antibiotic cassette of pX1918G (23) was ligated into the dephosphorylated unique *Xma*I site of pEX5938, which disrupted the *ditU* gene, and was used to transform S17-1 to generate pEX5938KO. Successful transformants of pEX5906KO and pEX5938KO were selected as described in Chapter 2. Homologous recombination of the mutated allele into strain LB400 was accomplished by diparental conjugation as in (4) and described in Chapter 3. Successful strains were designated DitQKO and DitUKO.

Homologous recombination of pEX5906KO was confirmed by PCR of a 2.7-kbp PCR product from strains growing on LB (-NaCl) agar plates containing 10 μg of gentamycin/ml using PCR primers XylE5906R and HISLEFT5906 under annealing condition of 57.8°C for 30 seconds and 30 cycles. Homologous recombination of pEX5938KO was verified by amplification of a ~ 3kp fragment from gentamycin resistant strains using primers HISLEFT5938 and HISRIGHT5938 at 60.0°C for 30 seconds. Amplicons generated from both DitQKO and DitUKO were sequenced and compared to the expected product.

Cell suspension and growth assays. Cell Suspensions and growth assays were conducted as described in Chapter 3 using LB400, DitQKO or DitUKO.

Proteome Cultures

Succinate. LB400 was streaked out from frozen stock on 1.5 % purified agar K1 plates, which were inverted over a petri dish lid containing biphenyl crystals and incubated for 3-4 days. The initial growth on biphenyl was used as a selection. Colonies were then used to inoculate 50 ml of K1 containing 1 g per litre of succinate. After 24 hours the culture reached late-log phase with an OD_{600} of ~ 0.9, and cells were transferred to fresh K1 containing 1 g per litre of succinate for an initial OD_{600} of 0.001. After 18 hours, the culture reached mid-log phase (OD_{600} 0.68). Cells from this culture were used to inoculate 1 litre Erlenmeyer flasks of K1 containing 1g per litre succinate. After 18 hours of incubation, cultures reached mid-log phase growth with an OD_{600} of ~ 0.5 and were collected as described below.

Abietic acid. LB400 cells used for proteomic analysis of AbA catabolism were first grown on biphenyl as described above for succinate grown cultures. A colony from biphenyl grown cells was used to inoculate 100-200 ml K1 medium containing 1g per litre of succinate. After the culture reached late-log phase (OD_{600} ~0.9), cells were transferred to fresh succinate-containing K1 for an initial OD of 0.001 and allowed to reach mid-log phase with an OD_{600} of ~0.7 (~18 hours). Cells from this second succinate culture were used to inoculate a 200 ml culture of K1

containing 90 mg per litre of AbA for an initial OD_{600} of 0.01. After an incubation of ~300 hours, AbA grown cells were used to inoculate fresh K1 medium containing 90 mg per litre of AbA at an initial OD_{600} of 0.001 or 0.01 and incubated until OD_{600} reached 0.04-0.0475. Cells from the second AbA culture were used to inoculate 1-3 litres of K1 containing 90 mg per litre of AbA for an initial OD_{600} of 0.001 and incubated for 30-35 hours until mid-log phase (OD_{600} ~ 0.05) and harvested as described below.

Dehydroabietic Acid. LB400 cells used for proteomic analysis of growth on DhA were first grown on biphenyl and subsequent succinate cultures as described above for both succinate and AbA grown cultures. As described above for AbA, succinate-grown cells were used to inoculate 100-300 ml of K1 medium for an initial OD_{600} of 0.01 containing 90 mg per litre of DhA. After incubation of approximately 150 hours these DhA grown cells were used to inoculate 50-100 ml of fresh K1 containing 90 mg per litre of DhA for an initial OD_{600} of 0.001-0.005 and incubated until cultures had reached late-log phase (~ 48 hours). Cells from the second DhA culture were used to inoculate 1 litre of K1 containing 90 mg per litre of DhA for an initial OD_{600} of 0.001. The culture was incubated until it reached mid-log phase (OD_{600} ~ 0.06) and harvested as described below.

Cell harvest and washing. Cells were harvested by centrifugation at 10,000 rpm for 20 min at 25°C, decanted, frozen using liquid nitrogen, and stored at –80°C. Pellets were thawed on ice and then kept cool on ice throughout the remaining steps. Pellets were suspended in a small amount of chilled sterile saline (0.8%) and then saline was added to the original culture volume prior to centrifugation, and mixed vigorously by shaking. The suspension was then centrifuged at 10,000 rpm at 4°C for 7 min and decanted immediately. The pellet was then suspended in 3 ml of chilled TE (10 mM Tris/HCl, 1 mM EDTA, pH 8.0) and aliquoted into pre-chilled 1.7 ml Eppendorf tubes. Suspensions were then centrifuged for 5 min at 13,200 rpm at 4°C, decanted with pipetting to remove all remaining fluid, and stored at –80°C.

Protein extraction and quantification. Pellets were thawed on ice and suspended in 300 µl of lysis buffer (4% cholamidopropyldimethylammoniopropanesulfoate [CHAPS], 30 mM Tris pH 6.5) by vortexing. Next, protease inhibitor cocktail [one tablet of Mini Complete per 10 ml solution; Roche] was added to the cell pellet (1:100, vol/vol) and incubated on ice for 20 min. Lysate was then added to 0.3 g of sterile beads (0.1-mm zirconia/silica beads; BioSpec Products Inc., Bartlesvilles, OK). The lysate was bead beaten using a Fast Prep Bio 101 Thermo Savant bead beater 5 times for 15 seconds at speed setting 6.0 with a 3 minute incubation on ice between runs to facilitate lysate cooling. The lysate was then centrifuged for 10-20 min at 13,200 rpm at 4°C to remove unbroken cells and debris. The supernatant was then removed and placed in a 1.7 ml Eppendorf tube. This centrifugation step was repeated until supernatant was clear and free of beads and then aliquoted into pre-chilled Eppendorf tubes and stored at –80°C. Proteins were quantified using 2D Quant kit (Amersham Biosciences) as per manufacturer's instructions.

Proteomic analysis. Proteomic analysis was carried out as described previously (5, 21). Briefly, after protein extraction, 2D gels were run for each of three biological replicates for LB400 cells grown on succinate, dehydroabietic acid, or abietic acid. The first-dimension separation was carried out using non-linear IPG strips (24 cm, pH 3 to 7). The IPG strips were rehydrated "in-gel" using 90 mg protein extract suspended in 400 µl rehydration solution (10 M urea, 2 M thiourea, 30 mM dithiothreitol, 3% CHAPS, Pharmalyte pH 3 to 10). To minimize carbamylation, the temperature was maintained between 20 and 25°C during protein solubilization. Isoelectric focusing in the IPG strips was carried out for a total of 73.5 kVh at 20°C under mineral oil using ETTAN IPGphor (Amersham Biosciences). The IPG strips were then equilibrated and run into 12% sodium dodecyl sulfate (SDS)-polyacrylamide gel electrophoresis (PAGE) gels (24 by 20 cm) using the ETTAN DALTtwelve system (Amersham Biosciences). Broad-range molecular mass markers (Invitrogen) were run on each side of the gel. Protein was detected using the fluorescent stain Sypro Ruby, and the gels were imaged using a

variable mode imager Typhoon 9400 (excitation 488 nm, emission 610 nm; Amersham Biosciences).

Analysis of 2D gels and protein identification. The 2D gel images were differentially analyzed using Progenesis Workstation software (Nonlinear Dynamics, Durham, NC). A signal intensity was assigned to each spot; and the signal intensity of each spot was normalized against the total signal intensity of all spots on the gel. The normalized signal intensity of each spot was then averaged over gels obtained from three different cultures. Averaged gels included only proteins spots that were present in at least two of three replicate gels. Only spots with a minimum normalized signal intensity of 0.002 or greater were analyzed further. Molecular mass values were assigned using the broad-range molecular mass markers (Invitrogen) run on each side of the gel. Isoelectric point values were assigned using an application provided with the Progenesis Workstation software. Theoretical molecular mass and isoelectric point values were predicted based on protein sequence using Expasy compute pI/Mw tool, available at http://ca.expasy.org/tools/pi_tool.html. For proteins appearing on the gel as a horizontal series of spots, likely due to carbamylation, the pI and mass of only the major spot in the series were recorded, and the difference in abundance was calculated based on the summed signal intensities of all the spots in the series. Protein spots whose intensities were at least twofold higher or lower versus the control (succinate-grown cells) were recorded as more or less abundant, respectively. Spots of interest were excised from gels and digested in-gel using trypsin (12). Mass spectrometry analyses were performed using a Voyager DESTR matrix-assisted laser desorption ionization-time of flight (MALDI-TOF) (Applied Biosystems). Proteins were identified as described previously (21) using the MASCOT search engine (www.matrixscience.com) using a database generated by in silico digestion of the total LB400 proteome predicted from the complete genome sequence (http://genome.ornl.gov/microbial/bfun/). A protein was considered identified if the hit fulfilled four criteria: 1) the hit was statistically significant (a MASCOT

search score above 52 for the LB400 database); 2) the number of matched peptides was five or higher; 3) the protein sequence coverage was above 20%; and, 4) the predicted mass and pI values were consistent with the experimentally determined ones. When two or more significant hits were returned, it was usually possible to narrow the identification to a single hit based on listed criteria (e.g., the pI and mass of some hits did not match that of the spot). Otherwise, the identification was excluded from the data set.

Substrate Binding. Cultures of *E. coli* DH5α containing pEX5938, pEX5906, or pEX18Ap were prepared and analyzed as described in Chapter 2 with the following exception. Instead of a French Press, two passes through an Emulsiflex C-5 cell disrupter operated at 15000 psi homogenizing pressure were used for cell lysis. DitQ was assayed at concentrations from 0.46 to 0.77 μM and DitU was assayed at concentrations for 0.61 to 0.70 μM.

In vitro P450 Assay. DitQ-LB400, or DitU-LB400 was collected and quantified in *E. coli* crude lysate as described for substrate binding assays in Chapter 2. Both ferredoxin DitA3 from *P. abietaniphila* –BKME-9 and ferredoxin reductase BphG from *Comamonas testosteroni* were purified to homogeneity and kindly provided by L. Eltis. Vials containing both DitA3 and BphG were sparged with argon for approximately 1 minute prior to the activity assay. BphG (1.8 μM), DitA3 (3.6 μM), *E. coli* crude lysate containing DitQ or DitU (1.0 μM), NADH (350 μM) and 100 μM abietane diterpenoid were combined and incubated for 5 min at room temperature or 30 min at 30°C. Controls included acidified reaction mixture or assays using IPTG induced *E. coli* crude lysate containing pEX18Ap.

4.3 Results

4.3.1 Succinate, DhA and AbA proteomes

Approximately 800 protein spots were detected in each of the proteomes of LB400 grown on succinate, AbA, and DhA as sole organic substrates (Fig. 4.1, See Appendix). Of the 551 protein spots common to the three proteomes, 52 were greater than 2-fold more abundant on both AbA and DhA than on succinate. Of the 679 protein spots common to the DhA and AbA proteomes, 128 were not detected in the succinate proteome. Of the protein spots significantly more abundant on the abietane diterpenoid substrates, 23 were identified (Table 4.3). Of these, genes of the LB400 megaplasmid *dit* cluster encode 16 proteins. They include two P450 monooxygenases, one of which is DitQ, encoded by BxeC0599, and detected in both AbA and

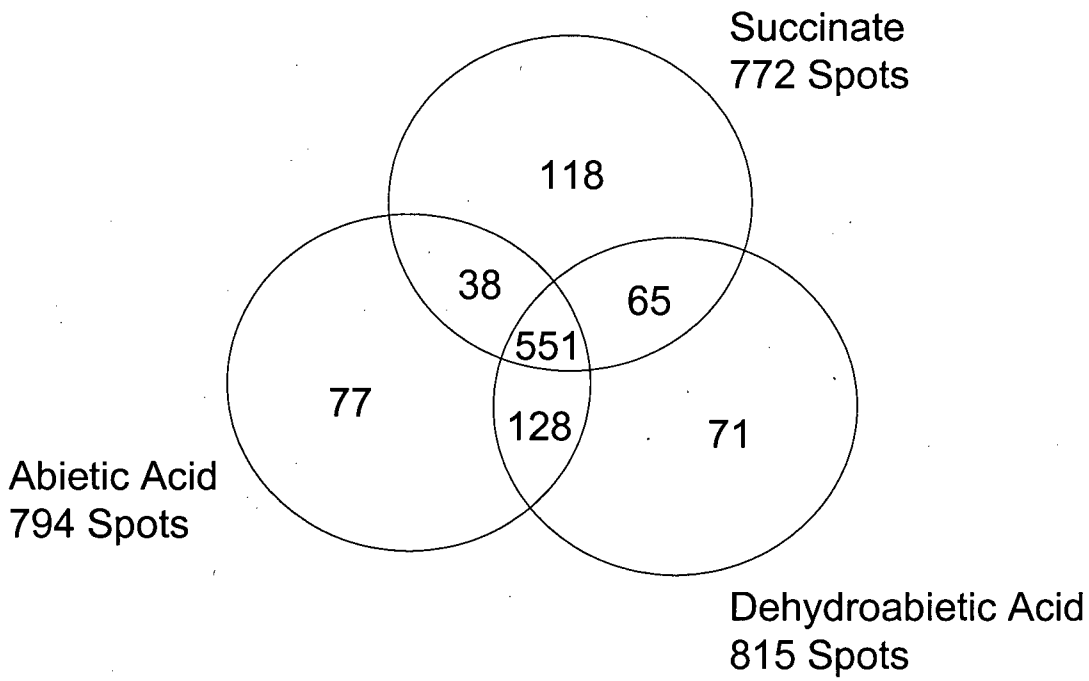

Figure 4.1 Global analysis of 3 LB400 proteomes. Circles represent proteomes of LB400 grown on succinate, AbA, or DhA as sole organic substrates. Numbers within each circle represent protein spots (n=3). Numbers outside circles represent the total number of protein spots present on each proteome with greater than or equal to 0.002 normalized signal intensity. Overlap between circles indicates protein spots that were present on more than one proteome.

Table 4.3 Proteins involved in abietane diterpenoid catabolism identified by MASCOT-based analysis of MALDI-TOF spectra

Gene no.[a]	Gene name	Protein name	Theor. pI[b]	Theor. MW[b]	Exp. pI[b]	Exp. MW[b]	# P[c]	Mascot score[c]	SC[c]	Normalized Signal Intensity		
										Succ	DhA	AbA
BxeC0585	*ditH*	Putative Hydrolase	5.3	37.9	5.0	39.2	16	185	57	ND	0.47	0.57
BxeC0586	*ditA1*	Alpha subunit of Ring Hydroxylating Dioxygenase	5.7	52.5	5.6	54.6	9	72	26	0.70	1.00	1.26
BxeC0587	*ditA2*	Beta subunit of Ring Hydroxylating Dioxygenase	5.8	21.1	5.8	22.1	8	115	61	ND	0.89	0.72
BxeC0592	*ditJ*	Putative CoA Ligase	5.8	60.0	5.8	64.9	9	65	20	ND	0.57	0.19
BxeC0594		Conserved Hypothetical	6.0	40.7	6.1	39.3	9	61	32	0.34	1.06	1.24
BxeC0597	*ditO*	Putative Thiolase	5.9	41.8	6.0	42.9	11	93	35	0.02	0.32	0.46
BxeC0599	*ditQ*	Cytochrome P450	6.0	46.9	6.1	47.7	17	100	42	ND	0.15	0.34
BxeC0602		Putative Acyl CoA Dehydrogenase	5.9	41.8	6.0	41.8	12	128	38	ND	0.68	0.35
BxeC0606		Conserved Hypothetical	5.6	49.5	5.4	48.7	10	71	33	0.02	2.02	2.17
BxeC0619		Putative Short Chain Dehydrogenase	5.6	29.4	5.7	26.1	8	63	43	0.09	0.19	0.17
BxeC0630		Conserved Hypothetical	5.8	39.1	5.8	39.6	7	56	23	ND	ND	0.42
BxeC0631	*ditU*	Cytochrome 450	5.9	47.6	6.1	48.1	23	153	64	ND	ND	0.50
BxeC0639	*ditB*	Putative Dehydrogenase	6.1	26.7	5.0	29.5	11	123	66	ND	0.40	0.86
BxeC0640	*ditC*	Ring Cleavage Dioxygenase	10.4	49.6	6.4	36.7	13	88	35	ND	0.69	0.46
BxeC0644		Conserved Hypothetical	6.1	37.2	6.0	37.4	13	113	51	ND	1.41	LR
BxeC0647		Conserved Hypothetical	6.0	51.2	5.5	47.7	17	137	49	ND	0.42	0.24
BxeC1186	*bphD*	Hydrolase	6.1	32.1	4.8	38.5	6	61	25	0.01	0.12	0.26
BxeB0962		Putative CoA Hydratase	5.2	28.5	4.5	26.8	14	120	70	ND	0.16	0.19
BxeB0963		Putative Biotin Carboxylase	5.4	72.9	5.0	76.4	19	127	36	ND	0.16	0.13
BxeB1203		Putative Isocitrate Lyase and Phosphorylmutase family protein	5.6	31.5	5.4	32.2	10	106	56	0.04	0.55	0.43
BxeB2301		Aconitate Hydratase	5.5	94.6	5.3	96.3	32	200	47	ND	0.56	0.50
BxeA1366		Putative 3-oxoacid CoA-transferase alpha subunit	5.7	25.5	5.7	27.1	7	67	67	0.05	0.43	0.27
BxeA2466		Putative LysR type Regulator	6.0	34.5	6.1	37.2	11	77	38	ND	0.42	LR

Abbreviations, Theo., Theoretical; Exp., Experimental; MW, molecular weight; pI, Isoelectric point; Succ, succinate; DhA, dehydroabietic acid; AbA, abietic acid.

[a] LB400 genome sequence available at http://genome.ornl.gov/microbial/bfun/

[b] See Methods and Materials for description of how Theor. And Exp. pI and MW were calculated

[c] Number of peptides matched (#P) and sequence coverage (SC) in MASCOT analysis. MASCOT-generated probability-based Mowse score. In the LB400 protein database scores greater than 52 are significant ($P < 0.05$)

[d] Average normalized signal intensities from three biological replicates under each of the tested growth conditions; Succ, succinate.

ND, not detected. LR, low resolution in area where spot was expected.

DhA proteomes (Fig.4.2). The second one is DitU, encoded by BxeC0631, unique to the AbA proteome. DitQ and DitU have similar pIs and molecular weights and, as expected, are located next to each other on the AbA proteome map (Fig 4.2).

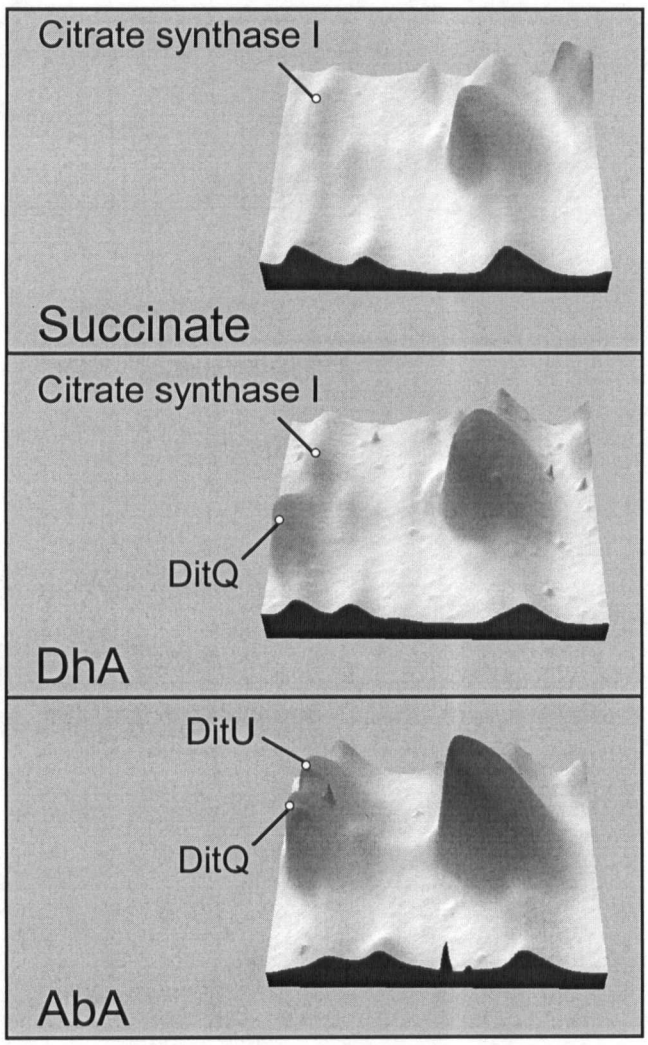

Figure 4.2 Differential expression of DitU. Three dimensional representation of 2D PAGE of the Succinate, DhA, and AbA proteomes of LB400 grown on the respective substrates showing the same relative area of each gel.

The DhA proteome contained a protein of low abundance with similar mobility as DitU, but this protein was identified as citrate synthase I, with a tryptic digest containing no peptide fragments corresponding to DitU (Fig. 4.2). An additional seven proteins not encoded within the *dit* gene cluster were unique to the AbA and DhA proteomes or were up-regulated on those

substrates relative to the succinate proteome (Table 4.3). These include proteins encoded by BxeC1186, BxeB0962, BxeB0963, BxeB1203, BxeB2301, BxeA1366, and BxeA2466.

4.3.2 Growth of mutant strains

To investigate the function of the identified P450s in abietane diterpenoid metabolism, two mutant strains were prepared, DitQKO and DitUKO, whose corresponding genes were disrupted by insertion. The *ditQ* disruption completely abolished the ability of LB400 to grow on DhA, but did not affect its growth on 7-oxo-DhA (Fig. 4.3). DitQKO grew on AbA with a similar doubling time and similar maximum protein concentration as LB400, but the lag phase was extended by approximately 100 hours. DitQKO grew on PaA to a similar maximum protein concentration as the LB400, but the lag phase was longer, and the doubling time greater. DitUKO was not able to grow on AbA; however, it showed similar lag phases, doubling times and maximum protein concentrations as LB400 on 7-oxo-DhA and DhA. Similar to DitQKO, growth of DitUKO on PaA reached a maximum protein concentration similar to the LB400, but the lag phase was longer and the doubling time greater.

4.3.3 Cell suspension assays

Cell suspensions assays were conducted to examine substrate removal and potential metabolite accumulation and/or removal.

AbA. LB400 and DitQKO were able to completely remove AbA within 72 hours (Fig. 4.4A). By contrast, DitUKO was only able to reduce the initial concentration of AbA by 34%, which indicates that *ditU* is involved in the catabolism of AbA. Trace amounts of 7-oxo-DhA were detected in all the cell suspensions on AbA at time zero, as this was a contaminant of the AbA reagent. LB400 and DitQKO increased amounts of 7–oxo-DhA, whereas, DitUKO did not increase 7-oxo-DhA above the initial concentration. This suggests that 7-oxo-DhA is a metabolite formed during AbA catabolism, and its formation requires DitU. A second metabolite

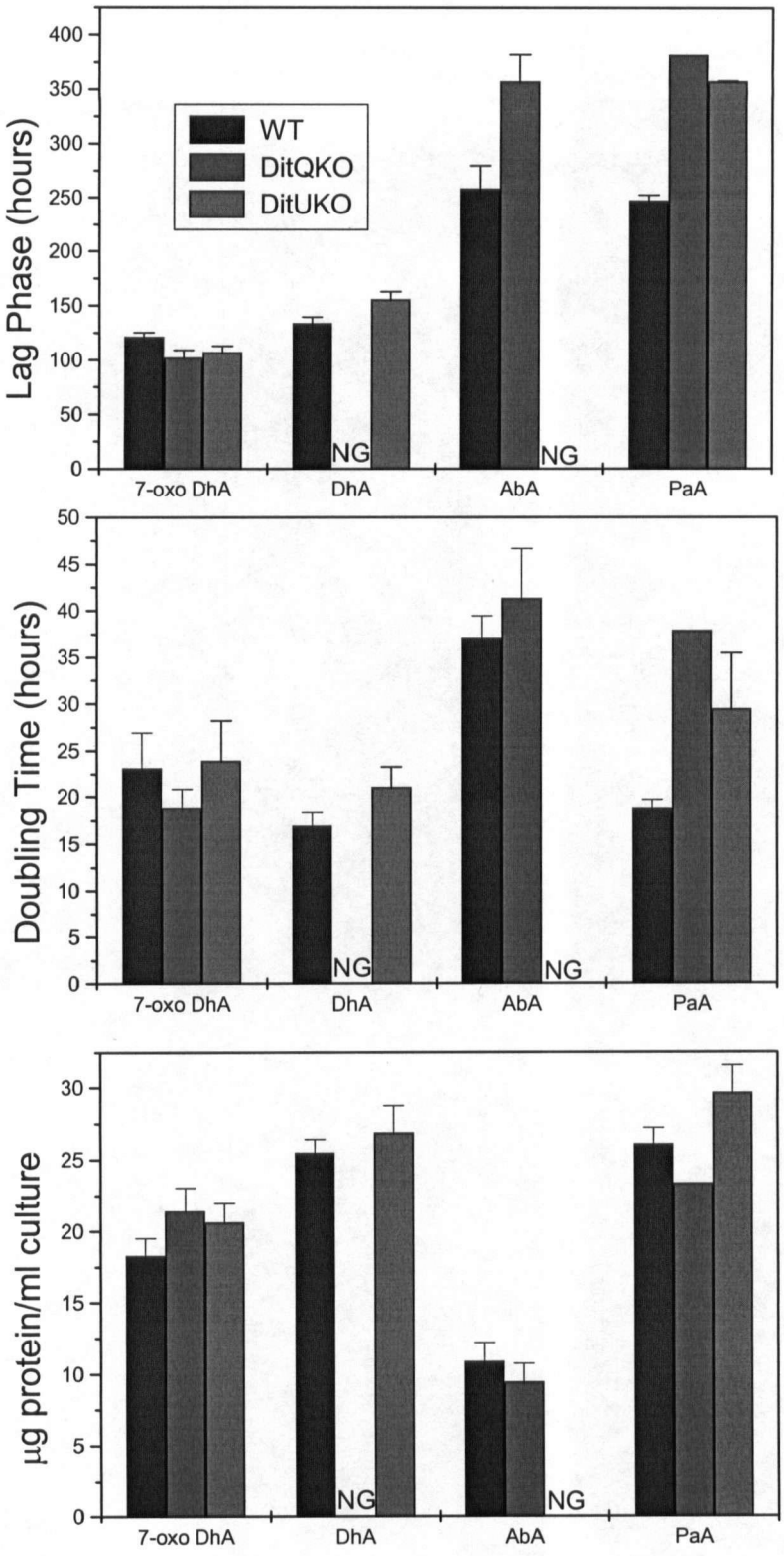

Figure 4.3 Growth characteristics of LB400 and two mutant strains, DitUKO and DitQKO on four abietane diterpenoids. Initial inoculum for each culture was ~2 x 10^6 cells/ml grown to mid-log phase on succinate. NG denotes no growth. Error bars indicate standard error.

with similar accumulation and removal patterns seen with 7-oxo-DhA could not be confidently identified using a NIST library search. This same metabolite was previously observed in cell suspensions of DitA1KO on AbA or PaA (Chapter 3) and was named Unknown I, and tentatively identified as 7-oxo-PaA (see Fig. 4.7). A third metabolite, identified as 2,4-dimethyl heptanedioic acid (DMHDA), was observed in LB400, DitQKO, and DitUKO cell suspensions. This same metabolite was also identified in an LB400 cell suspension assay reported in Chapter 3.

DhA. LB400 and DitUKO completely removed DhA within 72 hours, whereas DitQKO decreased concentrations of DhA by 40%, but was not able to remove it after 72 hours (Fig. 4.4 B). No 7-oxo-DhA or DMHDA accumulation was observed in DitQKO cell suspensions incubated on DhA, whereas LB400 and DitUKO with DhA showed the accumulation of both metabolites.

PaA. LB400 and DitQKO respectively removed 91% and 80% of the initial PaA by 72 hours; whereas, DitUKO removed only 22% by the same time (Fig. 4.4 C). With a longer incubation of 144 hours, DitUKO decreased the PaA concentration by 73%. All strains showed the accumulation of DhA, 7-oxo-DhA, DMHDA and Unknown I during PaA removal, which was not observed in heat-killed cell controls, supporting an enzymatic transformation of substrates and intermediates.

7-oxo-DhA. Cell suspensions of all strains completely removed 7-oxo-DhA within 24 hours (data not shown). This is an indication that neither DitQ nor DitU is essential for catabolism of 7-oxo-DhA.

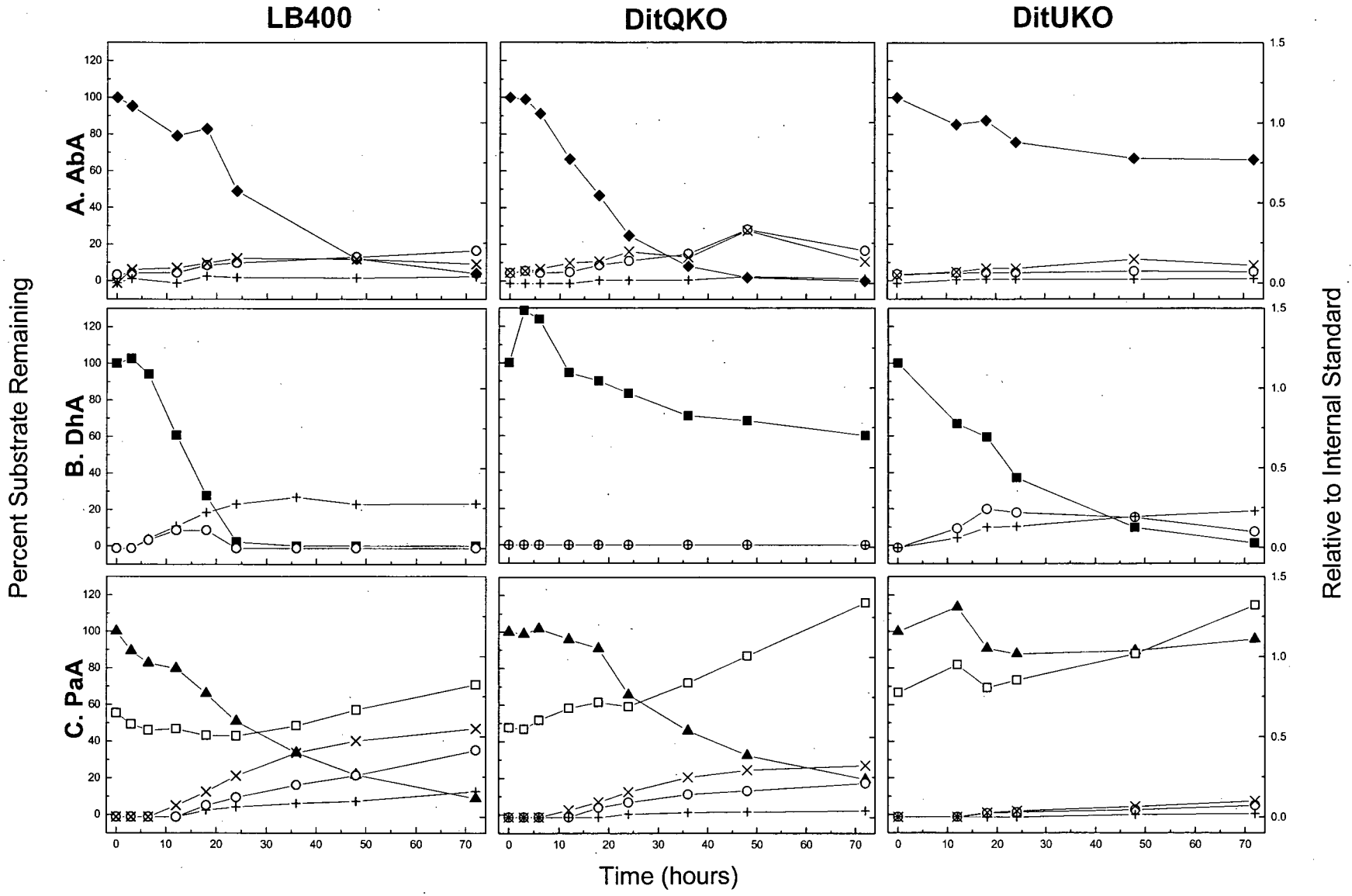

265 **Figure 4.4 Metabolite analysis of cell suspensions of LB400, DitQKO and DitUKO with AbA, DhA, and PaA.** A, AbA cell suspension. B, DhA cell suspension. C, PaA cell suspension. Closed symbols indicate values corresponding to the left y-axis and open or stick symbols correspond to the right y-axis, Symbols: ♦-AbA, ■ and □- DhA, ▲- PaA, ● and ○- 7-oxo-DhA, +-dimethyl heptanedioic acid, ×- Unknown I

4.3.4 Binding assays

To confirm that *ditQ* and *ditU* encode functional cytochromes P450, carbon monoxide binding assays were conducted. Both DitQ and DitU, expressed in the crude lysate of *E. coli,* bound carbon monoxide and produced a Soret maximum absorbance between 447 and 450 nm with little absorbance at 420 nm. This indicates that both DitQ and DitU are members of the P450 Superfamily and are expressed in *E. coli* in a native conformation. To investigate the possible range of compounds that bind to DitQ and DitU, substrate-binding assays were conducted. Binding of DhA to DitQ produced a typical substrate binding spectrum with dissociation constants (K_d) of 0.98 $\pm$ 0.01 μM (Fig. 4.5). This is a strong indication that DhA is a substrate for DitQ. Binding of PaA to DitQ produced a type I-like curve, which indicates that PaA is likely a substrate for DitQ, however an isosbestic point at 407 nm was not observed and therefore the dissociation constant could not be determined (Fig. 4.5). Binding of AbA to DitQ perturbed the heme environment; however, the binding equation curve could not be fitted to the data points and therefore results were inconclusive. 7-oxo-DhA did not alter the spectrum of DitQ at concentrations up to 25 μM, indicating that it is not likely a substrate for DitQ. The same assay was used to investigate binding of abietane diterpenoids to DitU, however, results were inconclusive. This may indicate that none of the assayed diterpenoids bind to DitU and therefore are not substrates for this enzyme, however other possibilities may exist, as discussed below.

4.3.5 P450 in vitro activity assay

To investigate the catalytic activity of DitQ and DitU, in vitro P450 activity assays were conducted. The crude lysate of *E. coli* containing expressed DitQ was combined with purified *Comamonas testosteroni* ferredoxin reductase BphG, purified *P. abietaniphila* BKME-9 ferredoxin DitA3, NADH, and either AbA, DhA, PaA or 7-oxo-DhA. BphG is the reductase component of the electron transport system of the biphenyl ring-hydroxylating dioxygenase. The gene encoding an LB400 homologue of DitA3 was up-regulated during growth on DhA versus

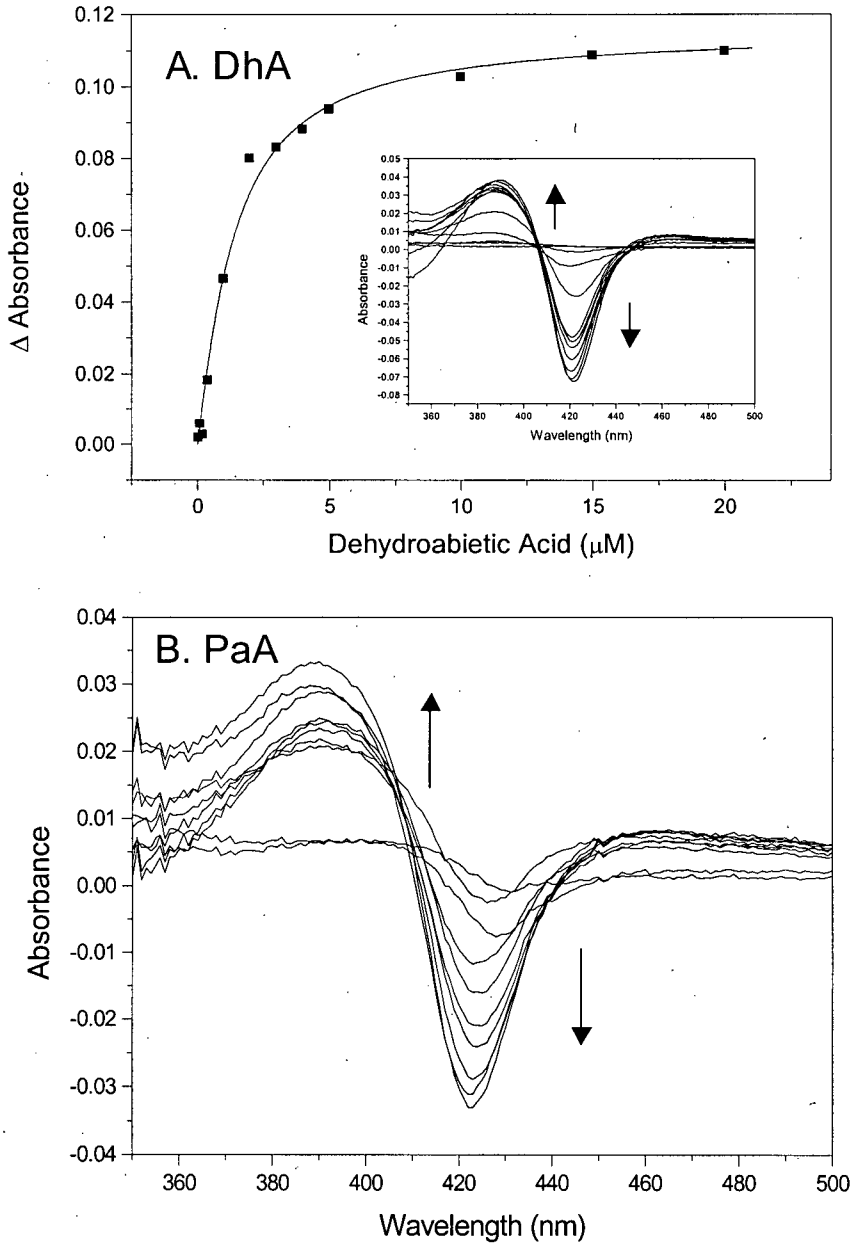

295 **Figure 4.5 Binding spectra for DhA or PaA to DitQ**. A. DhA binding to DitQ. Data points represent the difference in absorbance between 387 and 421 nm caused by increasing DhA concentrations. The curve represents a best fit of the binding equation to the data in which K_d = 0.98 ± 0.01 μM and Δ A_{max} = 1.16 x 10^{-1} ± 6.55 x 10^{-3}. Insets. UV-visible difference spectra of DitQ with increasing concentrations of DhA. B. PaA binding to DitQ. UV-visible difference
300 spectra of DitQ with increasing concentrations of PaA. Arrows indicate increases in the amplitude of maximum or minimum absorbance caused by increasing concentration of DhA or PaA.

on succinate in transcriptomic analysis (Chapter 3). GCMS analysis of the diazomethane-derivatized reactions incubated with DhA revealed the formation of a single peak at a retention time of 1.11 relative to that of DhA (Fig. 4.6). The mass spectrum of this peak indicated that the product is 7-hydroxy-DhA (Fig. 4.6, 4.7). Incubation of expressed DitQ with other diterpenoids did not yield a detectable product. The same assay was conducted using DitU expressed in *E. coli* under the same conditions and incubated with the same diterpenoids as used above, but no product was detected.

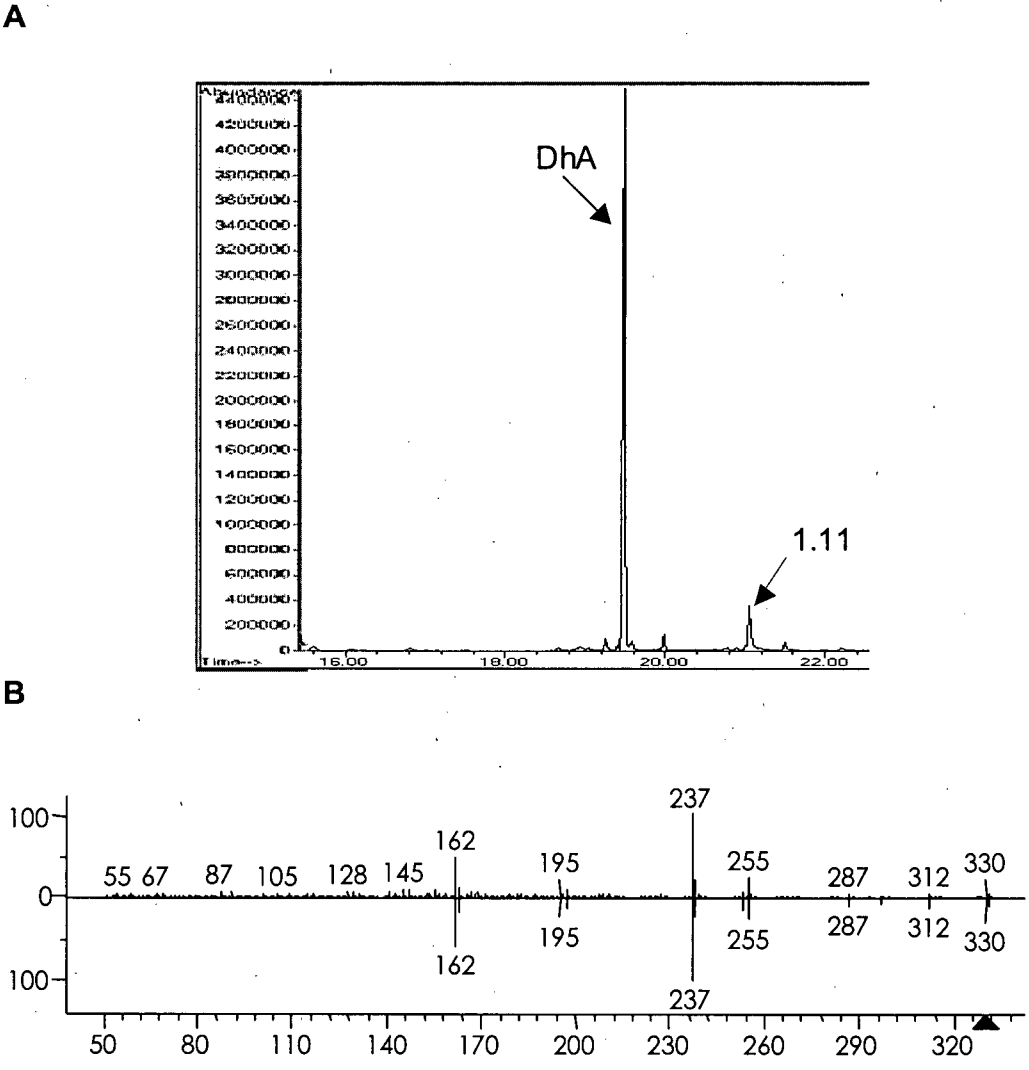

Figure 4.6 In vitro DitQ activity assay. A. Gas chromatograph of in vitro DitQ P450 reaction mixture incubated with DhA. B. Head to tail mass spectrum of peak with relative retention of 1.11. Fragmentation pattern above the zero line corresponds to the peak identified from DitQ with DhA in vitro activity assay. Fragmentation pattern below the zero line corresponds to 7-hydroxy-DhA mass spectrum from NIST library.

4.4 Discussion

This is the first proteomic investigation of bacteria grown on abietane diterpenoids (Fig. 4.1). This study provides the first conclusive evidence for the involvement of two cytochromes P450, DitQ (CYP226A1) and DitU (CYP226A2) of the LB400 *dit* cluster in the degradation of abietane diterpenoids. The results indicate that the P450s function in the catabolic pathways of AbA and/or DhA and are required in the formation of the central intermediate 7-oxo-DhA (Fig 4.7). We also provide the previously missing evidence for the C7 hydroxylating activity of DitQ.

4.4.1 Consistency of proteome and transcriptome

The protein spots identified as being up-regulated in the DhA proteome agree with the up-regulated genes of the DhA transcriptome reported in Chapter 3. All identified protein spots, which are products of the LB400 *dit* cluster genes, were also up-regulated in the transcriptome. Of the 7 identified proteins that are encoded by genes outside of the *dit* cluster, only one corresponding gene was not significantly up-regulated. Genes BxeB0962 and BxeA2466 (see Table 4.3) were up-regulated > 1.8 fold with p-values of < 0.01 and are clustered with up-regulated genes BxeB0961 and BxeB0963 involved in CoA-dependent metabolism, and BxeA2467, BxeA2469 and BxeA2470 involved in a possible sulfate transport cluster. Gene BxeA1366 was not significantly up-regulated but clustered with the up-regulated gene BxeA1367 both of which are also involved in CoA-dependent metabolism. Gene BxeC1186, which encodes a serine hydrolase, BphD of the biphenyl catabolic operon, was up-regulated 1.4 fold with a p-value of 0.0007. These results indicate consistency between the proteome and transcriptome.

4.4.2 Cytochromes P450 DitQ and DitU

Characterization of the LB400 *dit* cluster revealed two genes coding for cytochromes P450, *ditQ* and *ditU* (Chapter 3). The annotated LB400 genome revealed six putative cytochromes P450, four encoded on the megaplasmid and two on chromosome 1. Of these six

P450s, only DitU and/or DitQ were identified as having increased abundance during growth on AbA or DhA relative to growth on succinate (Fig. 4.2). DitQ and DitU are closely related, sharing 60% amino acid sequence identity (see Table 4.4), while their identity with the other four P450s of LB400 ranges from 19.5 to 24.4%. While DitQ is expressed during growth on both DhA and AbA, DitQKO mutant phenotypes showed that DitQ is required for catabolism of DhA and not of AbA, indicating non-essential expression of DitQ during growth of AbA (Figs. 4.2-4.4). On the other hand, DitU is expressed only during growth on AbA, with DitUKO mutant phenotypes confirming its essential role in the catabolism of AbA but not DhA. The expression of DitQ and not DitU during growth on DhA is consistent with transcriptomic results presented in Chapter 3.

A reporter construct in BKME-9 demonstrated that *ditQ* was induced by AbA, DhA or PaA. There is no conclusive evidence that a second P450 is involved in BKME-9 abietane diterpenoid catabolism. However, growth phenotypes of a BKME-9 *ditQ* knockout (Chapter 2) suggested that a second monooxygenase is able to complement DitQ during growth on DhA and PaA. This mutant strain showed that growth was only impaired and not abolished on both DhA and PaA. Note that a similar result was obtained for a knockout of the *ditQ* homologue identified in *P. diterpeniphila* A19-6a (17). The mutant strain was still able to grow on both AbA and DhA, however removal of both substrates was impaired. This raised the possibility of a second monooxygenase in both BKME-9 and A19-6a, possibly homologous to DitU in LB400. If this were the case, these previous findings would imply that the DitU homologues in BKME-9 and A19-6a were up-regulated or constitutively expressed during growth on DhA, which was not the case for LB400. This also raises the possibility that DitU-LB400 may also be able to transform DhA; however, because the enzyme is not expressed by LB400 during growth on DhA it cannot complement DitQ activity.

4.4.3 Binding properties of DitQ

The binding of DhA to DitQ (Fig. 4.5) agrees with our previous report for DitQ-BKME-9 (Chapter 2). However, DitQ-BKME-9 has a lower K_d than DitQ-LB400, which indicates that the affinity of DitQ-BKME-9 for DhA is greater than that of DitQ-LB400. DitQ-LB400 showed a type I-like binding spectrum for PaA, whereas titration of PaA with DitQ-BKME-9 caused a perturbation of the heme environment but results were inconclusive. Recently, however, atypical type I red-shifted binding spectra, similar to the one observed for DitQ-BKME-9 bound to PaA, have been reported for P450 EpoK bound to the polyketide epothilone D (19). EpoK has been shown to cause the epoxidation of epothilone D. This result raises the possibility that DitQ-BKME-9, which shares 71% amino acid identity with DitQ-LB400 (see Table 4.4), also binds PaA. Alternatively, it could be that the substrate range of DitQ-LB400 is wider than DitQ-BKME-9.

Both proteomic and mutant phenotype analysis imply that DitU is involved in the catabolism of AbA,. however, substrate binding assays and in vitro activity assays were inconclusive. This may indicate that the natural substrate for this enzyme has not been identified or the in vitro assay system for this enzyme was ineffective. In a recent report, Simgen et al. (25) were able to catalyze the 15β-hydroxylation of deoxycorticosterone with the purified $P450_{meg}$ (CYP106A2), adrenodoxin and adrenodoxin reductase. They were not, however, able to show evidence of binding using UV-Vis methods (25). Similarly, results from an investigation of $P450_{mor}$, isolated from *Mycobacterium* sp. Strain HE5, did not show evidence of binding of morpholine (up to 50 mM) to the purified HIS-tagged $P450_{mor}$. Morpholine is a putative native substrate for the enzyme. However, an in vitro P450 assay utilizing the purified enzyme in the presence of its native ferredoxin and ferredoxin reductase showed turnover of this substrate [29 $\pm$ 3.0 nmol morpholine^{-1} min^{-1} (nmol P450)$^{-1}$] (24). Further investigation with purified catalytic

subunits and electron transfer components may be necessary to establish the substrate range and activity of DitU.

4.4.4 Demonstration of DitQ activity

This thesis provides the missing evidence that DitQ catalyzes the C7 hydroxylation of DhA (Fig. 4.6). This conclusion is supported by the mutant phenotypes. Both LB400 and DitUKO accumulated 7-oxo-DhA in cell suspensions with DhA, whereas, DitQKO was not able to transform DhA, indicating that DitQ is required for this activity. DhA showed the lowest K_d with DitQ, which was the only substrate yielding a detectable product. This product was reported as a metabolite found in cultures of *A. eutrophus* incubated with DhA (2) and more recently as a biotransformation product of *Aspergillus niger* (10), however, no enzyme responsible for this transformation has been identified.

Even though PaA was shown to bind to DitQ-LB400, no transformation product from this substrate was observed in the in vitro activity assay. Inefficient electron transfer to the catalytic subunit using non-native electron transport components may have contributed to the lack of turnover of PaA, as suggested for DitU. Further investigation is needed to determine the substrate range of DitQ with native electron transport components (see below).

4.4.5 Proposed initial steps of the diterpenoid pathway

Both DitU and DitQ likely function in the conversion of abietane diterpenoids to 7-oxo-DhA (Fig. 4.7). During growth on DhA (V), *ditQ* is up-regulated and expressed. DitQ then binds DhA and catalyzes hydroxylation to 7-hydroxy-DhA (VII). The hydroxyl group is presumably further oxidized to 7-oxo-DhA (VIII) by an unidentified dehydrogenase. 7-oxo-DhA (VIII) is a substrate for DitA dioxygenase activity (14).

Previous reports on BKME-9 suggested that AbA (I, Fig. 4.7) is transformed to DhA (V) followed by catabolism as described above (13, 15, 16). However, there is no direct evidence of aromatization of the C ring or conversion of AbA to DhA prior to C7 hydroxylation neither in

BKME-9 nor in LB400. The current study provides new evidence that suggests a different route for AbA degradation (Fig. 4.7). The main route of AbA (I) degradation requires the activity of DitU, even though growth on AbA leads to the expression of both DitU and DitQ. Accumulation of 7-oxo-DhA (VIII) by a *ditA1* knockout on AbA supports that 7-oxo-DhA is an intermediate in AbA catabolism (Chapter 3). DitUKO cell suspensions reported in this Chapter revealed that DitU is required for transformation of AbA to 7-oxo-DhA. This raises the possibility that DitU catalyzes a step in the transformation of AbA to 7-oxo-DhA. Others have speculated that transformation of AbA involves the formation of 7-hydroxy-AbA (3), and 7,8 epoxy-AbA (III) (22). Chemical transformations of AbA have produced 7-acetoxy-DhA in a single step reaction with mercuric acetate (1). Also, fungal biotransformation of pimaradiene diterpenes, containing a B ring structure with a 7,8 double bond similar to AbA, revealed that the main products contained the epoxidation of the 7,8 double bond and 7-oxo derivatives (Chapter 1, Table 1.1) (6-8). Fraga et al. (6) speculated that the 7,8 epoxide rearranged to the 7-ketone by opening of the oxirane ring. A 7-oxo product of AbA catabolism would require elimination or shift in the 7,8 double bond. Such a shift could result in 7-oxo-PaA (VI), which was tentatively identified in extracts of both PaA and AbA cell suspensions with the DitA1KO mutant strain (Chapter 3) and in the present cell suspensions as Unknown I (Fig. 4.3). Perhaps 7-oxo-PaA (VI) is a common intermediate in AbA (I) and PaA (II) metabolism prior to aromatization of the C ring yielding 7-oxo-DhA (VIII) (see discussion below) (Fig. 4.7). A gene or enzyme leading to the aromatized ring C product has not been identified.

Two pathways may exist for the degradation of PaA (II) by LB400 that can be catalyzed by either DitQ or DitU (Fig. 4.7). Cells incubated in the presence of PaA revealed that both DitQKO and DitUKO mutant strains were able to transform PaA to DhA (Fig. 4.4) as was

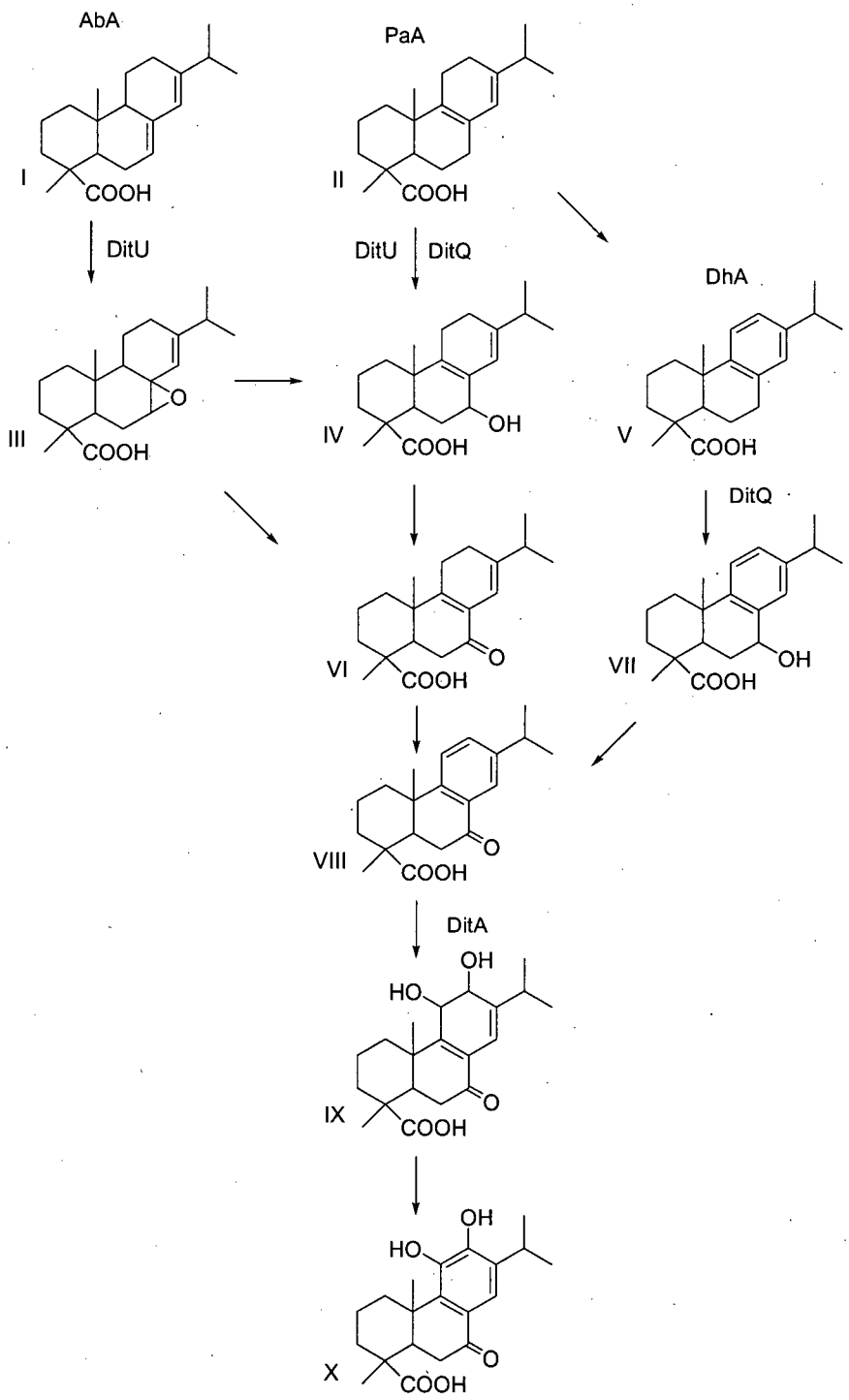

440

Figure 4.7 Proposed convergent pathway for abietane diterpenoid degradation by LB400. I. AbA; II, palustric acid; III, 7,8-epoxy-abietic acid; IV, 7-hydroxy-palustic acid ; V, dehydroabietic acid; VI, 7-oxo-palustric acid; VII, 7-hydroxy-dehydroabietic acid; VIII, 7-oxo-dehydroabietic acid; IX, 7-oxo-11,12-dihydroxy-8,13-abieadien acid; X 7-oxo-11,12-
445 dihydroxydehydroabietic acid. Enzymes next to arrows indicate the reaction proposed to be catalyzed by that enzyme.

observed with DitA1KO (Chapter 3). It follows that DhA (V) would then be degraded as described above via 7-hydroxy-DhA (VII). Alternatively, in Chapter 3 evidence was given for hydroxylation of PaA prior to aromatization of the C ring resulting in 7-oxo-PaA (VI) which would be degraded as described above via 7-oxo-DhA (VIII). In LB400 the question is, is DitQ or DitU involved in one or both of these pathways or is there redundancy between the activities of the two P450s? Substrate binding assays showed that DitQ binds PaA and is therefore likely a substrate for the enzyme. DitQ could then catalyze the transformation of PaA (II) to 7-hydroxy-PaA (IV). However, if only DitQ is expressed during growth on PaA this would not allow for growth or substrate removal by DitQKO on PaA (Fig 4.3, 4.4 & 4.7). On the other hand, if only DitU is expressed during growth on PaA this would not allow for growth or substrate removal by DitUKO on PaA. However, if both DitQ and DitU are up-regulated, then during growth and in cell suspensions of DitQKO on PaA, DitU could transform PaA to 7-hydroxy-PaA (IV). It is also possible, as speculated in BKME-9 DitQ knockouts, that DitU is able to bind and transform DhA (V) to 7-hydroxy-DhA (VII). During growth and cell suspensions of DitUKO, DitQ could catalyze the same transformations of PaA and DhA. More experimentation is required to determine the expression pattern of both P450s and transformations catalyzed by the two enzymes.

4.4.6. Electron transport ferredoxins

In the previous chapter, the possibility of a single ferredoxin reductase component functioning with both P450s and the ring hydroxylating dioxygenase was presented. The evidence there suggests that *ditA3* encoding a 3Fe-4S ferredoxin functions with the dioxygenase. This class of ferredoxin can function in P450 electron transport (20), raising the possibility that DitA3 also functions with DitQ and/or DitU. The BKME-9 homologue of DitA3 was used in the in vitro P450 assay for substrate transformation of DhA to 7-hydroxy-DhA, whereas assays which did not include DitA3 where not able to form a detectable product. This suggests that

DitA3 is used in both dioxygenase and monooxygenase electron transport systems. However, other evidence from a BKME-9 DitA3 mutant strain suggests that expression of DitA3 is not required for P450 activity (13). This mutant was not able to grow on DhA but did transform the substrate to 7-oxo-DhA. This finding supports its role in DitA catalytic function, but also suggests that another ferredoxin must be capable of electron transport in any P450(s) involved in oxygenation of C7. BxeC0601, located two ORFs downstream of *ditQ,* is predicted to encode a typical plant-type 2Fe-2S ferredoxin component. Perhaps this second ferredoxin functions in electron transport for one or both of the *dit* P450s. If this were the case it would result in a complex system of electron transfer involving a single reductase, two ferredoxins, one a 3Fe-4S and the other a 2Fe-2S, two cytochromes P450 and a ring hydroxylating dioxygenase. Further study is needed with purified electron transfer and catalytic components.

4.4.7.CYP226A family

DitQ-LB400 and DitU-LB400 are members of the cytochrome P450 CYP226A family. Based on sequence identity, there are six identified members of the CYP226A family (Table 4.4) (18), four of which are from bacteria that grow on abietane diterpenoids as a sole source of carbon and energy. DitQ-LB400 and DitU-LB400 have been designated CYP226A1 and CYP226A2, respectively. The only other classified member of this family is TdtD (CYP226A3) from the abietane diterpenoid degrading *Pseudomonas diterpeniphila* A19-6a (17). The BKME-9 homologue of DitQ has not yet been classified, but according to sequence identity of greater than 60% with other members of the family, DitQ from BKME-9 would also be included in this family. The remaining two P450s were identified in the recently sequenced genome of *P. aeruginosa* 2192 and are included in a putative 2192 *dit* cluster (Chapter 3). We suspect that this bacterium is also able to catabolize abietane diterpenoids, however this has not yet been confirmed. It is also worth noting that homologues of both CYP226A1 and CYP226A2 were identified in the Sargasso Sea metagenome (27). It is possible that all members of the CYP226A

P450 family are involved in diterpenoid catabolism. This may allow for the prediction of other abietane diterpenoid degrading strains based on the presence of high sequence similarity with members of CYP226A.

Table 4.4 CYP226A family

	DitQ-LB400	DitQ-BKME-9	DitQ-A19-6a	DitQ-2192	DitU-LB400	DitU-2192
DitQ-LB400	ID	70.8	72.2	70.8	60.9	56.7
DitQ-BKME-9	70.8	ID	84.1	84.4	62.1	60.7
DitQ-A19-6a	72.2	84.1	ID	93.8	63.0	61.6
DitQ-2192	70.8	84.4	93.8	ID	62.1	61.4
DitU-LB400	60.9	62.1	63.0	62.1	ID	64.7
DitU-2192	56.7	60.7	61.6	61.4	64.7	ID

Deduced amino acid percent sequence identity matrix. ID, identical

4.5 Conclusion

To our knowledge, this is the first clear demonstration of an enzyme, DitQ, which is responsible for C7 hydroxylation of an abietane diterpenoid in a degradation pathway. This type of enzyme appears widespread, as similar transformation products are commonly identified in the lysates of organisms incubated with diterpenoids for the purpose of identifying possible metabolites in eukaryotic systems or for means of producing more effective drug candidates (Chapter 1). The evidence is less strong for an analogous role of DitU in the transformation of AbA, however, our findings are consistent for a role similar to DitQ. Further work will focus on understanding the kinetics of the purified P450s as well as elucidating electron transport systems required for the degradation of abietane diterpenoids.

4.6. References

1. **Barrero, A. F., E. J. Alvarez-Manzaneda, R. Alvarez-Manzaneda, R. Chahboun, R. Meneses, and M. Aparicio B.** 1999. Ring A functionalization of terpenoids by the unusual Baeyer-Villiger rearrangement of aliphatic aldehydes. Synlett:713-716.

2. **Biellmann, J. F., G. Branlant, M. Gero-Robert, and M. Poiret.** 1973. Degradation bacterienne de l'acide dehydroabietique par un *Pseudomonas* et une *Alcaligenes*. Tetrahedron **29:**1237-1241.

3. **Cross, B. E., and P. L. Myers.** 1968. The bacterial transformation of abietic acid. Biochem J **108:**303-10.

4. **de Lorenzo, V., and K. N. Timmis.** 1994. Analysis and construction of stable phenotypes in gram-negative bacteria with Tn5- and Tn10-derived minitransposons. Methods Enzymol **235:**386-405.

5. **Denef, V. J., M. A. Patrauchan, C. Florizone, J. Park, T. V. Tsoi, W. Verstraete, J. M. Tiedje, and L. D. Eltis.** 2005. Growth substrate- and phase-specific expression of biphenyl, benzoate, and C1 metabolic pathways in *Burkholderia xenovorans* LB400. J. Bacteriol. **187:**7996-8005.

6. **Fraga, B. M., P. Gonzalez, M. G. Hernandez, M. C. Chamy, and J. A. Garbarino.** 2003. Microbial transformation of 18-hydroxy-9,13-epi-ent-pimara-7,15-diene by *Gibberella fujikuroi*. J Nat Prod **66:**392-7.

7. **Fraga, B. M., P. Gonzalez, M. G. Hernandez, M. C. Chamy, and J. A. Garbarino.** 1998. The microbiological transformation of a 9-epi-ent-pimaradiene diterpene by Gibberella fujikuroi. Phytochemistry **47:**211-215.

8. **Fraga, B. M., M. G. Hernandez, P. Gonzalez, M. C. Chamy, and J. A. Garbarino.** 2000. The biotransformation of 18-hydroxy-9-epi-ent-pimara-7,15-diene by *Gibberella fujikuroi*. Phytochemistry **53:**395-399.

9. **Goris, J., P. De Vos, J. Caballero-Mellado, J. Park, E. Falsen, J. F. Quensen, 3rd, J. M. Tiedje, and P. Vandamme.** 2004. Classification of the biphenyl- and polychlorinated biphenyl-degrading strain LB400T and relatives as *Burkholderia xenovorans* sp. nov. Int J Syst Evol Microbiol **54:**1677-81.

10. **Gouiric, S. C., G. E. Feresin, A. A. Tapia, P. C. Rossomando, G. Schmeda-Hirschmann, and D. A. Bustos.** 2004. 1β,7β-Dihydroxydehydroabietic acid, a new biotransformation product of dehydroabietic acid by *Aspergillus niger*. World Journal of Microbiology and Biotechnology **20:**281-284.

11. **Hoang, T. T., R. R. Karkhoff-Schweizer, A. J. Kutchma, and H. P. Schweizer.** 1998. A broad-host-range Flp-FRT recombination system for site-specific excision of chromosomally-located DNA sequences: application for isolation of unmarked *Pseudomonas aeruginosa* mutants. Gene **212:**77-86.

12. **Kinter, M., and N. E. Sherman.** 2000. Protein sequencing and identification using tandem mass spectrometry. John Wiley, New York.

13. **Martin, V. J., and W. W. Mohn.** 2000. Genetic investigation of the catabolic pathway for degradation of abietane diterpenoids by *Pseudomonas abietaniphila* BKME-9. J Bacteriol **182:**3784-93.

14. **Martin, V. J., and W. W. Mohn.** 1999. A novel aromatic-ring-hydroxylating dioxygenase from the diterpenoid-degrading bacterium *Pseudomonas abietaniphila* BKME-9. J Bacteriol **181:**2675-82.

15. **Martin, V. J., Z. Yu, and W. W. Mohn.** 1999. Recent advances in understanding resin acid biodegradation: microbial diversity and metabolism. Arch Microbiol **172:**131-8.

16. **Martin, V. J. J.** 1999. Molecular genetic investigation of the abietane diterpenoid degradation pathway of *Pseudomonas abietaniphila* BKME-9. Doctor of Philosophy. University of British Columbia, Vancouver.

17. **Morgan, C. A., and R. C. Wyndham.** 2002. Characterization of tdt genes for the degradation of tricyclic diterpenes by *Pseudomonas diterpeniphila* A19-6a. Can J Microbiol **48:**49-59.

18. **Nelson, D. R., L. Koymans, T. Kamataki, J. J. Stegeman, R. Feyereisen, D. J. Waxman, M. R. Waterman, O. Gotoh, M. J. Coon, R. W. Estabrook, I. C. Gunsalus, and D. W. Nebert.** 1996. P450 superfamily: update on new sequences, gene mapping, accession numbers and nomenclature. Pharmacogenetics **6:**1-42.

19. **Ogura, H., C. R. Nishida, U. R. Hoch, R. Perera, J. H. Dawson, and P. R. Ortiz de Montellano.** 2004. EpoK, a cytochrome P450 involved in biosynthesis of the anticancer agents epothilones A and B. Substrate-mediated rescue of a P450 enzyme. Biochemistry **43:**14712-21.

20. **O'Keefe, D. P., K. J. Gibson, M. H. Emptage, R. Lenstra, J. A. Romesser, P. J. Litle, and C. A. Omer.** 1991. Ferredoxins from two sulfonylurea herbicide monooxygenase systems in Streptomyces griseolus. Biochemistry **30:**447-55.

21. **Patrauchan, M. A., C. Florizone, M. Dosanjh, W. W. Mohn, J. Davies, and L. D. Eltis.** 2005. Catabolism of benzoate and phthalate in *Rhodococcus* sp. strain RHA1: redundancies and convergence. J. Bacteriol. **187:**4050-4063.

22. **Prinz, S., U. Mullner, J. Heilmann, K. Winkelmann, O. Sticher, E. Haslinger, and A. Hufner.** 2002. Oxidation products of abietic acid and its methyl ester. J Nat Prod **65:**1530-4.

23. **Schweizer, H. P., and T. T. Hoang.** 1995. An improved system for gene replacement and *xylE* fusion analysis in *Pseudomonas aeruginosa*. Gene **158:**15-22.

24. **Sielaff, B., and J. R. Andreesen.** 2005. Kinetic and binding studies with purified recombinant proteins ferredoxin reductase, ferredoxin and cytochrome P450 comprising

the morpholine mono-oxygenase from *Mycobacterium* sp. strain HE5. Febs J **272:**1148-59.

25. **Simgen, B., J. Contzen, R. Schwarzer, R. Bernhardt, and C. Jung.** 2000. Substrate binding to 15β-Hydroxylase (CYP106A2) probed by FT infrared spectroscopic studies of the iron ligand CO stretch vibration. Biochemical and Biophysical Research Communications **269:**737-742.

26. **Simons, R., U. Priefer, and A. Puhler.** 1983. A broad host range mobilization system for in vivo genetic engineering: transposon mutagenesis in Gram negative bacteria. Bio/Techonology **1:**784-790.

27. **Venter, J. C., K. Remington, J. F. Heidelberg, A. L. Halpern, D. Rusch, J. A. Eisen, D. Wu, I. Paulsen, K. E. Nelson, W. Nelson, D. E. Fouts, S. Levy, A. H. Knap, M. W. Lomas, K. Nealson, O. White, J. Peterson, J. Hoffman, R. Parsons, H. Baden-Tillson, C. Pfannkoch, Y.-H. Rogers, and H. O. Smith.** 2004. Environmental genome shotgun sequencing of the Sargasso Sea. Science **304:**66-74.

5. Conclusion

This dissertation greatly advances our understanding of the microbial metabolism of diterpenoids. Previous to the work presented here, a 16.7-kbp cluster of genes in BKME-9, including those encoding ring hydroxylating and ring cleavage dioxygenases, (3) and a 9.18-kbp cluster of genes, including a putative P450, (4) had been reported. We expanded knowledge of the BKME-9 *dit* cluster, showing that it contained a sequence of genes, including one encoding a cytochrome P450, with high deduced amino acid sequence identity and identical gene order to the *tdt* cluster. Using the characterized BKME-9 *dit* cluster, we identified an 80.5-kbp LB400 cluster of genes in LB400 containing many homologues with high sequence similarity to the BKME-9 *dit* cluster. Finally, through transcriptomic and proteomic analysis we characterized the genes of the 80.5-kbp LB400 *dit* cluster up-regulated during growth on abietane diterpenoids. Recently, another putative *dit* cluster was identified in the sequenced genome of *Pseudomonas aeruginosa* 2192 (*Pseudomonas aeruginosa 2192* Sequencing Project, Broad Institute of Harvard and MIT (http://www.broad.mit.edu)). The *dit* cluster is emerging as a common catabolic set of genes in Proteobacterial genomes and likely will be found in more bacterial genomes as they become available.

There is still much that remains unclear regarding the genes of the LB400 *dit* cluster. Of the 72 genes identified, we can confidently assign functions to only 6 catabolic gene products, which are involved in the transformation of abietane diterpenoids to an aromatic diol intermediate, a substrate for ring cleavage (see Chapter 4 Fig. 4.7). The function of the other 66 genes is unclear, although they presumably encode all components required to import and transform abietane diterpenoids into common intermediates of the central catabolic pathways. Regarding uptake, the LB400 *dit* cluster encodes 4 putative transport proteins, which could

function in either uptake of substrate or export of toxic intermediates. Regarding downstream catalysis of the cleaved C ring product, the *dit* cluster encodes 3 putative hydrolases, which could function in hydrolysis of carbon-carbon bonds splitting the C20 compound into smaller units. β-oxidation would likely then play a role with the *dit* cluster encoding several genes putatively involved in acyl-CoA metabolism including a CoA ligase, at least four acyl-CoA dehydrogenases, two putative enoyl-CoA hydratases, one 3-hydroxyacyl-CoA dehydrogenase, one acetyl CoA acetyl transferase. Also encoded by the *dit* cluster are more than 20 genes encoding conserved hypothetical proteins with no known function. With such a large cluster of genes, many encoding homologous proteins, it raises questions regarding redundancy. Do homologous proteins catalyze the same reaction or are different homologues required for the catabolism of different substrates, possibly other varieties of diterpenoids? Further study is needed to answer these questions.

Members of the CYP226A family play a key role in the initial steps of the catabolism of abietane diterpenoids. Previous reports implicated a P450 in the degradation pathway but gave no conclusive evidence for its role (4). We have shown that not one but two P450s are involved in the degradation of abietanes in LB400 and gave evidence that this is likely also the case in BKME-9. Using the information gained from these studies of the two P450s in abietane metabolism we were able to provide a clear model of the initial steps in the catabolism of DhA to 7-oxo-DhA. Although, we were able to show that DitU is involved in AbA and PaA catabolism, we were not able to confidently identify a substrate for DitU or show enzymatic activity. With respect to PaA catabolism, the involvement of DitQ was implicated through substrate binding data using both DitQ-BKME-9 and DitQ-LB400, while our understanding of the involvement of

DitU is not clear. Further work on purified enzyme systems maybe necessary for a better understanding of the substrates and enzymes involved in this catabolic pathway.

The major components of the anabolic pathway for abietane diterpenoid production in conifers is fairly well understood as reviewed in Chapter 1. We have recently begun to gain insight into the catabolism of these natural products at a molecular level, leading to a better understanding of the complete carbon cycle of these abundant compounds. Previous to this study 3 pathways for DhA degradation had been identified, one via a 3-oxo intermediate (2), one via a 7-oxo-DhA intermediate (3), and a third via a combination of the 3-oxo and 7-oxo pathways (1). Does the newly gained knowledge presented here shed any light on the general scheme of microbial degradation of the broad range of tricyclic diterpenoids via 7-oxo intermediates? In Chapter 1 we posed the question, does degradation rely on a few enzymes with broad specificities, or does there seem to be a proliferation of divergent degradative enzymes specific for the broad range of terpenoids? Similar to a divergent synthetic pathway requiring few relatively few enzymes for the synthesis of a broad range of diterpenoids, (Chapter 1, Fig. 1.5) could the same scheme be utilized in their catabolism, that is relatively few enzymes are used to transform the broad range of diterpenoids into a common intermediate in a convergent degradation pathway. The limited range of substrates tested in this dissertation cannot clearly answer this question. However, with respect to abietane diterpenoid metabolism by BKME-9 and LB400, results are consistent with a few enzymes with broad substrate specificities required for conversion to a central intermediate in a convergent pathway (Chapter 4, Fig. 4.7).

What evidence exists for the catabolic pathways of other tricyclic diterpenoids? Included in this group is a class of compounds structurally related to abietane diterpenoids, the pimeranes. Pimeranes are synthesized from the same enzymes as abietanes, except that while the abietanes

have an isopropyl group at C13, the pimeranes have a methyl and a vinyl group (see Chapter 1 – Fig. 1.5). To date, we have very limited data regarding the pathway for pimerane catabolism. In general, gram negative bacteria that can grow on abietanes cannot necessarily utilize pimeranes, whereas strains that can grow on pimeranes usually utilize abietanes (5). Based on the observation that most pimerane-degrading strains can grow on abietane diterpenoids, it is possible that the pimeranes share a common intermediate with abietane catabolism. What are the genetic traits distinguishing these capabilities? Do they have additional genes required for transformation of pimeranes to a common intermediate, or do pimerane-degrading strains possess genes encoding the similar enzymes as abietane-degrading strains with a wider substrate range. If it is in fact a convergent pathway, what is the common intermediate? As more genome sequence data becomes available, a strain capable of growth on both classes of diterpenoids will likely be sequenced. Interestingly, the *P. aeruginosa* 2192 putative *dit* cluster possesses genes encoding a second set of alpha- and beta-subunits of a ring hydroxylating dioxygenase sharing greater than 60% amino acid identity with DitA1 and DitA2. Could this dioxygenase be required for conversion of pimeranes to a central intermediate of the diterpenoid pathway? Work presented in this dissertation has provided the background to experimentally investigate this and other questions regarding abietane diterpenoid degradation.

5.1 Comments on future research

Many possibilities exist for further work regarding the catabolism of abietane diterpenoids, including mechanisms of substrate transport, and genomic investigation of other putative abietane diterpenoid degrading strains, such as *P. aeruginosa* 2192. Recommendations for future work, however, focus on the P450s involved in abietane diterpenoid metabolism. Preliminary, biochemical analysis of both DitQ and DitU in this dissertation was conducted in

crude lysate of *E. coli.* Purification of DitQ and DitU and their putative electron transport components should lead to clarification of the role of these enzymes in the catabolism of abietane diterpenoids. These enzymes represent a novel family of P450s involved in natural product catabolism. Characterization of both DitQ and DitU and deciphering their complex electron transport system, potentially involving a single reductase functioning with 2 types of ferredoxins, a dioxygenase and 2 cytochromes P450 in a natural systems would be a novel finding and expand our understanding of electron transport in oxygenase systems.

5.4 References

1. **Biellmann, J. F., G. Branlant, M. Gero-Robert, and M. Poiret**. 1973. Degradation bacterienne de l'acide dehydroabietique par *Flavobacterium resinovorum*. Tetrahedron 29:1227-1236.

2. **Kieslich, K**. 1976. Microbial transformations of non-steroid cyclic compounds. J. Wiley, Chichester, Eng.

3. **Martin, V. J., and W. W. Mohn.** 2000. Genetic investigation of the catabolic pathway for degradation of abietane diterpenoids by *Pseudomonas abietaniphila* BKME-9. J Bacteriol 182:3784-93

4. **Morgan, C. A., and R. C. Wyndham.** 2002. Characterization of tdt genes for the degradation of tricyclic diterpenes by *Pseudomonas diterpeniphila* A19-6a. Can J Microbiol 48:49-59.

5. **Wilson, A. E., E. R. Moore, and W. W. Mohn.** 1996. Isolation and characterization of isopimaric acid-degrading bacteria from a sequencing batch reactor. Appl Environ Microbiol 62:3146-51.

APPENDIX

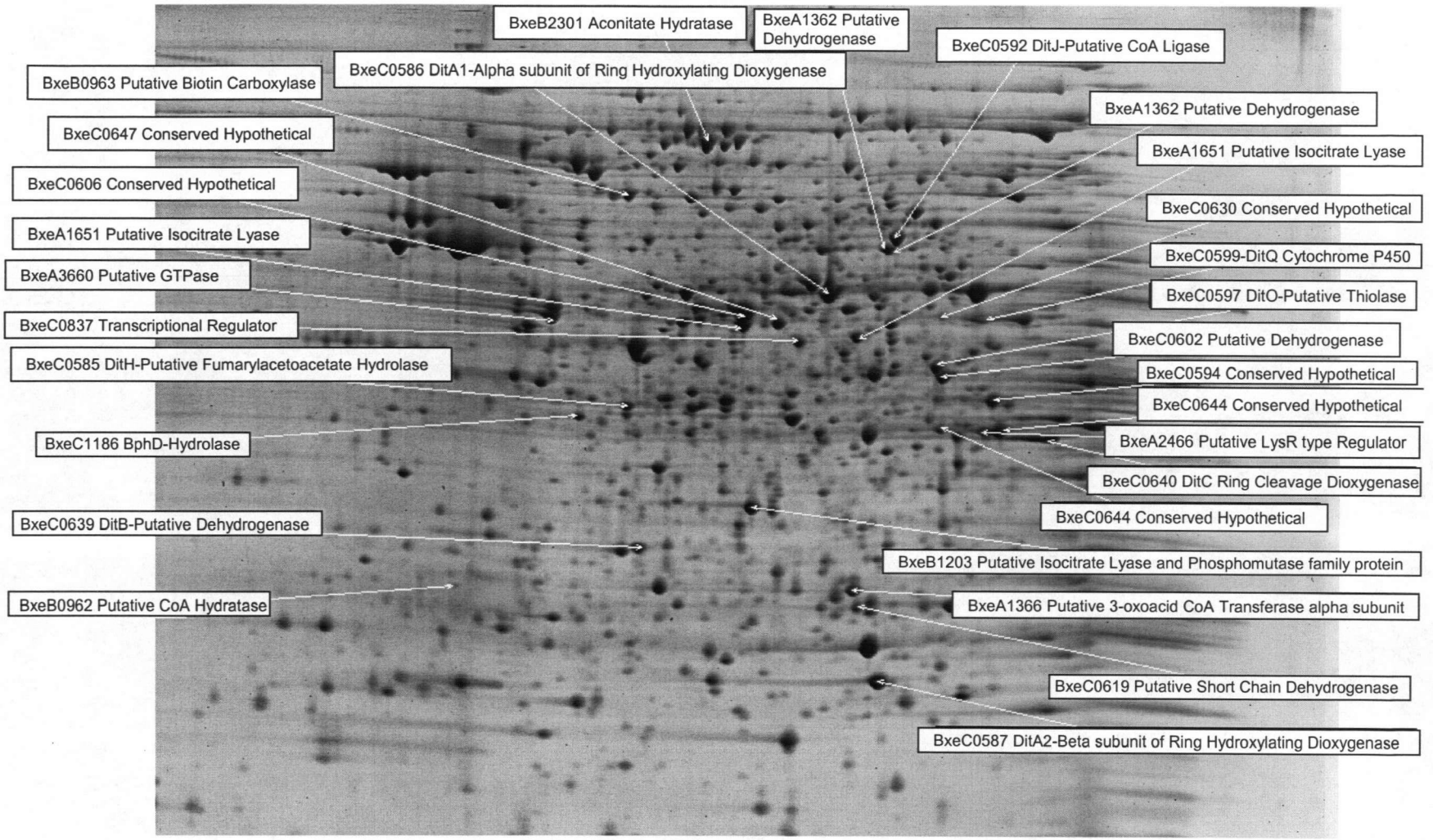

Figure A.1. Dehydroabietic Acid Proteome.

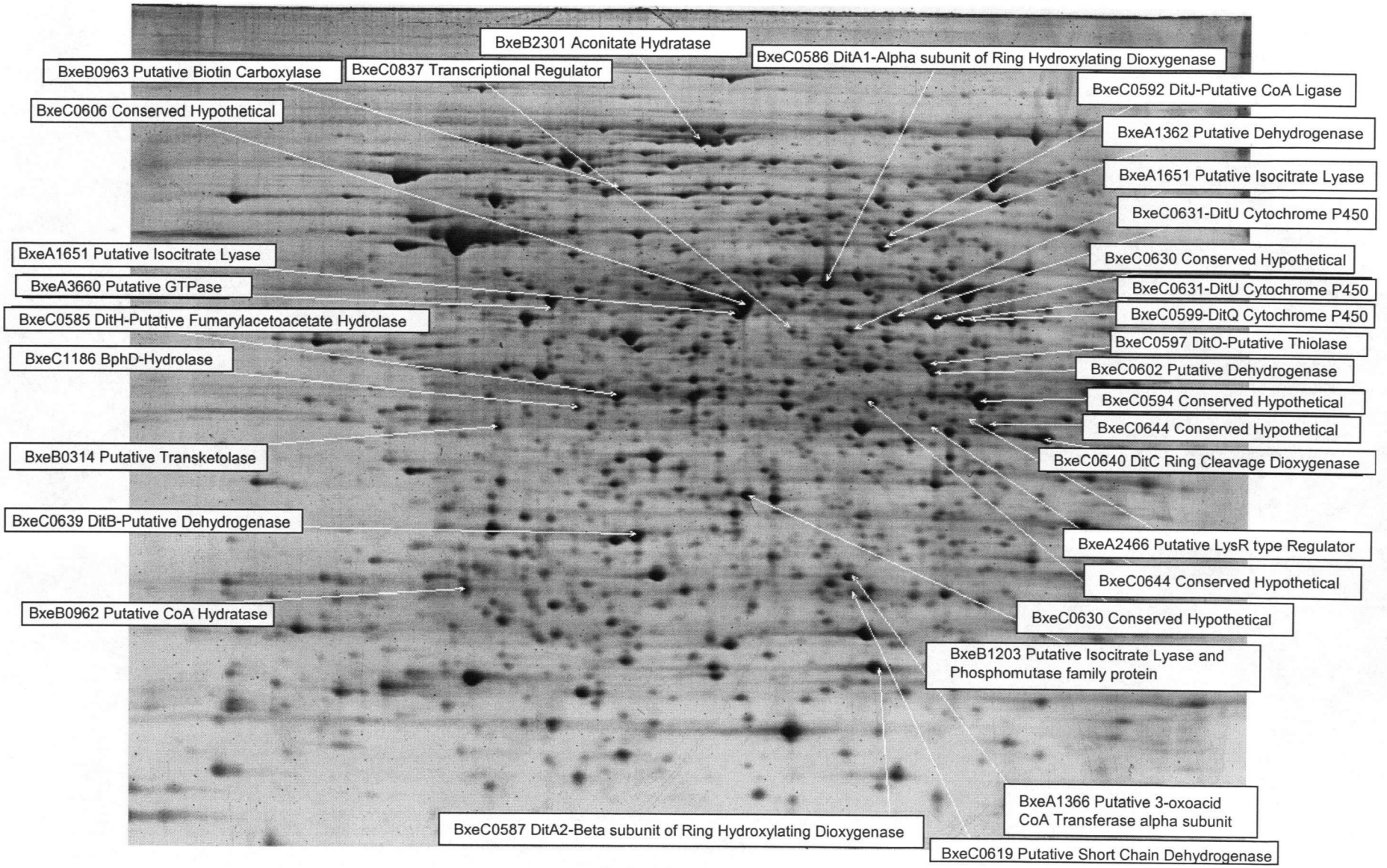

125 **Figure A.2 Abietic Acid Proteome**

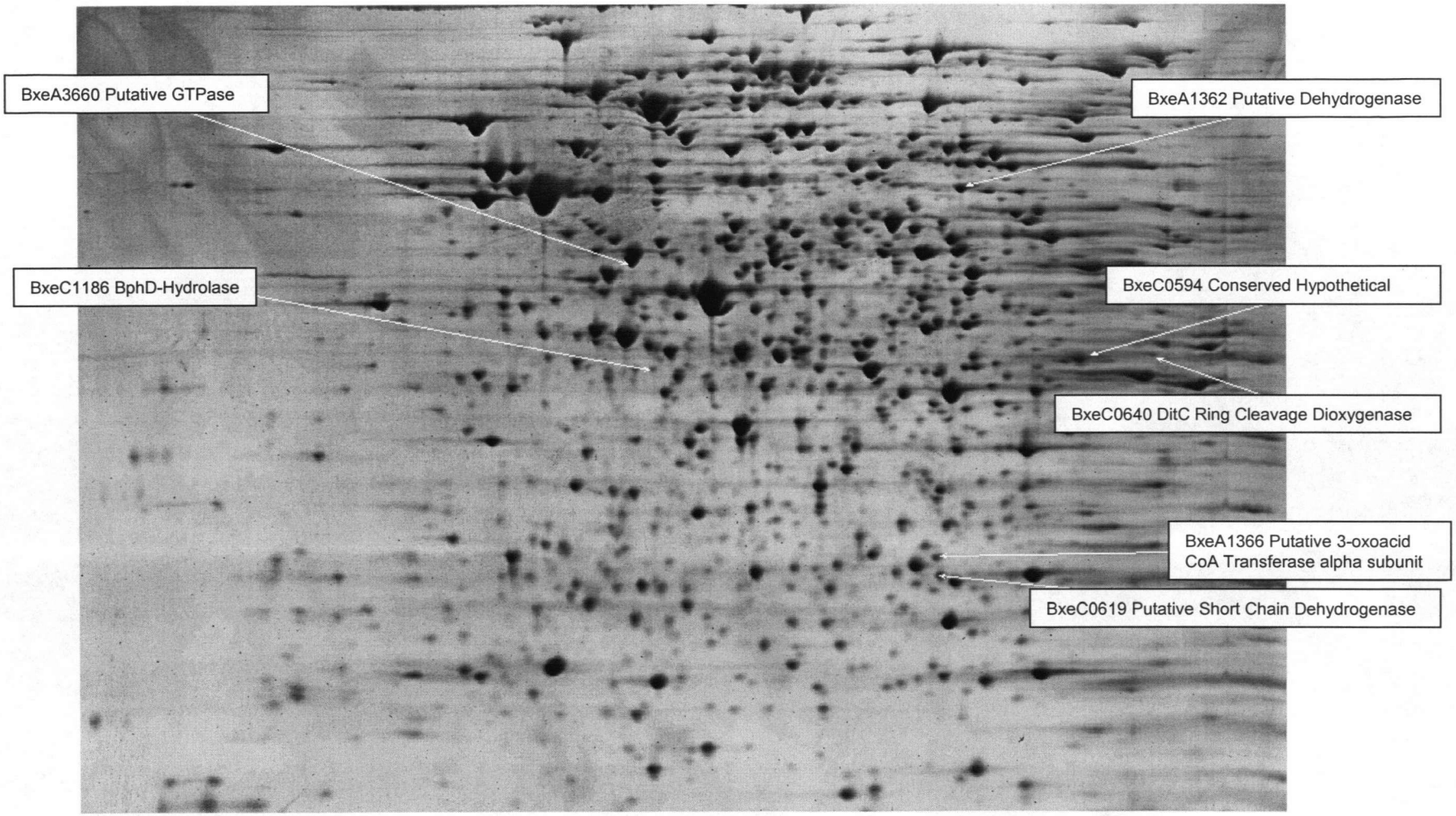

Figure A.3 Succinate Proteome